MR IMAGING OF THE PRETERM BRAIN

safer better faster stronger

Annemarie Plaisier

Cover design: Ton Everaers & Lucy Plaisier
Thesis layout: Ton Everaers
Printing: Print Partners Ipskamp

ISBN: 978-90-9028083-7

Part of the research in this thesis was financially supported by the "Ter Meulen Fonds".

The print and reproduction of this thesis was kindly supported by:
Chiesi Pharmaceuticals, Covidien Nederland, Esaote Benelux, Lammers Medical Technology, VCM Medical, Nutricia baby- en kindervoeding, AbbVie and ABNAMRO.

MR IMAGING OF THE PRETERM BRAIN

safer better faster stronger

Beeldvorming door middel van MRI van het premature brein
veiliger beter sneller krachtiger

Proefschrift

Ter verkrijging van de graad van doctor aan de
Erasmus Universiteit Rotterdam
op gezag van de rector magnificus
Prof.dr. H.A.P. Pols
en volgens besluit van het College voor Promoties

De openbare verdediging zal plaatsvinden op
dinsdag 25 maart 2014 om 13.30 uur

door

Annemarie Plaisier
geboren te Rotterdam

ERASMUS UNIVERSITEIT ROTTERDAM

Promotiecommissie:

Promotoren: Prof.dr. I.K.M. Reiss

Prof.dr. G.P. Krestin

Overige leden: Prof.dr. D. Tibboel

Prof.dr. W.J. Niessen

Prof.dr. S.J. Counsell

Copromotor: Dr. J. Dudink

Contents

Chapter 1 Introduction and aims *11*

Chapter 2 Optimal timing of cerebral MRI in preterm infants to predict long term neurodevelopmental outcome: a systematic review *27*
American Journal of Neuroradiology, May 2013

Chapter 3 Safety of routine early MRI in preterm infants *51*
Pediatric Radiology, 2012; 42:1205-11

Chapter 4 Acquisition guidelines and quality assessment tools for analyzing neonatal diffusion tensor MRI data *67*
American Journal of Neuroradiology, 2013; 34:1496-505

Chapter 5 Choice of diffusion tensor estimation approach affects fiber tractography of the fornix in the preterm brain *91*
American Journal of Neuroradiology, January 2014

Chapter 6 Standardized workflow for constructing a site-specific DTI template of the preterm brain *107*
In preparation

Chapter 7 Serial cranial ultrasonography and early MRI are complementary in detecting preterm brain injury *125*
Submitted

Chapter 8 General discussion and future perspectives *145*

Chapter 9 Samenvatting *159*
Summary *164*
About the author *168*
List of publications *170*
PhD Portfolio *172*
Dankwoord *174*
Color section *178*

CHAPTER 1

Introduction and Aims

Preterm brain injury

Human brain development and maturation consist of complex processes that span from the first trimester of pregnancy to adult life. These processes include: 1) neuronal proliferation, characterized by generation of neurons in the dorsal subventricular zone and ventral germinative epithelium of the ganglionic eminence; 2) migration, where neurons move from these zones to specific sites where they will reside for life; 3) organization, in which neurons differentiate to subplate neurons, align, orientate and connect through their axons and dendrites. Glial cells differentiate into astrocytes, oligodendrocytes and microglia, and 4) myelination, where oligodendrocytes produce myelin that will be deposited around axons[1, 2].

Preterm infants are born in this critical period, in which the brain is particularly vulnerable to exogenous and endogenous events. Perinatal hypoxia-ischemia, hyperoxia, infection and hypocarbia can result in fluctuations in cerebral blood flow, inflammation, increased excitotoxicity and oxidative stress, all of which can affect normal brain ontogenesis and cause irreversible injury[3, 4].

In general, the two most commonly recognized variants of preterm brain injury are: periventricular white matter (WM) injury and hemorrhage in the germinal matrix and lateral ventricle. These injury patterns will be discussed separately in the following sections.

White matter injury

Cerebral preterm WM injury is predominantly characterized by injury to vulnerable preoligodendrocytes, leading to a marked deficit of mature myelin-producing oligodendrocytes and hypomyelination. Although this results in an increase in oligodendroglial precursors, these progenitors seem not able to fully differentiate. Furthermore, they seem to be even more vulnerable to hypoxia-ischemia, which explains why the risk increases with decreasing gestational age. Another element of WM injury is caused by injury to subplate neurons and late migrating neurons, resulting in neuronal loss, axonal degeneration, abnormal thalamocortical connectivity and gliosis that can be found throughout the brain[3, 5].

Lesions can vary from diffuse non-cystic components to focal necrosis with loss of all cellular elements, also known as cystic periventricular leukomalacia (Fig 1). Due to important advances in neonatal care[6], this is seen less frequently nowadays. However, because of extensive destruction and developmental disruption, diffuse non-cystic WM injury has far reaching consequences and remains to be accounted for most neurological sequelae in infants born preterm[7-9].

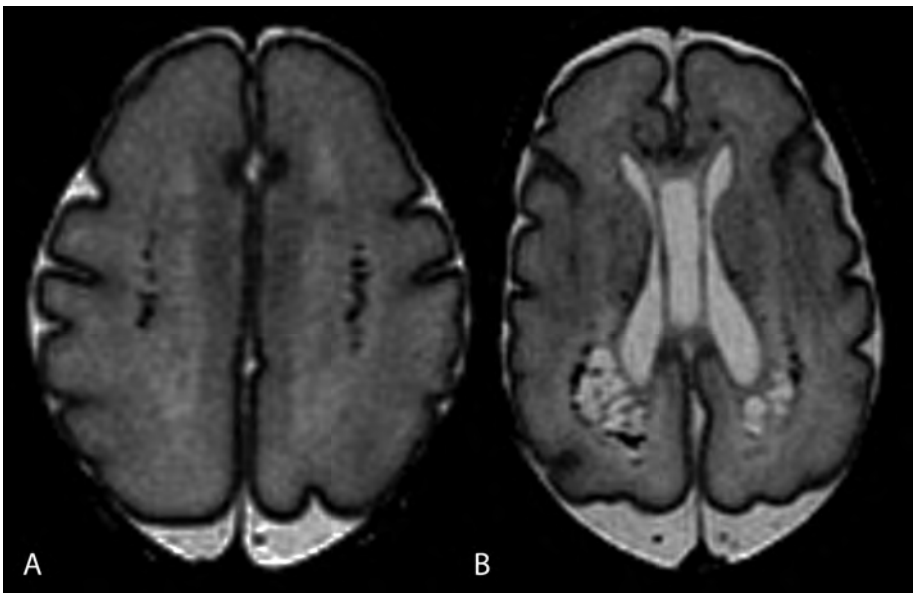

Figure 1 – Examples of periventricular white matter injury on transversal T2-weighted images, scanned at 30 weeks postmenstrual age. **A**, punctate white matter lesions, and **B**, periventricular leukomalacia.

Germinal matrix and intraventricular hemorrhage

The dorsal subventricular zone, or germinal matrix, is located near the lateral ventricles, is highly vascularized and contains neuronal and glial precursors of subplate neurons, oligodendrocytes and astrocytes. After proliferation, these progenitors migrate from the germinal matrix towards their permanent destination. Volume of the germinal matrix peaks at 25 weeks and slowly regresses at 36 weeks of gestation.

Because of its high vascularization and due to perinatal hemodynamic and inflammatory factors, the germinal matrix is prone to hemorrhage, resulting in germinal matrix hemorrhage (GMH) or, if hemorrhage is extended to the ventricles, in intraventricular hemorrhage (IVH)[10, 11]. Main predicting factor for poor outcome of GMH-IVH is the presence of associated WM injury, such as in periventricular hemorrhagic infarction, due to obstructed cerebral venous drainage. Post-hemorrhagic ventricular dilatation is caused by impaired reabsorption of cerebrospinal fluid, subsequent to inflammation and aqueductal obstruction by blood clot, disrupted ependym and reactive gliosis (Fig 2)[10]. But, even in the absence of these complications, cognitive deficits are still encountered and could be attributed to secondary injury patterns. These include: injury to the developing cerebellum by subarachnoid blood products and impaired cortical maturation, as a consequence of destruction to neuroglial progenitors, resulting in decreased cortical thickness[12-14].

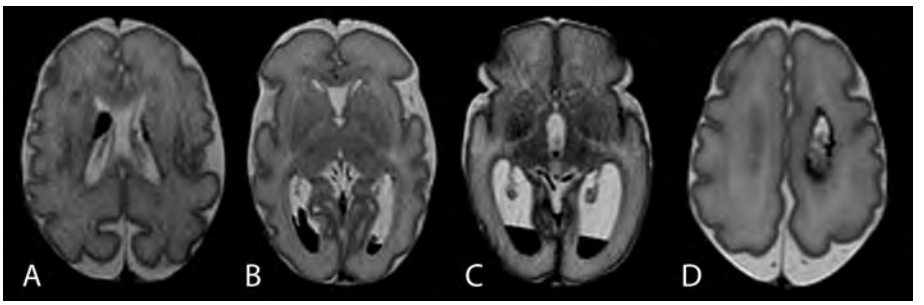

Figure 2 – Gradation of germinal matrix and intraventricular hemorrhage on transversal T2-weighted images. **A**, bilateral germinal matrix hemorrhage; **B**, intraventricular hemorrhage; **C**, post-hemorrhagic ventricular dilatation, and **D**, periventricular hemorrhagic infarction.

Imaging biomarkers of outcome

Preterm birth and subsequent brain injury are becoming global health care problems because of high financial costs and social-emotional burden due to high mortality and morbidity rates[15]. Persistent disabilities such as cerebral palsy, neurodevelopmental delay, neuro-sensory impairment and neurocognitive dysfunction (learning disabilities, attention deficit and social behavior disorders), are frequently encountered in survivors of prematurity and increase with decreasing gestational age[6, 16-20]. With growing numbers of infants born extremely premature (born below 26 weeks of gestation), early detection of abnormal neurodevelopment is urgently needed. Early biomarkers of long term outcome would provide accurate information to doctors and parents and are essential in the design of neuro-protective intervention strategies[21, 22].

Structural neonatal neuroimaging techniques

In order to improve prediction of outcome, neuroimaging is increasingly performed in neonatal intensive care units[23-25]. Cranial ultrasonography (CUS) is most frequently used, relatively cheap, often directly available and allows serial bedside scanning with little disturbance to the infant. Traditionally, CUS is used to detect focal lesions, such as GMH-IVH, post-hemorrhagic ventricular dilatation and cystic periventricular leukomalacia. Owing to ongoing technical developments, such as raw data analysis, multimodal imaging, usage of supplemental acoustic windows and quantitative abilities, its usefulness for preterm infants is enhancing[26-31]. Experienced and careful application of CUS might be as effective as MRI in lesion detection. Furthermore, with color Doppler imaging, sequential monitoring of cerebral microcirculation and intracranial hemodynamic adaptations after birth is possible. Limitations of CUS include observer-dependency, lower sensitivity to detect posterior fossa abnormalities and congenital malformations and the lack of objective measurements to provide early predictors of outcome[32-34].

Magnetic resonance imaging (MRI) is a powerful imaging technique that has substantially evolved to provide high-resolution images to evaluate the brain without ionizing radiation[35-38]. Structural MRI, such as T1- and T2-weighted images (Fig 3), are well able to assess brain development and presence of lesions, related to neurodevelopmental deficits[39, 40]. However, because these deficits seem to occur even in absence of significant brain injury, the use of quantitative MRI techniques to assess microstructural alterations of brain development is rapidly increasing[41].

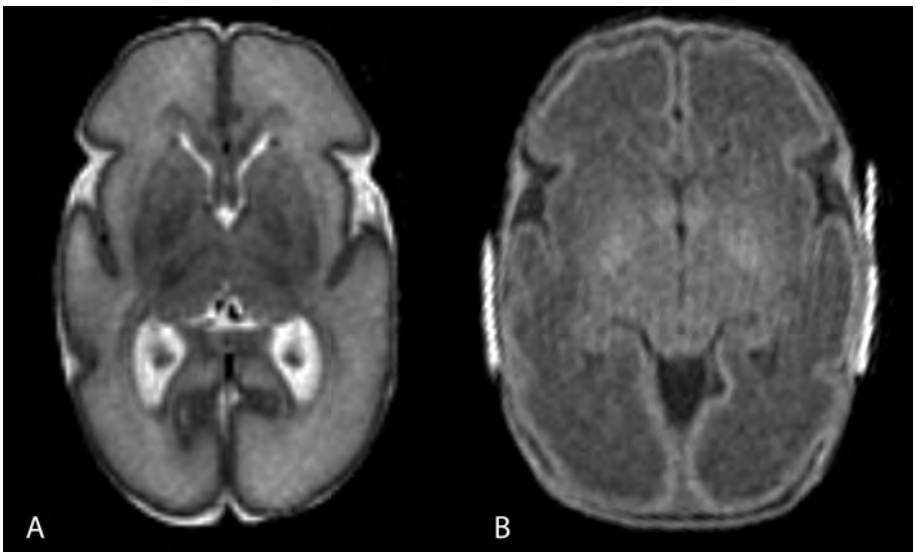

Figure 3 – Conventional structural MRI sequences: **A**, transversal T2-weighted fast-spin echo, and **B**, transversal 3D T1-SPGR images.

Characteristics, benefits and disadvantages of most common used quantitative MRI techniques that have been developed will be discussed in the next section.

Quantitative MRI techniques

By segmenting brain MR images into specific regions or tissues, volumes of these segments can be calculated. Previous volumetric MRI studies have provided quantification of maturational changes in brain volumes during gestation. In general, preterm infants at term corrected age have reduced tissue volumes and increased cerebrospinal fluid volumes compared to healthy term born infants[42-45]. Cortical folding processes mostly take place after 26 weeks' gestational age (Fig 4) and can be quantified by calculating ratios between cortical surface area and total brain volume or by similar measurements[46]. These quantitative surrogates of cortical development have been used to demonstrate maturational disturbances in

preterm infants that are correlated to long term neurodevelopmental impairment[23, 45, 47, 48]. Main limitations of these techniques include their time consuming nature, high variability due to large heterogeneity and the necessity of complex algorithms and post processing methods that limit clinical application.

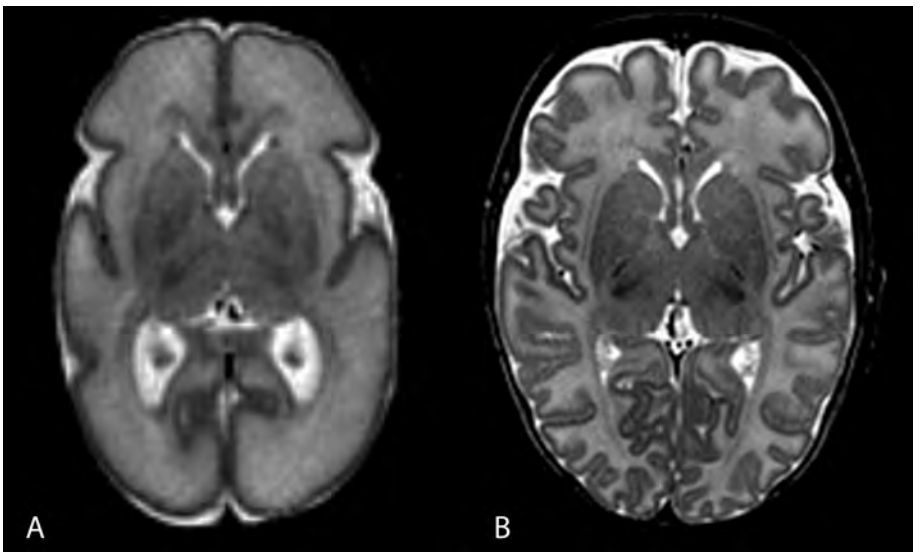

Figure 4 – Transversal T2-weighted images showing the imposing cortical folding process during brain maturation. Note the marked difference between gyrification between 30 weeks postmenstrual age (**A**) and at term-equivalent age (**B**).

Brain tissue metabolites can be quantitatively assessed with proton magnetic resonance spectroscopy. Objective evaluation of the N-acetyl aspartate/choline ratio seems particularly valuable in prematurity, as this ratio increases with synthesis by oligodendrocyte progenitor cells. Thus, proton magnetic resonance spectroscopy enables quantification of WM injury[49]. However, clinical impact is limited due to lack of reference values and correlation to long term outcome.

Diffusion tensor imaging (DTI) allows not only to visualize specific WM tracts, but also to assess pre-myelinating processes during development and to quantify brain abnormalities that are not detectable on conventional MRI sequences. Furthermore, DTI has unique abilities to evaluate microstructural brain properties and seems particularly suitable as neuroimaging biomarker to provide quantification of brain maturation and injury. Many DTI studies using different tools have revealed substantial insights into disturbed brain connectivity and functionality of infants born preterm[50-55]. Technical developments regarding mapping macrostructural brain connections, aimed to find the human 'connectome', are promising and might unravel origins of future adult diseases.

Technical background of DTI is however complex: acquisition, processing and interpretation are not as straightforward as with conventional MRI sequences and need caution. Because many pitfalls must be addressed when using DTI, a reasonable part of this thesis is focused on this technique.

Basic principles of diffusion

Diffusion is random motion of water molecules that varies across brain regions due to underlying tissue characteristics: in cerebrospinal fluid, water molecules can move freely in all directions and displacement is equally distributed, this is called isotropic diffusion. In highly organized tissue, such as in the WM, diffusion is hindered perpendicular to, and facilitated along fiber directions. This is called anisotropic diffusion[56-59]. By assessing diffusion in brain tissue, DTI is able to assess specific tissue features, such as myelination, fiber density and complexity. Frequently used quantitative parameters are fractional anisotropy (FA) and apparent diffusion coefficient (ADC). FA increases proportionally with the degree of tissue organization and ranges from zero to one. During brain development, FA increases and ADC decreases exponentially in WM as a result of decreased water content and increased (pre-) myelination[60-62]. DTI studies have demonstrated that deviations from these developmental trends are considered diagnostic of WM injury and correlate with impaired outcome in preterm infants[8, 50-53, 55, 63, 64].

DTI measures diffusion in more than six non-collinear directions. The diffusion tensor is calculated to describe orientation and directionality of diffusion in the studied tissue. This is usually displayed as an ellipsoid, with the long axis representing the direction with the highest diffusivity and perpendicular axis representing less and least diffusivity respectively. Assessment of spatial organization of WM structures is based on this mathematical background and can be visualized using different techniques.

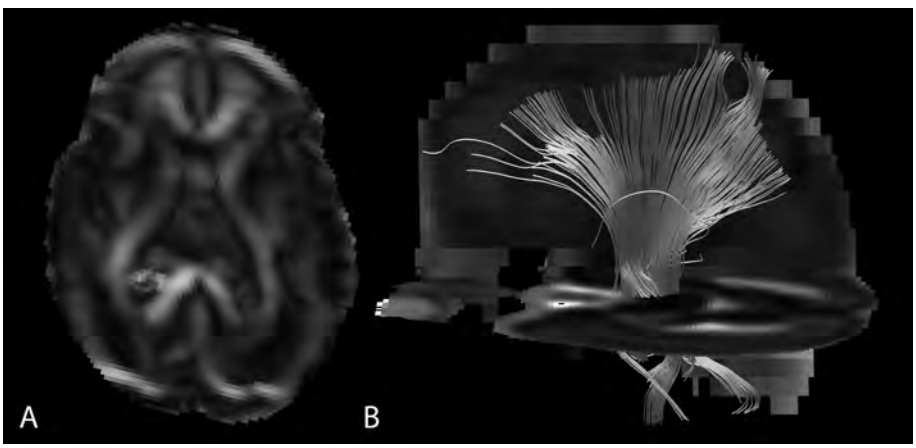

Figure 5 – Applications of diffusion tensor imaging: **A**, color-coded maps; red stands for left–right direction, blue for superior–inferior, and green for anterior–posterior. Brightness of colors is weighted by the FA value. **B**, fiber tractography of the corticospinal tract. (A full color version of this illustration can be found in the color section).

Color maps (Fig 5A) indicate direction of highest diffusivity. As this is considered to correspond with orientation of WM fibers, color maps represent position and direction of WM tracts. Fiber tractography enables delineation of specific WM pathways (Fig 5B), this is usually performed by tracking highest diffusivity from voxel to voxel throughout the brain.

Feasibilty of neonatal MRI in clinical care

In order to enable early parental counseling and administration of rehabilitative strategies, MRI scanning is increasingly performed serially and at early preterm age[48, 61, 65, 66]. In addition, quantitative MRI techniques potentially have invaluable possibilities to provide early, objective biomarkers of microstructural WM changes and subsequent outcome and might become essential for neuroprotective intervention trials for evaluating efficacy.

Because of high likelihood of respiratory, hemodynamic and thermoregulatory instability, scanning vulnerable preterm infants is extremely challenging[67-70]. Also, in order to apply MRI sequences efficiently, thorough knowledge of timing, nature and presentation of preterm brain injury is crucial[71, 72]. Moreover, obtaining reliable MR images and reference values is not straightforward due to tissue characteristics of the developing brain and many technical issues that complicate reliable analysis, such as: hardware setup, image acquisition and processing methodology[73-75]. These important matters require dedication and comprehensiveness adapted to the preterm population to pave the way for MRI to provide clinical biomarkers of injury.

Thesis outline and aims

This thesis is aimed to address safety aspects, dedicated use of sequences and quality issues of cerebral MRI scans in preterm infants.

MRI scans are increasingly performed in preterm infants to detect brain injury and to predict neurodevelopmental outcome. However, there seems no consensus on optimal timing of MRI scanning. **Chapter 2** presents therefore a systematic review of current literature regarding optimal timing of MRI scans in preterm infants with regard to best prediction of long term outcome. Moreover, early MRI scans are increasingly performed, but may be complicated by safety issues because of the high vulnerability in this population. **Chapter 3** addresses these aspects in a retrospective study.

DTI has great potentials to provide unique imaging biomarkers of WM microstructure. However, this technique is based on complex aspects and therefore highly sensitive to many factors that may influence the final results. **Chapter 4** describes guidelines to acquire neonatal DTI from a clinical perspective and recommends high-quality data acquisition and processing. The importance of these aspects is further emphasized in **chapter 5**, where the impact of processing methodology and data quality on tractography results of the fornix in the preterm brain is prospectively investigated. In addition, due to the numerous aspects that may complicate analysis, DTI measurements can typically not be exchanged across centers. Because such values are highly needed for clinical individual purposes, using brain DTI templates site-specifically might be a solution. As such, **chapter 6** introduces a workflow for the construction of a site-specific preterm brain DTI template. Efficacy of the method will be tested in a proof of concept study.

Based on the aforementioned chapters, the clinical use of early MRI scans in preterm infants might be limited. Because of the great potentials MRI could offer us in the near future, these limitations need to be addressed. **Chapter 7**, raises awareness regarding clinical restrictions of MRI by investigating detection efficacy and clinical feasibility of serial advanced CUS scans, performed by an experienced observer, compared with an early MRI scan, in a large prospective cohort study.

Chapter 8 summarizes main findings and conclusions of this thesis and discusses future directions.

References

1. Volpe JJ. Neuronal Proliferation, Migration Organization and Myelination. In: *Neurology of the Newborn*. (ed). Philadelphia: Saunders; 2008.
2. Kostovic I, Jovanov-Milosevic N. The development of cerebral connections during the first 20-45 weeks' gestation. *Semin Fetal Neonatal Med* 2006;11:415-22.
3. Volpe JJ. Brain injury in premature infants: a complex amalgam of destructive and developmental disturbances. *Lancet Neurol* 2009;8:110-24.
4. Deng W. Neurobiology of injury to the developing brain. *Nat Rev Neurol* 2010;6:328-36.
5. Supramaniam V, Vontell R, Srinivasan L, Wyatt-Ashmead J, Hagberg H, Rutherford M. Microglia activation in the extremely preterm human brain. *Pediatr Res* 2013;73:301-9.
6. Moore T, Hennessy EM, Myles J, Johnson SJ, Draper ES, Costeloe KL, Marlow N. Neurological and developmental outcome in extremely preterm children born in England in 1995 and 2006: the EPICure studies. *BMJ* 2012;345:e7961.
7. Rutherford MA, Supramaniam V, Ederies A, Chew A, Bassi L, Groppo M, Anjari M, Counsell S, Ramenghi LA. Magnetic resonance imaging of white matter diseases of prematurity. *Neuroradiology* 2010;52:505-21.
8. Huppi PS, Murphy B, Maier SE, Zientara GP, Inder TE, Barnes PD, Kikinis R, Jolesz FA, Volpe JJ. Microstructural brain development after perinatal cerebral white matter injury assessed by diffusion tensor magnetic resonance imaging. *Pediatrics* 2001;107:455-60.
9. Khwaja O, Volpe JJ. Pathogenesis of cerebral white matter injury of prematurity. *Arch Dis Child Fetal Neonatal Ed* 2008;93:F153-61.
10. Volpe JJ. Intracranial Hemorrhage: Germinal Matrix-Intraventricular Hemorrhage of the Premature Infant. In: *Neurology of the Newborn.* (ed). Philadelphia: Saunders; 2008.
11. Raets MM, Dudink J, Govaert P. Neonatal disorders of germinal matrix. *J Matern Fetal Neonatal Med* 2013.
12. Folkerth RD. Germinal matrix haemorrhage: destroying the brain's building blocks. *Brain* 2011;134:1261-3.
13. Bassan H. Intracranial hemorrhage in the preterm infant: understanding it, preventing it. *Clin Perinatol* 2009;36:737-62.
14. Volpe JJ. Cerebellum of the premature infant: rapidly developing, vulnerable, clinically important. *J Child Neurol* 2009;24:1085-104.
15. Gulland A. Fifteen million and rising--the number of premature births every year. *BMJ* 2012;344:e3084.
16. Incidence of and risk factors for neonatal morbidity after active perinatal care: extremely preterm infants study in Sweden (EXPRESS). *Acta Paediatr* 2010;99:978-92.
17. Larroque B, Ancel PY, Marret S, Marchand L, Andre M, Arnaud C, Pierrat V, Roze JC, Messer J, Thiriez G, Burguet A, Picaud JC, Breart G, Kaminski M. Neurodevelopmental disabilities and special care of 5-year-old children born before 33 weeks of gestation (the EPIPAGE study): a longitudinal cohort study. *Lancet* 2008;371:813-20.
18. Marlow N, Wolke D, Bracewell MA, Samara M. Neurologic and developmental disability at six years of age after extremely preterm birth. *N Engl J Med* 2005;352:9-19.
19. Saigal S, Doyle LW. An overview of mortality and sequelae of preterm birth from infancy to adulthood. *Lancet* 2008;371:261-9.
20. Wood NS, Marlow N, Costeloe K, Gibson AT, Wilkinson AR. Neurologic and developmental disability after extremely preterm birth. EPICure Study Group. *N Engl J Med* 2000;343:378-84.

21. Ment LR, Hirtz D, Huppi PS. Imaging biomarkers of outcome in the developing preterm brain. *Lancet Neurol* 2009;8:1042-55.
22. Rees S, Harding R, Walker D. The biological basis of injury and neuroprotection in the fetal and neonatal brain. *Int J Dev Neurosci* 2011;29:551-63.
23. Inder TE, Tao J, Neil JJ. Common lesions in the newborn brain. *Top Magn Reson Imaging* 2011;22:25-32.
24. Ramenghi LA, Rutherford M, Fumagalli M, Bassi L, Messner H, Counsell S, Mosca F. Neonatal neuroimaging: going beyond the pictures. *Early Hum Dev* 2009;85:S75-7.
25. de Vries LS, Benders MJ, Groenendaal F. Imaging the premature brain: ultrasound or MRI? *Neuroradiology* 2013;55:13-22.
26. Govaert PP, de Vries L.S. *An atlas of neonatal brain sonography.* 2nd ed. London, Cambridge: Mac Keith Press; 2010.
27. Leijser LM, de Vries LS, Cowan FM. Using cerebral ultrasound effectively in the newborn infant. *Early Hum Dev* 2006;82:827-35.
28. Leijser LM, Srinivasan L, Rutherford MA, Counsell SJ, Allsop JM, Cowan FM. Structural linear measurements in the newborn brain: accuracy of cranial ultrasound compared to MRI. *Pediatr Radiol* 2007;37:640-8.
29. Steggerda SJ, Leijser LM, Wiggers-de Bruine FT, van der Grond J, Walther FJ, van Wezel-Meijler G. Cerebellar injury in preterm infants: incidence and findings on US and MR images. *Radiology* 2009;252:190-9.
30. van Wezel-Meijler G, Steggerda SJ, Leijser LM. Cranial ultrasonography in neonates: role and limitations. *Semin Perinatol* 2010;34:28-38.
31. Horsch S, Skiold B, Hallberg B, Nordell B, Nordell A, Mosskin M, Lagercrantz H, Aden U, Blennow M. Cranial ultrasound and MRI at term age in extremely preterm infants. *Arch Dis Child Fetal Neonatal Ed* 2010;95:F310-4.
32. Reynolds PR, Dale RC, Cowan FM. Neonatal cranial ultrasound interpretation: a clinical audit. *Arch Dis Child Fetal Neonatal Ed* 2001;84:F92-5.
33. Mirmiran M, Barnes PD, Keller K, Constantinou JC, Fleisher BE, Hintz SR, Ariagno RL. Neonatal brain magnetic resonance imaging before discharge is better than serial cranial ultrasound in predicting cerebral palsy in very low birth weight preterm infants. *Pediatrics* 2004;114:992-8.
34. Whyte HEA, Blaser S. Limitations of routine neuroimaging in predicting outcomes of preterm infants. *Neuroradiology* 2013;55:3-11.
35. Counsell SJ, Rutherford MA, Cowan FM, Edwards AD. Magnetic resonance imaging of preterm brain injury. *Arch Dis Child Fetal Neonatal Ed* 2003;88:F269-74.
36. Huppi PS, Inder TE. Magnetic resonance techniques in the evaluation of the perinatal brain: recent advances and future directions. *Semin Neonatol* 2001;6:195-210.
37. Rutherford MA. What's new in neuroimaging? Magnetic resonance imaging of the immature brain. *Eur J Paediatr Neurol* 2002;6:5-13.
38. Boardman JP, Craven C, Valappil S, Counsell SJ, Dyet LE, Rueckert D, Aljabar P, Rutherford MA, Chew AT, Allsop JM, Cowan F, Edwards AD. A common neonatal image phenotype predicts adverse neurodevelopmental outcome in children born preterm. *Neuroimage* 2010;52:409-14.
39. Woodward LJ, Anderson PJ, Austin NC, Howard K, Inder TE. Neonatal MRI to predict neurodevelopmental outcomes in preterm infants. *N Engl J Med* 2006;355:685-94.
40. Woodward LJ, Clark CA, Bora S, Inder TE. Neonatal white matter abnormalities an important predictor of neurocognitive outcome for very preterm children. *PLoS One* 2012;7:e51879.

41. Counsell SJ, Edwards AD, Chew AT, Anjari M, Dyet LE, Srinivasan L, Boardman JP, Allsop JM, Hajnal JV, Rutherford MA, Cowan FM. Specific relations between neurodevelopmental abilities and white matter microstructure in children born preterm. *Brain* 2008;131:3201-8.
42. Keunen K, Kersbergen KJ, Groenendaal F, Isgum I, de Vries LS, Benders MJ. Brain tissue volumes in preterm infants: prematurity, perinatal risk factors and neurodevelopmental outcome: a systematic review. *J Matern Fetal Neonatal Med* 2012;25 Suppl 1:89-100.
43. Inder TE, Warfield SK, Wang H, Huppi PS, Volpe JJ. Abnormal cerebral structure is present at term in premature infants. *Pediatrics* 2005;115:286-94.
44. Srinivasan L, Dutta R, Counsell SJ, Allsop JM, Boardman JP, Rutherford MA, Edwards AD. Quantification of deep gray matter in preterm infants at term-equivalent age using manual volumetry of 3-tesla magnetic resonance images. *Pediatrics* 2007;119:759-65.
45. Dubois J, Benders M, Borradori-Tolsa C, Cachia A, Lazeyras F, Ha-Vinh Leuchter R, Sizonenko SV, Warfield SK, Mangin JF, Huppi PS. Primary cortical folding in the human newborn: An early marker of later functional development. *Brain* 2008;131:2028-41.
46. Dubois J, Benders M, Cachia A, Lazeyras F, Ha-Vinh Leuchter R, Sizonenko SV, Borradori-Tolsa C, Mangin JF, Huppi PS. Mapping the early cortical folding process in the preterm newborn brain. *Cereb Cortex* 2008;18:1444-54.
47. Kapellou O, Counsell SJ, Kennea N, Dyet L, Saeed N, Stark J, Maalouf E, Duggan P, Ajayi-Obe M, Hajnal J, Allsop JM, Boardman J, Rutherford MA, Cowan F, Edwards AD. Abnormal cortical development after premature birth shown by altered allometric scaling of brain growth. *PLoS Med* 2006;3:1382-90.
48. Rathbone R, Counsell SJ, Kapellou O, Dyet L, Kennea N, Hajnal J, Allsop JM, Cowan F, Edwards AD. Perinatal cortical growth and childhood neurocognitive abilities. *Neurology* 2011;77:1510-5.
49. Huppi PS, Lazeyras F. Proton magnetic resonance spectroscopy ((1)H-MRS) in neonatal brain injury. *Pediatr Res* 2001;49:317-20.
50. Bassi L, Ricci D, Volzone A, Allsop JM, Srinivasan L, Pai A, Ribes C, Ramenghi LA, Mercuri E, Mosca F, Edwards AD, Cowan FM, Rutherford MA, Counsell SJ. Probabilistic diffusion tractography of the optic radiations and visual function in preterm infants at term equivalent age. *Brain* 2008;131:573-82.
51. Ball G, Boardman JP, Aljabar P, Pandit A, Arichi T, Merchant N, Rueckert D, Edwards AD, Counsell SJ. The influence of preterm birth on the developing thalamocortical connectome. *Cortex* 2013;34:1124-36.
52. de Bruine FT, van Wezel-Meijler G, Leijser LM, van den Berg-Huysmans AA, van Steenis A, van Buchem MA, van der Grond J. Tractography of developing white matter of the internal capsule and corpus callosum in very preterm infants. *Eur Radiol* 2011;21:538-47.
53. Anjari M, Srinivasan L, Allsop JM, Hajnal JV, Rutherford MA, Edwards AD, Counsell SJ. Diffusion tensor imaging with tract-based spatial statistics reveals local white matter abnormalities in preterm infants. *Neuroimage* 2007;35:1021-7.
54. Dudink J, Buijs J, Govaert P, van Zwol AL, Conneman N, van Goudoever JB, Lequin M. Diffusion tensor imaging of the cortical plate and subplate in very-low-birth-weight infants. *Pediatr Radiol* 2010;40:1397-404.
55. van Kooij BJ, de Vries LS, Ball G, van Haastert IC, Benders MJ, Groenendaal F, Counsell SJ. Neonatal tract-based spatial statistics findings and outcome in preterm infants. *AJNR Am J Neuroradiol* 2012;33:188-94.
56. Dudink J, Kerr JL, Paterson K, Counsell SJ. Connecting the developing preterm brain. *Early Hum Dev* 2008;84:777-82.

57. Huppi PS, Dubois J. Diffusion tensor imaging of brain development. *Semin Fetal Neonatal Med* 2006;11:489-97.
58. Jones DK. Studying connections in the living human brain with diffusion MRI. *Cortex* 2008;44:936-52.
59. Pandit AS, Ball G, Edwards AD, Counsell SJ. Diffusion magnetic resonance imaging in preterm brain injury. *Neuroradiology* 2013;55 Suppl 2:65-95.
60. Neil JJ, Shiran SI, McKinstry RC, Schefft GL, Snyder AZ, Almli CR, Akbudak E, Aronovitz JA, Miller JP, Lee BC, Conturo TE. Normal brain in human newborns: apparent diffusion coefficient and diffusion anisotropy measured by using diffusion tensor MR imaging. *Radiology* 1998;209:57-66.
61. Drobyshevsky A, Bregman J, Storey P, Meyer J, Prasad PV, Derrick M, MacKendrick W, Tan S. Serial diffusion tensor imaging detects white matter changes that correlate with motor outcome in premature infants. *Dev Neurosci* 2007;29:289-301.
62. Miller SP, Vigneron DB, Henry RG, Bohland MA, Ceppi-Cozzio C, Hoffman C, Newton N, Partridge JC, Ferriero DM, Barkovich AJ. Serial quantitative diffusion tensor MRI of the premature brain: development in newborns with and without injury. *J Magn Reson Imaging* 2002;16:621-32.
63. Counsell SJ, Allsop JM, Harrison MC, Larkman DJ, Kennea NL, Kapellou O, Cowan FM, Hajnal JV, Edwards AD, Rutherford MA. Diffusion-weighted imaging of the brain in preterm infants with focal and diffuse white matter abnormality. *Pediatrics* 2003;112:1-7.
64. Counsell SJ, Shen Y, Boardman JP, Larkman DJ, Kapellou O, Ward P, Allsop JM, Cowan FM, Hajnal JV, Edwards AD, Rutherford MA. Axial and radial diffusivity in preterm infants who have diffuse white matter changes on magnetic resonance imaging at term-equivalent age. *Pediatrics* 2006;117:376-86.
65. Dyet LE, Kennea N, Counsell SJ, Maalouf EF, Ajayi-Obe M, Duggan PJ, Harrison M, Allsop JM, Hajnal J, Herlihy AH, Edwards B, Laroche S, Cowan FM, Rutherford MA, Edwards AD. Natural history of brain lesions in extremely preterm infants studied with serial magnetic resonance imaging from birth and neurodevelopmental assessment. *Pediatrics* 2006;118:536-48.
66. Miller SP, Ferriero DM, Leonard C, Piecuch R, Glidden DV, Partridge JC, Perez M, Mukherjee P, Vigneron DB, Barkovich AJ. Early brain injury in premature newborns detected with magnetic resonance imaging is associated with adverse early neurodevelopmental outcome. *J Pediatr* 2005;147:609-16.
67. Benavente-Fernandez I, Lubian-Lopez PS, Zuazo-Ojeda MA, Jimenez-Gomez G, Lechuga-Sancho AM. Safety of magnetic resonance imaging in preterm infants. *Acta Paediatrica* 2010;99:850-3.
68. Stokowski LA. Ensuring safety for infants undergoing magnetic resonance imaging. *Adv Neonatal Care* 2005;5:14-27; quiz 52-4.
69. Mathur AM, Neil JJ, McKinstry RC, Inder TE. Transport, monitoring, and successful brain MR imaging in unsedated neonates. *Pediatr Radiol* 2008;38:260-4.
70. Merchant N, Groves A, Larkman DJ, Counsell SJ, Thomson MA, Doria V, Groppo M, Arichi T, Foreman S, Herlihy DJ, Hajnal JV, Srinivasan L, Foran A, Rutherford M, Edwards AD, Boardman JP. A patient care system for early 3.0 Tesla magnetic resonance imaging of very low birth weight infants. *Early Hum Dev* 2009;85:779-83.
71. Rutherford M, Biarge MM, Allsop J, Counsell S, Cowan F. MRI of perinatal brain injury. *Pediatr Radiol* 2010;40:819-33.
72. van Wezel-Meijler G, Leijser LM, de Bruine FT, Steggerda SJ, van der Grond J, Walther FJ. Magnetic resonance imaging of the brain in newborn infants: practical aspects. *Early Hum Dev* 2009;85:85-92.

73. Jones DK, Cercignani M. Twenty-five pitfalls in the analysis of diffusion MRI data. *NMR Biomed* 2010;23:803-20.
74. Mukherjee P, Chung SW, Berman JI, Hess CP, Henry RG. Diffusion tensor MR imaging and fiber tractography: technical considerations. *AJNR Am J Neuroradiol* 2008;29:843-52.
75. Pannek K, Guzzetta A, Colditz PB, Rose SE. Diffusion MRI of the neonate brain: acquisition, processing and analysis techniques. *Pediatric Radiology* 2012;42:1169-82.

CHAPTER 2

Optimal Timing of Cerebral MRI in Preterm Infants to Predict Long Term Neurodevelopmental Outcome: A Systematic Review

A. Plaisier
P. Govaert
M.H. Lequin
J. Dudink

American Journal of Neuroradiology, May 2013

Abstract

Advances in neonatal neuroimaging have improved detection of preterm brain injury responsible for abnormal neuromotor and cognitive development. Increasingly sophisticated magnetic resonance imaging (MRI) setups allow scanning during early preterm life.

In this review, we investigated how brain MRI in preterm infants should be timed to best predict long term outcome. Given the strong evidence that structural brain abnormalities are related to long term neurodevelopment, MRI should preferably be done at term-equivalent age. Early MRI scans are promising as they can guide early neuroprotective intervention studies and are indispensable in ongoing research on the understanding of preterm brain injury.

Introduction

Preterm birth with subsequent brain injury is an increasing public health concern. Advances in neonatal intensive care have significantly improved survival rates among very low birth weight infants, but survivors are still at considerable risk to develop cognitive, behavioral, neurosensory and motor disabilities[1-5]. The most common preterm brain injury patterns are: white matter (WM) injury, germinal matrix-intraventricular hemorrhage and its correlates; post-hemorrhagic ventricular dilatation and periventricular hemorrhagic venous infarction (Fig 1). Cystic periventricular leukomalacia is seen less often now. Diffuse non-cystic types of WM injury, including punctate WM lesions (PWML) and diffuse excessive high signal intensity (DEHSI), are therefore most frequent[6-10] and leading cause of disturbed brain growth, connectivity and functionality[11-13].

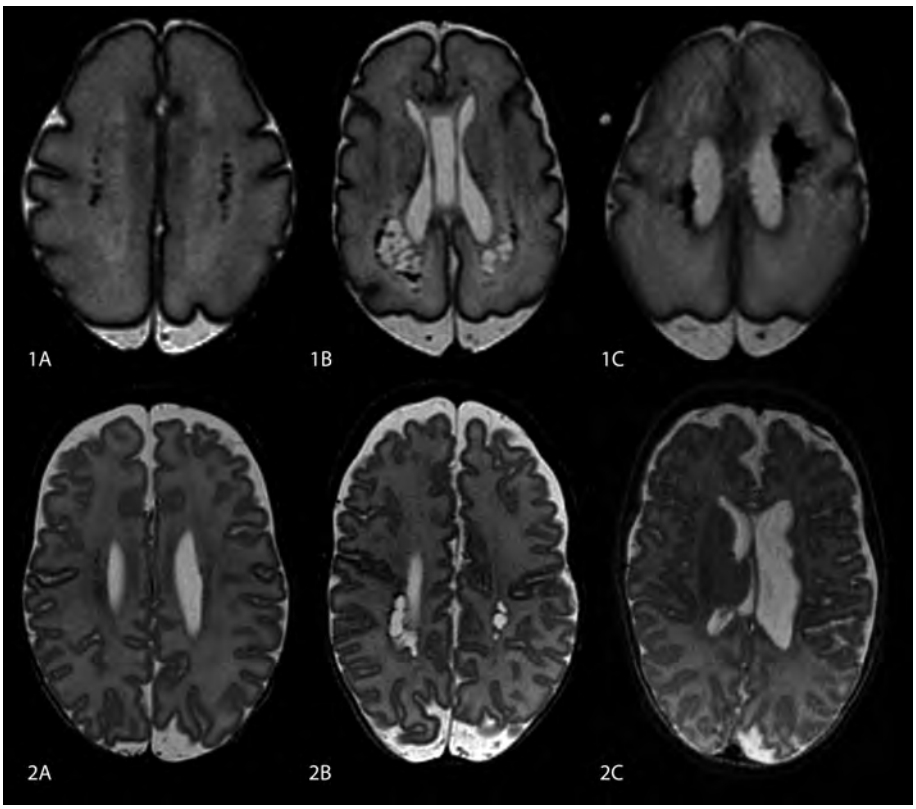

Figure 1 – Evolution of common types of preterm brain injury. 1, at 30 weeks' postmenstrual age and 2, at term-equivalent age. Transversal T2-weighted fast-spin-echo images of: **A**, punctate white matter lesions; **B**, periventricular leukomalacia, and **C**, periventricular hemorrhagic venous infarction. Note that images **2B** and **2C** are slightly oblique.

Although MRI is superior to cranial ultrasonography in detecting diffuse WM injury[14-17], structural MRI studies fail to precisely predict outcome[6, 8, 18]. One reason is that conventional MRI is not sensitive enough to measure changes in microstructure[19]. However, advanced MRI acquisition sequences and post processing techniques, such as diffusion tensor imaging (DTI), volumetric MRI measurements and proton MR spectroscopy (^{1}H-MRS), may be a solution.

DTI allows quantification of WM at a microstructural level by measuring the diffusion of water molecules in tissues[20, 21]. DTI studies have shown increasing fractional anisotropy (FA) and decreasing apparent diffusion coefficient (ADC) during brain maturation, which is ascribed to the decreased water content and increased WM complexity due to myelination[20, 22]. Deviations from these developmental trends are considered diagnostic of perinatal WM injury[23-25].

WM injury in preterm infants has been related to significantly reduced brain volume[26, 27], but brain growth in extremely preterm infants may also be disturbed in absence of evident WM abnormalities. Volumes of brain regions and structures are correlated to perinatal complications and are inversely related to gestational age at birth[28, 29]. Smaller volumes are often associated with impaired neuropsychological function at later age[29, 30].

Assessment of cortical folding during early brain development, with the use of post processing software[31], has provided insight into the underlying mechanisms of normal development, regional specialization and functional lateralization[32, 33]. Anomalous cortical folding, demonstrated in preterm infants, has been proposed as an early biomarker of neurocognitive impairment[34, 35].

Metabolic integrity of tissues can be measured in vivo with ^{1}H-MRS. The N-acetyl aspartate/choline ratio is of special interest in neonatal neuroimaging, as the ratio increases during brain maturation as an effect of synthesis by proliferating oligodendrocyte progenitor cells[36].

Early MRI provides early biomarkers of preterm brain injury and enables early parental counseling. However, systematic use of such MRI scans has its limitations due to hemodynamic, respiratory and thermodynamic instability seen in most preterm infants[37]. Moreover, technical aspects like smaller heads result in a lower signal-to-noise ratio[38]. As in most studies obtained at term-equivalent age[18, 30], less is known about the value of scanning at a lower postmenstrual age (PMA). Furthermore, brain injury can also occur in the late preterm period. MRI at term has the disadvantage that parents and caregivers are not fully informed until their child reaches term age. Furthermore, logistic issues may emerge in centers where infants are transferred to other hospitals once certain criteria are met.

As there seems to be no consensus on optimal timing of MRI, we reviewed the literature on prediction of neurodevelopmental outcome with the use of brain MRI performed at either early preterm or term age.

Methods

The Embase, Medline OvidSP, Cochrane and PubMed databases were systematically searched for relevant papers published between 1979 and November 2012. The strategy included synonyms and combinations of the following keywords: "prematurity," "neuroimaging," "brain" and "MRI" (full research strategy is available on-line). The search was limited to human research that involved original patient data and only articles written in English were included.

Studies were eligible under the following conditions: 1) they included preterm infants born at <32 weeks' gestation; 2) MRI was performed in the neonatal period, and 3) neurodevelopmental outcome was linked to MRI findings. To avoid large variations in MRI determinants, we only included structural MRI studies if they evaluated the findings according to a reproducible classification.

The initial search resulted in 2104 citations. Two reviewers (AP, JD) screened all abstracts of these citations for relevance and reached consensus after discussion in case of disagreement. Sixty-two articles were incorporated in this review. In the "Results" section, we present findings according to type of MRI technique: conventional structural MRI (such as T1- and T2-weighted scans), DTI, volumetric MRI and proton MR spectroscopy. Further classification was based on the timing of MRI: serial, before 35 weeks' or after 35 weeks' PMA.

Results

Conventional structural MRI

Serial MRI (Table 1)

Three serial neuroimaging studies correlated injury to outcome. One was a prospective consecutive MRI study by Dyet et al[8], regarding 327 MRI scans of 119 preterm infants. Only major destructive cerebral and cerebellar lesions seen at the initial scan within two days after birth were related to poorer neurodevelopmental outcome. DEHSI and post-hemorrhagic ventricular dilatation at term-equivalent age were significantly related to adverse outcome. Isolated hemorrhage or PWML did not seem to predict adverse neurodevelopmental outcome. The second, by Miller et al[39], demonstrated that moderately severe abnormalities, such as WM injury, ventriculomegaly and intraventricular hemorrhage on early scans were associated with adverse neurodevelopmental outcome as strongly (or even more strongly) as abnormalities on the term-equivalent scans: the relative risk was 5.6 and 5.3 respectively. The third, a large serial MRI study by Tam et al[40], demonstrated that not only large, but also small cerebellar hemorrhages, not detected on cranial ultrasonography, were associated with abnormal neurologic examination at 3-6 years of age. The presence of these small cerebellar hemorrhages was associated with a 5.0 odds ratio of abnormal neurologic examination at a mean age of 4.8 years.

MRI at ≤35 weeks' PMA (Table 2)

The presence of cystic PVL and cerebellar hemorrhage at 35 weeks' PMA was significantly correlated to abnormal neurologic examination at 30 months in a retrospective neuroimaging study by Cornette et al[41]. Isolated PWML was not correlated to abnormal neurodevelopmental outcome at the age of 30 months.

MRI at >35 weeks' PMA (Table 3)

Twenty-six studies correlated brain injury at conventional MRI at 35 weeks' PMA with outcome. The impact of overt WM lesions at term on neurodevelopment has been extensively investigated. Severity of WM abnormalities is often assessed according to a comprehensive scoring system[15] and is assumed to be directly associated with the incidence of neuromotor impairment until five years of age[9, 10, 15-17, 42-49] and inversely correlated to Bayley scales[50] up to 30 months[15, 16, 42, 51-54] and cognitive performance to nine years of age[55-60]. The presence of WM injury has an odds ratio of 8.3 for low full-scale intelligence quotient (IQ<70)[59]. Moderate to severe WM abnormalities highly predict severe motor delay; odds ratios up to 10.0 and positive predictive values up to 100% have been demonstrated[15, 42, 44, 45, 52, 59].

The association between subtle diffuse WM injury and neurodevelopmental outcome is not clear[61]. Some research groups demonstrated a significant association between PWML and impaired neurodevelopmental outcome[10, 46, 62], whereas others suggest the contrary, provided that no other major lesions were observed[8, 52]. DEHSI was associated with adverse outcome in a large serial imaging study by Dyet et al[8], but others could not confirm this finding[10, 42, 51, 59, 62, 63]. The lack of clarity is thought to be due to the absence of objective definitions for these patterns of brain injury[24, 48, 64] and raises the importance of objective assessment of diffuse WM injury.

Extensive intraventricular hemorrhage and venous infarctions according to Papile[65] are associated with neurodevelopmental impairment[16, 17, 48, 53]. Post-hemorrhagic ventricular dilatation is associated with neurological impairment to six years of age[66]. In a study by de Vries et al[67] asymmetrical myelination of the posterior limb of the internal capsule (PLIC) at term age in preterm infants with venous infarction seemed to be an early predictor of future hemiplegia.

Although commonly described in cranial ultrasonography studies[68], caudothalamic cysts were not related to cognitive and neuropsychological impairment in a MRI study by Lind et al[69].

The impact of gray matter abnormalities remains unclear. They were significantly associated with abnormal neurobehavioral outcome at term in a study by Brown et al[47] and with decreased Bayley scales at two years in a study by Woodward et al[15], but others[9, 59] found no significant relation between injury to the cerebral gray matter and neuromotor function at term[9] or cognitive outcome at nine years of age[59].

Table 1: Details of included serial MRI studies

MRI modality		Population	Timing of MRI (wk)	Main findings
Structural conventional	Dyet et al[8]	119 Infants <30 wks	Serial	Abnormal outcome[a] at 18 mos was related to major destructive lesions, DEHSI, cerebellar hemorrhage and post-hemorrhagic ventricular dilatation
	Miller et al[39]	89 Infants <34 wks	32 + 37	Abnormal outcome[b] at 18 mos was related to severity of WM injury, ventriculomegaly and intraventricular hemorrhage on first (RR, 5.6) and second (RR, 5.3) MRI
	Tam et al[40]	131 Infants <34 wks	32 + 37	Abnormal neurologic examination findings at 4.8 yrs were related to large and small cerebellar hemorrhage, OR for small hemorrhage was 5.0
DTI	Drobyshevsky et al[70]	24 Infants <32 wks	30 + 36	PDI [b] at 24 mos correlated to FA of the PLIC at 30 wks (r = 0.55), faster increase of FA/wk in internal capsule (r = -0.63) and occipital WM (r = -0.59)
	Glass et al[71]	Nine infants <34 wks	33 + 38	FA of the optic radiation was correlated with visual-evoked-potential amplitude (r = 0.7) at 10.5 mos
Volumetric	Dubois et al[72]	45 Infants <36 wks	32 + 41	Functional assessment at term was associated with inner cortical surface and sulcation index
	Kapellou et al[73] Rathbone et al[74]	119 Infants <30 wks	Serial	Growth of the cortical surface area was related to neurodevelopmental outcome[a] at 24 mos and full-scale IQ at six yrs

Note: mos indicates months; DEHSI, diffuse excessive high signal intensity; WM, white matter; RR, relative risk; yrs, years; OR, odds ratio; PDI, psychomotor development index; FA, fractional anisotropy, and PLIC, posterior limb of the internal capsule.

[a] Griffiths Mental Developmental Scales.

[b] Bayley Scales of Infant Development.

Diffusion tensor imaging

Serial MRI (Table 1)

Two serial DTI studies found a significant correlation with cognitive and neurosensory outcome. Drobyshevsky et al[70] demonstrated that Bayley's performance index at 24 months was correlated with FA of the PLIC at 30 weeks (r = 0.55) and faster increase of FA per week in the internal capsule (r = -0.63) and occipital WM (r = -0.59). Increased FA values in the optic radiation at 33 and 37 weeks were associated with increased visual-evoked-response amplitudes at 10.5 months (r = 0.7)[71]. However, this may not necessarily mean that eventually visual function is better.

MRI at ≤35 weeks' PMA

None of the included studies related early DTI measurements to long term outcome.

MRI at >35 weeks' PMA (Table 3)

In a tract-based spatial statistics study by van Kooij et al[75], FA values of the corpus callosum were correlated to cognitive scores. Gross motor scores were correlated to radial diffusion of the corpus callosum and internal and external capsules. Fine motor scores were correlated to FA throughout the WM. Other DTI studies have demonstrated similar correlations: DTI parameters of the corpus callosum, PLIC, right orbital frontal cortex and centrum semiovale were correlated to cognitive performance[76-79]. In other studies, DTI measurements of the corpus callosum, PLIC and corona radiata were correlated to motor function[77, 80-82]. Furthermore, FA values of the optic radiation were directly correlated to visual assessment scores at term-equivalent age[83].

Table 2: Details of included MRI studies, scanned at ≤35 week' postmenstrual age

MRI modality		Population	Timing of MRI (wk)	Main findings
Structural conventional	Cornette et al[41]	50 Infants <37 wks	35	Major cerebral abnormalities were correlated to abnormal outcome at 30 mos; isolated PWML were not related to neurodevelopmental impairment
Volumetric	Badr et al[84]	59 Infants <37 wks	31	WM volume was correlated significantly to PDI[a] (r = 0.29) and MDI[a] (r = 0.31) at 18 mos

Note: mos indicates months; PWML, punctate white matter lesions; WM, white matter; PDI, psychomotor development index, and MDI, mental development index.
[a] Bayley Scales of Infant Development.

Volumetric MRI

Serial MRI (Table 1)

Three serial volumetric MRI studies demonstrated that early structural abnormalities are predictors of neurobehavioral outcome. Dubois et al[72] concluded that at term-corrected age, neurobehavioral development was significantly associated with quantitative surrogates of cortical folding. Kapellou et al[73] found that the ratio between cortical surface area and cerebral volume was directly related to neurodevelopment at 24 months. The same group showed that growth of the cortical surface area was also significantly related to intelligence at six years: a faster growth of 0.032% per week resulted in an increase of one IQ point[74].

MRI at ≤35 weeks' PMA (Table 2)

Badr et al[84] found that WM volumes on MRI at a mean PMA of 31 weeks were significantly correlated to Bayley's psychomotor development index (PDI) ($r = 0.29$) and mental development index (MDI) ($r = 0.31$) at 18 months.

MRI at >35 weeks' PMA (Table 3)

Volumetric MRI studies in preterm infants with neurodevelopmental impairment have demonstrated significantly smaller total brain volume[54, 66, 85] and that of several cerebral structures or regions, including the cerebellum[66, 86-89], total WM[90], total[28, 91] and deep[66, 79] gray matter, occipital lobes[92], hippocampus[93, 94] and brainstem[95], as well as significantly larger ventricles [28, 96]. These findings were irrespective of the presence of overt brain injury. Simple linear metric assessment, such as biparietal and cerebellar diameter on MRI also significantly correlated with neurocognitive function[97, 98]. Impaired social-emotional development at five years was associated with decreased hippocampal volume in girls and decreased frontal lobe growth in boys[78].

Proton MR Spectroscopy

MRI at >35 weeks' PMA (Table 3)

^{1}H-MR spectroscopy is an accurate quantitative biomarker for the prediction of neurodevelopmental outcome after hypoxic-ischemic encephalopathy in term infants[99]. It is not clear whether this holds true for preterm infants. Cerebellar NAA/Cho ratio at term is suggested to correlate with cognitive outcome at 24 months[89]. However, Gadin et al found no correlation between MR spectroscopy of the periventricular WM and motor development at six months[91].

Table 3: Details of included MRI studies, scanned at >35 week' postmenstrual age

MRI modality		Population	Timing of MRI (wk)	Main findings
Structural conventional	Sie et al[52]	43 Infants <37 wks	36	Severe WM abnormalities had a PPV of 85-100% for PDI[a] <70 at 18 mos and 100% PPV for CP
	Skiold et al[42]	117 Infants <27 wks	38–41	Moderate/severe WM abnormalities were related to neurodevelopment[a] at 30 mos; PPV for the development of CP was 50%; patients with DEHSI had a normal outcome[a]
	Jeon et al[10]	126 Infants <32 wks	37	Cystic PVL and PWML were significantly related to CP; DEHSI was not related to adverse neurodevelopment[a] at 24 mos
	Iwata et al[59]	76 Infants <32 wks	38–42	WM injury predicted low full-scale IQ (OR, 8.3), CP (OR, 10.0) and requirements for special assistance at school (OR, 7.0) at nine yrs. DEHSI and gray matter abnormalities were not associated with impaired outcome
	Woodward et al[57]	110 Infants <32 wks	Term	Extent of WM abnormalities was significantly related to executive-function abilities at four yrs
	Spittle et al[45]	227 Infants <30 wks	38–42	Severity of WM abnormalities was related to proportion of severe motor impairment at five yrs; mild WM abnormalities had an OR of 5.6 for severe motor impairment
	Kidokoro et al[63]	160 Infants <30 wks	40	DEHSI was not related to neurodevelopmental outcome[a] at 24 mos
	Hart et al[51]	67 Infants <35 wks	37–44	Overt abnormalities were related to neurodevelopmental outcome[a] at 18 mos; DEHSI was not related to abnormal outcome
	de Bruine et al[62]	110 Infants <32 wks	40–44	PWML (OR, 18.38) and ventricular dilatation (OR, 4.57) predicted motor delay at 24 mos; PWML was also related to MDI[a] at 24 mos; DEHSI was not related to abnormal outcome
	Munck et al[53]	180 Infants <1500 g	Term	Major cerebral abnormalities were significantly correlated to decreased outcome[a] at 24 mos

MRI modality		Population	Timing of MRI (wk)	Main findings
Structural conventional	Hnatyszyn et al[43]	23 Infants <36 wks	38–40	Asphyxiated brain injury was correlated to the development of CP at 24 mos
	De Vries et al[67]	12 Infants <36 wks	40	Asymmetrical PLIC caused by venous infarction predicted future hemiplegia
	Lind et al[69]	Five infants <1500 g	Term	Caudothalamic cysts were not correlated to neurodevelopment[a] at 24 mos or IQ at five yrs
	Clark et al[58]	103 Infants <33 wks	40	Severity of brain injury (white > gray matter) was strongly related to working memory at six yrs
	Spittle et al[55]	188 Infants <30 wks	38–42	WM abnormalities were associated with lower social-emotional competence at 24 mos
	Spittle et al[44]	86 Infants <30 wks	38–44	WM abnormalities were associated with motor outcome at 12 mos
	Brown et al[47]	168 Infants <30 wks	38–42	WM and gray matter abnormalities were correlated strongly to neurobehavioral performance at term
	Spittle et al[9]	86 Infants <30 wks	38–44	Severity of WM abnormalities was related to abnormal general movement at one and three mos
	Reidy et al[60]	198 Infants <30 wks	Term	WM abnormalities predicted several language abilities at seven yrs
	Edgin et al[56]	100 Infants <33 wks	39–41	Mild and moderate/severe WM abnormalities were correlated to lower executive-functioning performance at two and four yrs
	Nanba et al[46]	289 Infants <34 wks	36–43	PWML in the corona radiata above the PLIC were correlated to gross motor functions at 3-5 yrs
	Iwata et al[61]	210 Infants <36 wks	Term	Subtle WM injury was significantly related to full-scale IQ at six yrs

MRI modality		Population	Timing of MRI (wk)	Main findings
DTI	van Kooij et al[75]	64 Infants <31 wks	40–45	At 24 mos, PDI[a] was correlated to FA in the CC; fine motor performance,[a] to FA in major WM tracts; and gross motor performance[a] to FA in PLIC and fornix
	Woodward et al[15]	167 Infants <30 wks	38–42	Increasing severity of WM abnormalities was associated with lower outcome[a] at 24 mos
	Mirmiran et al[16]	61 Infants <30 wks	36–40	PPV of brain lesions was 60% for the development of CP at 31 mos
	Valkama et al[17]	50 Infants <34 wks	39	Parenchymal lesions predicted CP at 18 mos, sensitivity, 82%; specificity, 97%
	Aida et al[48]	15 Infants <33 wks	35–45	Parenchymal lesions predicted CP at 12 mos
	van Kooij et al[77]	69 Infants <31 wks	40-45	At 24 mos, PDI[a] was correlated to volume and length of CC and right PLIC in girls; fine motor performance[a] was correlated to volume and FA of left PLIC in boys
	Kaukola et al[80]	30 Infants <32 wks	38–42	Higher ADC in the corona radiata was associated with poorer gross motor outcome[b] at 24 mos
	Rose et al[81]	78 Infants <32 wks	33–42	Neurodevelopmental outcome at 18 mos[a] was correlated to FA of the right PLIC
	Bassi et al[83]	37 Infants <33 wks	39–43	FA of the optic radiation was correlated with visual function at term-equivalent age
	Krishnan et al[76]	38 Infants <34 wks	38–44	Without focal brain injury, lower ADC in the WM was correlated to developmental outcome[b] at 24 mos
	Arzoumanian et al[82]	63 Infants <34 wks	34–42	FA in the PLIC was reduced in infants with abnormal neurologic examination at 24 mos
	Rogers et al[78]	111 Infants <30 wks	37–43	Higher ADC in the orbitofrontal cortex correlated to social-emotional problems at five yrs

MRI modality		Population	Timing of MRI (wk)	Main findings
Volumetric	Boardman et al[79]	80 Infants ≤34 wks	38–44	Decreased development[b] was associated with decreased reduction of WM and deep gray matter
	Jary et al[66]	25 Infants <30 wks	38–47	In infants with PHVD, total cerebral volume was correlated to MDI[a] and PDI[a] at 24 mos, thalamic and cerebellar volume were correlated to PDI[a]
	Nguyen et al[97]	182 Infants <30 wks	40	Biparietal diameter correlated to neurodevelopmental outcome[a] at 24 mos
	Maunu et al[96]	225 Infants <1500 g	Term	Ventricular dilatation and brain pathology was associated with CP and outcome[a] at 24 mos
	Lind et al[86]	164 Infants <1500 g	Term	PDI[a] and MDI[a] scores at 24 mos <70 associated with larger ventricles and lower volumes of cerebrum, cerebellum, frontal lobe, basal ganglia, thalamus
	Spittle et al[98]	83 Infants <30 wks	38–40	Reduced cerebellar diameter was correlated to abnormal general movements at three mos
	Lind et al[87]	97 Infants <1500 g	Term	Reduced cerebellar volume was associated with poorer executive function and motor skills at five yrs
	Thompson et al[93]	184 Infants <30 wks	38–42	Reduced hippocampal volume was related to neurodevelopmental outcome[a] at 24 mos
	Tan et al[85]	65 Infants <29 wks	40–43	Total brain volume was correlated to MDI[a] at nine mos
	Beauchamp et al[94]	156 Infants <30 wks	38–42	Reduced hippocampal volume was related to working memory deficits at 24 mos
	Shah et al[92]	68 Infants <33 wks	Term	Inferior occipital brain regions were correlated to impaired oculomotor function control at 24 mos
	Shah et al[88]	83 Infants <32 wks	38–43	Reduced cerebellar volume was associated with WM injury and outcome[a] at 24 mos

MRI modality		Population	Timing of MRI (wk)	Main findings
Volumetric	Woodward et al[54]	92 Infants <32 wks	39–41	After correcting for WM injury, total brain volume was correlated to object working memory at 24 mos
	Inder et al[28]	119 Infants <33 wks	39–41	Decreased cortical and deep gray matter volumes and increased CSF volumes were correlated to neurodevelopmental disability at 12 mos
	Peterson et al[90]	10 Infants <37 wks	35	Sensorimotor and midtemporal WM volumes were correlated strongly with outcome[a] at 20 mos
	Valkama et al[95]	51 Infants <34 wks	Term	Reduced brainstem volume was associated with neurosensory disability at 18 mos
^{1}H-MRS	Gadin et al[91]	38 Infants <30 wks	36	Decreased subcortical gray matter was associated with low PDI[a] at 6 mos; MRS measurements did not correlate with neurodevelopmental outcome[a]
	van Kooij et al[89]	112 Infants <31 wks	39–45	Cerebellar volume and cerebellar NAA/Cho ratio were positively correlated to MDI[a] at 24 mos

Note: WM indicates white matter, PPV, positive predictive value; PDI, psychomotor development index; mos, months; CP, cerebral palsy; DEHSI, diffuse excessive high signal intensity; PVL periventricular leukomalacia; PWML, punctate white matter lesions; OR, odds ratio; yrs, years; MDI, mental development index, PLIC, posterior limb of the internal capsule; CC, corpus callosum; ADC, apparent diffusion coefficient; PHVD, post-hemorrhagic ventricular dilatation; MRR magnetic resonance spectroscopy, and CSF, cerebrospinal fluid.

[a] Bayley Scales of Infant Development.

[b] Griffiths Mental Developmental Scales.

Discussion

This systematic review included eight serial MRI studies, two performed at ≤35 weeks, and fifty-two MRI studies performed at >35 weeks. The results of these studies made clear that the extent of structural abnormalities, microstructural deviations and global reductions in brain volumes, both at preterm and term-equivalent age, is directly related to the level of neuromotor and neurocognitive performance in childhood. Involvement of WM in preterm brain injury seems paramount. Accurate assessment of WM integrity, therefore, may help predict long term outcome in preterm infants and is one of the challenging goals in the field of neonatal neurology.

These studies do not provide clear evidence on the optimal timing of MRI. Although an increasing number of neuroimaging studies used early MRI to show that brain abnormalities are often present during early preterm life[22, 100, 101], only two of the studies linked these findings to outcome. Dyet et al[8] demonstrated that MRI within the first two days after birth was of limited additional value for predicting outcome. On the other hand, Miller et al[39] reported that early MRI findings at 32 weeks' of gestation were as reliable for predicting neurodevelopment as MRI at term age. This finding suggests that predictive MRI may be performed well before term-equivalent age, provided it is after the first week of life.

Neonatal care would benefit from identifying brain injury early in preterm life, in terms of effective and timely parental counseling, tailored rehabilitation strategies and better understanding of neuropathology. Currently, we have no efficacious therapy for preterm brain injury, but trials on possible neuroprotective agents, such as erythropoietin, melatonin, stem cell therapy and magnesium sulfate are being conducted or planned for the near future[102, 103]. Early MRI could provide early biomarkers that trials could target.

Image acquisition, processing and interpretation are not as straightforward as with conventional MRI, though sophisticated techniques such as DTI allow objective and quantifiable assessment of cerebral tissue. Because measurement accuracy depends on various aspects, including scanner type, hardware set-up, acquisition settings and clinical characteristics, reproducibility of the same measurements in different imaging centers is low. Furthermore, the availability of normal ADC and FA values of specific WM structures is limited. In addition, DTI is especially sensitive to image artifacts and corruption[104]. Reliable conclusions can therefore only be drawn if quality assessment before post processing provided satisfactory data quality. In the included studies, quality assessment was often not performed.

MRI is expensive, time consuming and requires great experience and dedication to ensure patient safety[37] as well as good quality data and interpretation[105]. These limitations should be especially taken into account with regard to the individual clinical care for patients with normal cranial sonographic findings. This technique can reliably predict some aspects of the outcome of preterm infants and also allows serial neuroimaging in a fast, convenient and less

expensive manner[106, 107]. Moreover, advanced applications, such as color Doppler imaging, also allow objective and quantitative brain assessment.

Several limitations of this systematic review need to be addressed. First, heterogeneity of the study populations was due to variation in age at MRI, acquisition settings, post processing methods for MRI evaluation, other technical aspects of MRI scanners, different ages at outcome measurement and different measures of outcome. Second, follow-up periods were relatively short. Third, because the search was restricted to articles in the English language, possible relevant studies might not have been included.

In conclusion, MRI remains an outstanding method to predict long term neurodevelopmental outcome and cerebral MRI should be part of standard clinical care for preterm infants. Early MRI allows timely parental counseling, targeting of rehabilitation strategies and availability of early biomarkers. However, the individual prognostic information provided by early scanning remains inferior to that provided by term scanning. As long as the correlation of brain injury from early MRI with outcome is not clear, we would argue that standard MRI should preferably be performed at term-equivalent age. On the other hand, early MRI yields important information about the pathogenesis of preterm brain injury and therefore is indispensable in research on preterm brain injury.

References

1. Saigal S, Doyle LW. An overview of mortality and sequelae of preterm birth from infancy to adulthood. *Lancet* 2008;371:261-9.
2. Bhutta AT, Cleves MA, Casey PH, Cradock MM, Anand KJ. Cognitive and behavioral outcomes of school-aged children who were born preterm: a meta-analysis. *JAMA* 2002;288:728-37.
3. Larroque B, Ancel PY, Marret S, Marchand L, Andre M, Arnaud C, Pierrat V, Roze JC, Messer J, Thiriez G, Burguet A, Picaud JC, Breart G, Kaminski M. Neurodevelopmental disabilities and special care of 5-year-old children born before 33 weeks of gestation (the EPIPAGE study): a longitudinal cohort study. *Lancet* 2008;371:813-20.
4. Marlow N, Wolke D, Bracewell MA, Samara M. Neurologic and developmental disability at six years of age after extremely preterm birth. *N Engl J Med* 2005;352:9-19.
5. Williams J, Lee KJ, Anderson PJ. Prevalence of motor-skill impairment in preterm children who do not develop cerebral palsy: a systematic review. *Dev Med Child Neurol* 2010;52:232-7.
6. Rutherford MA, Supramaniam V, Ederies A, Chew A, Bassi L, Groppo M, Anjari M, Counsell S, Ramenghi LA. Magnetic resonance imaging of white matter diseases of prematurity. *Neuroradiology* 2010;52:505-21.
7. Inder TE, Wells SJ, Mogridge NB, Spencer C, Volpe JJ. Defining the nature of the cerebral abnormalities in the premature infant: a qualitative magnetic resonance imaging study. *J Pediatr* 2003;143:171-9.
8. Dyet LE, Kennea N, Counsell SJ, Maalouf EF, Ajayi-Obe M, Duggan PJ, Harrison M, Allsop JM, Hajnal J, Herlihy AH, Edwards B, Laroche S, Cowan FM, Rutherford MA, Edwards AD. Natural history of brain lesions in extremely preterm infants studied with serial magnetic resonance imaging from birth and neurodevelopmental assessment. *Pediatrics* 2006;118:536-48.
9. Spittle AJ, Brown NC, Doyle LW, Boyd RN, Hunt RW, Bear M, Inder TE. Quality of general movements is related to white matter pathology in very preterm infants. *Pediatrics* 2008;121:e1184-e9.
10. Jeon TY, Kim JH, Yoo S-Y, Eo H, Kwon J-Y, Lee J, Lee M, Chang YS, Park WS. Neurodevelopmental outcomes in preterm infants: comparison of infants with and without diffuse excessive high signal intensity on MR images at near-term-equivalent age. *Radiology* 2012;263:518-26.
11. Volpe JJ. Brain injury in premature infants: a complex amalgam of destructive and developmental disturbances. *Lancet Neurol* 2009;8:110-24.
12. Khwaja O, Volpe JJ. Pathogenesis of cerebral white matter injury of prematurity. *Arch Dis Child Fetal Neonatal Ed* 2008;93:F153-61.
13. Huppi PS, Murphy B, Maier SE, Zientara GP, Inder TE, Barnes PD, Kikinis R, Jolesz FA, Volpe JJ. Microstructural brain development after perinatal cerebral white matter injury assessed by diffusion tensor magnetic resonance imaging. *Pediatrics* 2001;107:455-60.
14. Inder TE, Anderson NJ, Spencer C, Wells S, Volpe JJ. White matter injury in the premature infant: a comparison between serial cranial sonographic and MR findings at term. *Am J Neuroradiol* 2003;24:805-9.
15. Woodward LJ, Anderson PJ, Austin NC, Howard K, Inder TE. Neonatal MRI to predict neurodevelopmental outcomes in preterm infants. *New Engl J Med* 2006;355:685-94.
16. Mirmiran M, Barnes PD, Keller K, Constantinou JC, Fleisher BE, Hintz SR, Ariagno RL. Neonatal brain magnetic resonance imaging before discharge is better than serial cranial ultrasound in predicting cerebral palsy in very low birth weight preterm infants. *Pediatrics* 2004;114:992-8.

17. Valkama AM, Paakko ELE, Vainionpaa LK, Lanning FP, Ilkko EA, Koivisto ME. Magnetic resonance imaging at term and neuromotor outcome in preterm infants. *Acta Paediatr Int J Paediatr* 2000;89:348-55.
18. Ment LR, Hirtz D, Huppi PS. Imaging biomarkers of outcome in the developing preterm brain. *Lancet Neurol* 2009;8:1042-55.
19. Counsell SJ, Rutherford MA, Cowan FM, Edwards AD. Magnetic resonance imaging of preterm brain injury. *Arch Dis Child Fetal Neonatal Ed* 2003;88:F269-74.
20. Huppi PS, Dubois J. Diffusion tensor imaging of brain development. *Semin Fetal Neonatal Med* 2006;11:489-97.
21. Jones DK. Studying connections in the living human brain with diffusion MRI. *Cortex* 2008;44:936-52.
22. Dudink J, Lequin M, van Pul C, Buijs J, Conneman N, van Goudoever J, Govaert P. Fractional anisotropy in white matter tracts of very-low-birth-weight infants. *Pediatr Radiol* 2007;37:1216-23.
23. Miller SP, Vigneron DB, Henry RG, Bohland MA, Ceppi-Cozzio C, Hoffman C, Newton N, Partridge JC, Ferriero DM, Barkovich AJ. Serial quantitative diffusion tensor MRI of the premature brain: development in newborns with and without injury. *J Magn Reson Imaging* 2002;16:621-32.
24. Counsell SJ, Allsop JM, Harrison MC, Larkman DJ, Kennea NL, Kapellou O, Cowan FM, Hajnal JV, Edwards AD, Rutherford MA. Diffusion-weighted imaging of the brain in preterm infants with focal and diffuse white matter abnormality. *Pediatrics* 2003;112:1-7.
25. Counsell SJ, Shen Y, Boardman JP, Larkman DJ, Kapellou O, Ward P, Allsop JM, Cowan FM, Hajnal JV, Edwards AD, Rutherford MA. Axial and radial diffusivity in preterm infants who have diffuse white matter changes on magnetic resonance imaging at term-equivalent age. *Pediatrics* 2006;117:376-86.
26. Inder TE, Huppi PS, Warfield S, Kikinis R, Zientara GP, Barnes PD, Jolesz F, Volpe JJ. Periventricular white matter injury in the premature infant is followed by reduced cerebral cortical gray matter volume at term. *Ann Neurol* 1999;46:755-60.
27. Thompson DK, Warfield SK, Carlin JB, Pavlovic M, Wang HX, Bear M, Kean MJ, Doyle LW, Egan GF, Inder TE. Perinatal risk factors altering regional brain structure in the preterm infant. *Brain* 2007;130:667-77.
28. Inder TE, Warfield SK, Wang H, Huppi PS, Volpe JJ. Abnormal cerebral structure is present at term in premature infants. *Pediatrics* 2005;115:286-94.
29. Keunen K, Kersbergen KJ, Groenendaal F, Isgum I, de Vries LS, Benders MJ. Brain tissue volumes in preterm infants: prematurity, perinatal risk factors and neurodevelopmental outcome: a systematic review. *J Matern Fetal Neonatal Med* 2012;25 Suppl 1:89-100.
30. Mathur A, Inder T. Magnetic resonance imaging--insights into brain injury and outcomes in premature infants. *J Commun Disord* 2009;42:248-55.
31. Dubois J, Benders M, Cachia A, Lazeyras F, Ha-Vinh Leuchter R, Sizonenko SV, Borradori-Tolsa C, Mangin JF, Huppi PS. Mapping the early cortical folding process in the preterm newborn brain. *Cereb Cortex* 2008;18:1444-54.
32. Dubois J, Benders M, Lazeyras F, Borradori-Tolsa C, Leuchter RH, Mangin JF, Huppi PS. Structural asymmetries of perisylvian regions in the preterm newborn. *Neuroimage* 2010;52:32-42.
33. Dubois J, Hertz-Pannier L, Cachia A, Mangin JF, Le Bihan D, Dehaene-Lambertz G. Structural asymmetries in the infant language and sensori-motor networks. *Cereb Cortex* 2009;19:414-23.
34. Ajayi-Obe M, Saeed N, Cowan FM, Rutherford MA, Edwards AD. Reduced development of cerebral cortex in extremely preterm infants. *Lancet* 2000;356:1162-3.

35. Huppi PS, Schuknecht B, Boesch C, Bossi E, Felblinger J, Fusch C, Herschkowitz N. Structural and neurobehavioral delay in postnatal brain development of preterm infants. *Pediatr Res* 1996;39:895-901.
36. Huppi PS, Lazeyras F. Proton magnetic resonance spectroscopy ((1)H-MRS) in neonatal brain injury. *Pediatr Res* 2001;49:317-20.
37. Plaisier A, Raets MMA, van der Starre C, Feijen-Roon M, Govaert P, Lequin MH, Heemskerk AM, Dudink J. Safety of routine early MRI in preterm infants. *Pediatric Radiology* 2012;42:1205-11.
38. Hillenbrand CM, Reykowski A. MR Imaging of the Newborn: a technical perspective. *Magn Reson Imaging Clin N Am* 2012;20:63-79.
39. Miller SP, Ferriero DM, Leonard C, Piecuch R, Glidden DV, Partridge JC, Perez M, Mukherjee P, Vigneron DB, Barkovich AJ. Early brain injury in premature newborns detected with magnetic resonance imaging is associated with adverse early neurodevelopmental outcome. *J Pediatr* 2005;147:609-16.
40. Tam EWY, Rosenbluth G, Rogers EE, Ferriero DM, Glidden D, Goldstein RB, Glass HC, Piecuch RE, Barkovich AJ. Cerebellar hemorrhage on magnetic resonance imaging in preterm newborns associated with abnormal neurologic outcome. *J Pediatr* 2011;158:245-50.
41. Cornette LG, Tanner SF, Ramenghi LA, Miall LS, Childs AM, Arthur RJ, Martinez D, Levene MI. Magnetic resonance imaging of the infant brain: Anatomical characteristics and clinical significance of punctate lesions. *Arch Dis Child Fetal Neonatal Ed* 2002;86:F171-F7.
42. Skiold B, Vollmer B, Bohm B, Hallberg B, Horsch S, Mosskin M, Lagercrantz H, Den U, Blennow M. Neonatal magnetic resonance imaging and outcome at age 30 months in extremely preterm infants. *J Pediatr* 2012;160:559-66.e1.
43. Hnatyszyn G, Cyrylowski L, Czeszynska MB, Walecka A, Konefal H, Szmigiel O, Gizewska M, Dawid G. The role of magnetic resonance imaging in early prediction of cerebral palsy. *Turk J Pediatr* 2010;52:278-84.
44. Spittle AJ, Boyd RN, Inder TE, Doyle LW. Predicting motor development in very preterm infants at 12 months' corrected age: The role of qualitative magnetic resonance imaging and general movements assessments. *Pediatrics* 2009;123:512-7.
45. Spittle AJ, Cheong J, Doyle LW, Roberts G, Lee KJ, Lim J, Hunt RW, Inder TE, Anderson PJ. Neonatal white matter abnormality predicts childhood motor impairment in very preterm children. *Dev Med Child Neurol* 2011;53:1000-6.
46. Nanba Y, Matsui K, Aida N, Sato Y, Toyoshima K, Kawataki M, Hoshino R, Ohyama M, Itani Y, Goto A, Oka A. Magnetic resonance imaging regional T1 abnormalities at term accurately predict motor outcome in preterm infants. *Pediatrics* 2007;120:e10-e9.
47. Brown NC, Inder TE, Bear MJ, Hunt RW, Anderson PJ, Doyle LW. Neurobehavior at Term and White and Gray Matter Abnormalities in Very Preterm Infants. *J Pediatr* 2009;155:32-8.e1.
48. Aida N, Nishimura G, Hachiya Y, Matsui K, Takeuchi M, Itani Y. MR imaging of perinatal brain damage: Comparison of clinical outcome with initial and follow-up MR findings. *Am J Neuroradiol* 1998;19:1909-21.
49. Van Wezel-Meijler G, Van Der Knaap MS, Oosting J, Sie LTL, De Groot L, Huisman J, Valk J, Lafeber HN. Predictive value of neonatal MRI as compared to ultrasound in premature infants with mild periventricular white matter changes. *Neuropediatrics* 1999;30:231-8.
50. Bayley N. Bayley Scales of Infant and Toddler Development, Third edition. San Antonio, USA: Harcourt Assessment. 2006.

51. Hart A, Whitby E, Wilkinson S, Alladi S, Paley M, Smith M. Neuro-developmental outcome at 18 months in premature infants with diffuse excessive high signal intensity on MR imaging of the brain. *Pediatr Radiol* 2011;41:1284-92.
52. Sie LTL, Hart AAM, van Hof J, de Groot L, Lems W, Lafeber HN, Valk J, van der Knaap MS. Predictive value of neonatal MRI with respect to late MRI findings and clinical outcome. A study in infants with periventricular densities on neonatal ultrasound. *Neuropediatrics* 2005;36:78-89.
53. Munck P, Haataja L, Maunu J, Parkkola R, Rikalainen H, Lapinleimu H, Lehtonen L. Cognitive outcome at 2 years of age in Finnish infants with very low birth weight born between 2001 and 2006. *Acta Paediatr Int J Paediatr* 2010;99:359-66.
54. Woodward LJ, Edgin JO, Thompson D, Inder TE. Object working memory deficits predicted by early brain injury and development in the preterm infant. *Brain* 2005;128:2578-87.
55. Spittle AJ, Treyvaud K, Doyle LW, Roberts G, Lee KJ, Inder TE, Cheong JLY, Hunt RW, Newnham CA, Anderson PJ. Early Emergence of Behavior and Social-Emotional Problems in Very Preterm Infants. *J Am Acad Child Adolesc Psychiatry* 2009;48:909-18.
56. Edgin JO, Inder TE, Anderson PJ, Hood KM, Clark CAC, Woodward LJ. Executive functioning in preschool children born very preterm: Relationship with early white matter pathology. *J Int Neuropsychol Soc* 2008;14:90-101.
57. Woodward LJ, Clark CAC, Pritchard VE, Anderson PJ, Inder TE. Neonatal white matter abnormalities predict global executive function impairment in children born very preterm. *Dev Neuropsychol* 2011;36:22-41.
58. Clark CAC, Woodward LJ. Neonatal cerebral abnormalities and later verbal and visuospatial working memory abilities of children born very preterm. *Dev Neuropsychol* 2010;35:622-42.
59. Iwata S, Nakamura T, Hizume E, Kihara H, Takashima S, Matsuishi T, Iwata O. Qualitative brain MRI at term and cognitive outcomes at 9 years after very preterm birth. *Pediatrics* 2012;129:e1138-e47.
60. Reidy N, Morgan A, Thompson DK, Inder TE, Doyle LW, Anderson PJ. Impaired Language Abilities and White Matter Abnormalities in Children Born Very Preterm and/or Very Low Birth Weight. *J Pediatr* 2013;162:719-24.
61. Iwata S, Iwata O, Bainbridge A, Nakamura T, Kihara H, Hizume E, Sugiura M, Tamura M, Matsuishi T. Abnormal white matter appearance on term FLAIR predicts neuro-developmental outcome at 6 years old following preterm birth. *Int J Dev Neurosci* 2007;25:523-30.
62. De Bruine FT, Van Den Berg-Huysmans AA, Leijser LM, Rijken M, Steggerda SJ, Van Grond JD, Van Wezel-Meijler G. Clinical implications of MR imaging findings in the white matter in very preterm infants: A 2-year follow-up study. *Radiology* 2011;261:899-906.
63. Kidokoro H, Anderson PJ, Doyle LW, Neil JJ, Inder TE. High signal intensity on T2-weighted MR imaging at term-equivalent age in preterm infants does not predict 2-year neurodevelopmental outcomes. *Am J Neuroradiol* 2011;32:2005-10.
64. Hagmann CF, De Vita E, Bainbridge A, Gunny R, Kapetanakis AB, Chong WK, Cady EB, Gadian DG, Robertson NJ. T2 at MR imaging is an objective quantitative measure of cerebral white matter signal intensity abnormality in preterm infants at term-equivalent age. *Radiology* 2009;252:209-17.
65. Papile LA, Burstein J, Burstein R, Koffler H. Incidence and evolution of subependymal and intraventricular hemorrhage: a study of infants with birth weights less than 1,500 gm. *J Pediatr* 1978;92:529-34.
66. Jary S, De Carli A, Ramenghi LA, Whitelaw A. Impaired brain growth and neurodevelopment in preterm infants with posthaemorrhagic ventricular dilatation. *Acta Paediatrica* 2012;101:743-8.

67. De Vries LS, Groenendaal F, van Haastert IC, Eken P, Rademaker KJ, Meiners LC. Asymmetrical myelination of the posterior limb of the internal capsule in infants with periventricular haemorrhagic infarction: an early predictor of hemiplegia. *Neuropediatrics* 1999;30:314-9.
68. Horsch S, Kutz P, Roll C. Late germinal matrix hemorrhage-like lesions in very preterm infants. *J Child Neurol* 2010;25:809-14.
69. Lind A, Lapinleimu H, Korkman M, Lehtonen L, Parkkola R, Haataja L. Five-year follow-up of prematurely born children with postnatally developing caudothalamic cysts. *Acta Paediatr Int J Paediatr* 2010;99:304-7.
70. Drobyshevsky A, Bregman J, Storey P, Meyer J, Prasad PV, Derrick M, MacKendrick W, Tan S. Serial diffusion tensor imaging detects white matter changes that correlate with motor outcome in premature infants. *Dev Neurosci* 2007;29:289-301.
71. Glass HC, Berman JI, Norcia AM, Rogers EE, Henry RG, Hou C, Barkovich AJ, Good WV. Quantitative fiber tracking of the optic radiation is correlated with visual-evoked potential amplitude in preterm infants. *Am J Neuroradiol* 2010;31:1424-9.
72. Dubois J, Benders M, Borradori-Tolsa C, Cachia A, Lazeyras F, Ha-Vinh Leuchter R, Sizonenko SV, Warfield SK, Mangin JF, Huppi PS. Primary cortical folding in the human newborn: An early marker of later functional development. *Brain* 2008;131:2028-41.
73. Kapellou O, Counsell SJ, Kennea N, Dyet L, Saeed N, Stark J, Maalouf E, Duggan P, Ajayi-Obe M, Hajnal J, Allsop JM, Boardman J, Rutherford MA, Cowan F, Edwards AD. Abnormal cortical development after premature birth shown by altered allometric scaling of brain growth. *PLoS Med* 2006;3:1382-90.
74. Rathbone R, Counsell SJ, Kapellou O, Dyet L, Kennea N, Hajnal J, Allsop JM, Cowan F, Edwards AD. Perinatal cortical growth and childhood neurocognitive abilities. *Neurology* 2011;77:1510-5.
75. Van Kooij BJM, De Vries LS, Ball G, Van Haastert IC, Benders MJNL, Groenendaal F, Counsell SJ. Neonatal tract-based spatial statistics findings and outcome in preterm infants. *Am J Neuroradiol* 2012;33:188-94.
76. Krishnan ML, Dyet LE, Boardman JP, Kapellou O, Allsop JM, Cowan F, Edwards AD, Rutherford MA, Counsell SJ. Relationship between white matter apparent diffusion coefficients in preterm infants at term-equivalent age and developmental outcome at 2 years. *Pediatrics* 2007;120:e604-e9.
77. Van Kooij BJM, Van Pul C, Benders MJNL, Van Haastert IC, De Vries LS, Groenendaal F. Fiber tracking at term displays gender differences regarding cognitive and motor outcome at 2 years of age in preterm infants. *Pediatr Res* 2011;70:626-32.
78. Rogers CE, Anderson PJ, Thompson DK, Kidokoro H, Wallendorf M, Treyvaud K, Roberts G, Doyle LW, Neil JJ, Inder TE. Regional cerebral development at term relates to school-age social-emotional development in very preterm children. *J Am Acad Child Adolesc Psychiatry* 2012;51:181-91.
79. Boardman JP, Craven C, Valappil S, Counsell SJ, Dyet LE, Rueckert D, Aljabar P, Rutherford MA, Chew AT, Allsop JM, Cowan F, Edwards AD. A common neonatal image phenotype predicts adverse neurodevelopmental outcome in children born preterm. *Neuroimage* 2010;52:409-14.
80. Kaukola T, Perhomaa M, Vainionpaa L, Tolonen U, Jauhiainen J, Paakko E, Hallman M. Apparent diffusion coefficient on magnetic resonance imaging in pons and in corona radiata and relation with the neurophysiologic measurement and the outcome in very preterm infants. *Neonatology* 2010;97:15-21.
81. Rose J, Butler EE, Lamont LE, Barnes PD, Atlas SW, Stevenson DK. Neonatal brain structure on MRI and diffusion tensor imaging, sex, and neurodevelopment in very-low-birthweight preterm children. *Dev Med Child Neurol* 2009;51:526-35.

82. Arzoumanian Y, Mirmiran M, Barnes PD, Woolley K, Ariagno RL, Moseley ME, Fleisher BE, Atlas SW. Diffusion tensor brain imaging findings at term-equivalent age may predict neurologic abnormalities in low birth weight preterm infants. *Am J Neuroradiol* 2003;24:1646-53.
83. Bassi L, Ricci D, Volzone A, Allsop JM, Srinivasan L, Pai A, Ribes C, Ramenghi LA, Mercuri E, Mosca F, Edwards AD, Cowan FM, Rutherford MA, Counsell SJ. Probabilistic diffusion tractography of the optic radiations and visual function in preterm infants at term equivalent age. *Brain* 2008;131:573-82.
84. Badr LK, Bookheimer S, Purdy I, Deeb M. Predictors of neurodevelopmental outcome for preterm infants with brain injury: MRI, medical and environmental factors. *Early Hum Dev* 2009;85:279-84.
85. Tan M, Abernethy L, Cooke R. Improving head growth in preterm infants - A randomised controlled trial II: MRI and developmental outcomes in the first year. *Arch Dis Child Fetal Neonatal Ed* 2008;93:f342-f6.
86. Lind A, Parkkola R, Lehtonen L, Munck P, Maunu J, Lapinleimu H, Haataja L. Associations between regional brain volumes at term-equivalent age and development at 2 years of age in preterm children. *Pediatr Radiol* 2011;41:953-61.
87. Lind A, Haataja L, Rautava L, Valiaho A, Lehtonen L, Lapinleimu H, Parkkola R, Korkman M. Relations between brain volumes, neuropsychological assessment and parental questionnaire in prematurely born children. *Eur Child Adolesc Psychiatry* 2010;19:407-17.
88. Shah DK, Anderson PJ, Carlin JB, Pavlovic M, Howard K, Thompson DK, Warfield SK, Inder TE. Reduction in cerebellar volumes in preterm infants: Relationship to white matter injury and neurodevelopment at two years of age. *Pediatr Res* 2006;60:97-102.
89. Van Kooij BJM, Benders MJNL, Anbeek P, Van Haastert IC, De Vries LS, Groenendaal F. Cerebellar volume and proton magnetic resonance spectroscopy at term, and neurodevelopment at 2years of age in preterm infants. *Dev Med Child Neurol* 2012;54:260-6.
90. Peterson BS, Anderson AW, Ehrenkranz R, Staib LH, Tageldin M, Colson E, Gore JC, Duncan CC, Makuch R, Ment LR. Regional brain volumes and their later neurodevelopmental correlates in term and preterm infants. *Pediatrics* 2003;111:939-48.
91. Gadin E, Lobo M, Paul DA, Sem K, Steiner KV, Mackley A, Anzilotti K, Galloway C. Volumetric MRI and MRS and early motor development of infants born preterm. *Pediatr Phys Ther* 2012;24:38-44.
92. Shah DK, Guinane C, August P, Austin NC, Woodward LJ, Thompson DK, Warfield SK, Clemett R, Inder TE. Reduced occipital regional volumes at term predict impaired visual function in early childhood in very low birth weight infants. *Invest Ophthalmol Vis Sci* 2006;47:3366-73.
93. Thompson DK, Wood SJ, Doyle LW, Warfield SK, Lodygensky GA, Anderson PJ, Egan GF, Inder TE. Neonate hippocampal volumes: Prematurity, perinatal predictors, and 2-year outcome. *Ann Neurol* 2008;63:642-51.
94. Beauchamp MH, Thompson DK, Howard K, Doyle LW, Egan GF, Inder TE, Anderson PJ. Preterm infant hippocampal volumes correlate with later working memory deficits. *Brain* 2008;131:2986-94.
95. Valkama AM, Tolonen EU, Kerttula LI, Paakko ELE, Vainionpaa LK, Koivisto ME. Brainstem size and function at term age in relation to later neurosensory disability in high-risk, preterm infants. *Acta Paediatr Int J Paediatr* 2001;90:909-15.
96. Maunu J, Lehtonen L, Lapinleimu H, Matomaki J, Munck P, Rikalainen H, Parkkola R, Haataja L. Ventricular dilatation in relation to outcome at 2 years of age in very preterm infants: A prospective Finnish cohort study. *Dev Med Child Neurol* 2011;53:48-54.
97. Nguyen The Tich S, Anderson PJ, Hunt RW, Lee KJ, Doyle LW, Inder TE. Neurodevelopmental and perinatal correlates of simple brain metrics in very preterm infants. *Arch Pediatr Adolesc Med* 2011;165:216-22.

98. Spittle AJ, Doyle LW, Anderson PJ, Inder TE, Lee KJ, Boyd RN, Cheong JLY. Reduced cerebellar diameter in very preterm infants with abnormal general movements. *Early Hum Dev* 2010;86:1-5.
99. Thayyil S, Chandrasekaran M, Taylor A, Bainbridge A, Cady EB, Chong WK, Murad S, Omar RZ, Robertson NJ. Cerebral magnetic resonance biomarkers in neonatal encephalopathy: a meta-analysis. *Pediatrics* 2010;125:e382-95.
100. Nossin-Manor R, Chung AD, Whyte HEA, Shroff MM, Taylor MJ, Sled JG. Deep gray matter maturation in very preterm neonates: regional variations and pathology-related age-dependent changes in magnetization transfer ratio. *Radiology* 2012;263:510-7.
101. Smyser CD, Inder TE, Shimony JS, Hill JE, Degnan AJ, Snyder AZ, Neil JJ. Longitudinal analysis of neural network development in preterm infants. *Cereb Cortex* 2010;20:2852-62.
102. Doyle LW. Antenatal magnesium sulfate and neuroprotection. *Curr Opin Pediatr* 2012;24:154-9.
103. Rees S, Harding R, Walker D. The biological basis of injury and neuroprotection in the fetal and neonatal brain. *Int J Dev Neurosci* 2011;29:551-63.
104. Jones DK, Cercignani M. Twenty-five pitfalls in the analysis of diffusion MRI data. *NMR Biomed* 2010;23:803-20.
105. Pannek K, Guzzetta A, Colditz PB, Rose SE. Diffusion MRI of the neonate brain: acquisition, processing and analysis techniques. *Pediatric Radiology* 2012;42:1169-82.
106. De Vries LS, Van Haastert IL, Rademaker KJ, Koopman C, Groenendaal F. Ultrasound abnormalities preceding cerebral palsy in high-risk preterm infants. *J Pediatr* 2004;144:815-20.
107. Horsch S, Skiold B, Hallberg B, Nordell B, Nordell A, Mosskin M, Lagercrantz H, Aden U, Blennow M. Cranial ultrasound and MRI at term age in extremely preterm infants. *Arch Dis Child Fetal Neonatal Ed* 2010;95:F310-4.

CHAPTER 3

Safety of Routine Early MRI in Preterm Infants

A. Plaisier
M.M.A. Raets
C. van der Starre
M. Feijen - Roon
P. Govaert
M.H. Lequin
A.M. Heemskerk
J. Dudink

Pediatric Radiology, 2012; 42:1205-11

Abstract

Background

Routine cerebral magnetic resonance imaging (MRI) at 30 weeks postmenstrual age (PMA) is increasingly performed as part of standard clinical care in preterm infants. We evaluated safety of these early MRI procedures.

Methods

We retrospectively collected data on patient safety of preterm infants who underwent early MRI scans. Data was collected at fixed times before and after the MRI scan. MRI procedures were carried out according to a comprehensive guideline.

Results

A total of 52 infants underwent a MRI scan at 30 weeks PMA. Although no serious adverse events occurred and vital parameters remained stable during the procedure, minor adverse events were encountered in 26 infants (50%). The MRI was terminated in three infants (5.8%) because of respiratory instability. Increased respiratory support within 24 hours after the MRI was necessary for 12 infants (23.1%) and was significantly associated with gestational age, birth weight and the mode of respiratory support. Hypothermia (core temperature below 36˚C) occurred in nine infants (17.3%). Temperature dropped significantly after the MRI scan.

Conclusion

Minor adverse events after MRI procedures at 30 weeks PMA were common and should not be underestimated. A dedicated and comprehensive guideline for MRI procedures in preterm infants is essential.

Introduction

In preterm infants, early recognition of neonatal brain injury and assessment of risks of later impairment is a challenging goal of current neuroimaging studies[1-3]. Magnetic resonance imaging (MRI) provides clinicians and researchers objective, high-quality, in vivo information about brain anatomy, pathology and, due to recent advances, functional and physiological characteristics[4-10]. Early cerebral MRI scans at 30 weeks' postmenstrual age (PMA) and at term-equivalent age are increasingly being incorporated into standard care for very low birth weight (VLBW) infants (birth weight <1,500 grams). This provides early biomarkers for studying preterm brain injury related to neurodevelopmental outcome. These early determinants may contribute to the design of pharmacological and behavioral interventions to improve future outcome[6, 7, 11, 12].

MRI is considered a safe imaging technique. No evidence exists of serious harm to human tissue, besides loud acoustic noise, tissue heating and peripheral nerve stimulation[13-16]. Performing early MRI scans in VLBW infants is challenging, as they frequently require respiratory support and are vulnerable to hemodynamic instability. Consequently, early MRI scans of VLBW infants should be performed in a safe and controlled environment with the use of a dedicated protocol. Studies on the methods that promote patient safety and healthcare quality are ongoing. Previous studies regarding safety of MRI in VLBW infants suggest that MRI procedures are safe[17-19]. However, population-size and maturity-range varied widely in these studies. Furthermore, in some works, only adverse events during the scan were assessed[17, 18].

Our aim was to study the safety of routine MRI scans in preterm infants at a PMA of 30 weeks. To accomplish this, we collected data of these infants regarding safety incidents and (avoidable) adverse events over a long time-period: 24 hours before and 24 hours following the MRI scan.

Methods

Dedicated guideline

A tailored, center-specific guideline for MRI procedures in VLBW infants was developed in collaboration with representatives from the Radiology and Neonatology departments as well as a patient safety officer from the Erasmus Medical Center – Sophia's Children Hospital. The guideline was based on MR safety literature and our own experiences and was adjusted using the principles of the 'plan-do-study-act' quality improvement[20], an iterative process to improve outcomes (Fig 1). A description of this tailored guideline for MRI procedures in preterm infants is given in the attachment.

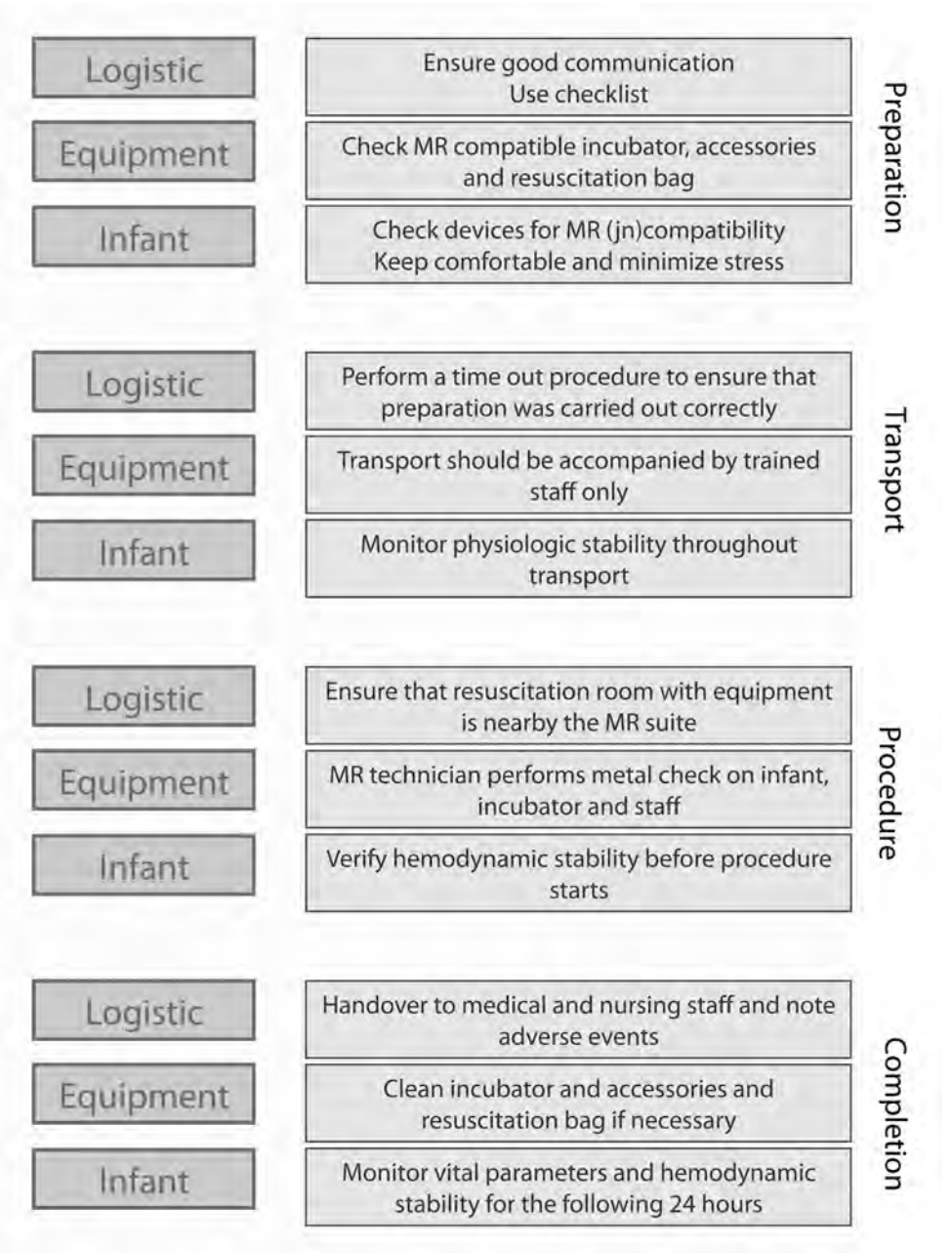

Figure 1 – Guideline for safe execution of MRI procedures in preterm infants.

Subjects

As part of standard clinical care practices, MRI scans were performed on VLBW infants that were born at a gestational age (GA) <29 weeks. These scans were performed at PMA of 30 weeks (29 4/7 – 30 4/7 weeks). In all patients, the MRI procedure was carried out according to our multi-disciplinary guideline (see attachment). The medical team (attending neonatologist and nursing staff) decided whether the infants were medically stable enough to undergo an MRI scan. The following criteria to define hemodynamic and respiratory instability were: high frequency oscillation ventilation, doxapram dependency, inotropic support and sepsis work-up within 12 hours before the MRI scan.

Data regarding patient safety, such as vital parameters, mode of respiratory support, number of episodes of bradycardia, apnea or oxygen desaturation and (avoidable) adverse events, were retrospectively collected from our electronic patient data management system. These data were sampled at fixed times: 24, 16 and 8 hours before the MRI scan, during the MRI procedure itself and 8, 16 and 24 hours after the MRI scan. The definitions of major and minor adverse events are listed in Table 1. Increased hemodynamic instability was defined as an increase of >5 episodes of bradycardia (heart rate <100/min), apnea (>20 seconds) or oxygen desaturation (saturation <85%) within the first 24 hours after the MRI, compared with the 24 hours before the scan. Increased respiratory support within 24 hours after the MRI was defined as increased inspiratory pressure, increased positive end expiratory pressure or increased frequency of ventilation. Hypothermia was defined as core temperature below 36˚C.

The study was approved by the medical ethical committee of the Erasmus Medical Centre Rotterdam, the Netherlands.

Table 1: Definitions of adverse events

Major adverse events	Respiratory compromise resulting in intubation
	Circulatory compromise resulting in need for inotropic agents
	Cardiac resuscitation
	Death
Minor adverse events	Respiratory instability during the procedure
	Respiratory compromise resulting in minor increased respiratory support
	Increased hemodynamic instability
	Hypothermia

Imaging

All MRI scans were performed using a 1.5-T GE Echo Speed scanner (General Electronics Medical Systems, Milwaukee, Wisconsin, USA). The standard imaging protocol included the following: axial T1-weighted spin-echo, axial T2-weigthed dual-spin-echo, sagittal T1-weighted spin-echo, axial 3DT1-weighted SPGR and echo planar diffusion tensor imaging. The acquisition times were approximately 5-6 minutes per sequence.

Data analysis

Statistical analysis was performed using SPSS v17.0.2 (SPSS, Illinois, USA). A repeated measures ANOVA using Wilk's Lambda test was conducted to test the stability of vital parameters during the MRI procedure. Correlations of adverse events with GA, birth weight, weight at image acquisition, gender, temperature drop, mode of respiratory support and total acquisition time were tested. Pearson's correlation coefficients were used for continuous variables. Pearson's Chi-squared test was performed for proportional differences between two categorically scaled variables. One-way ANOVA was used for mean differences between three or more groups holding the groups as a factor variable categorically scaled. A p-value of <.05 (two-sided) was considered statistically significant.

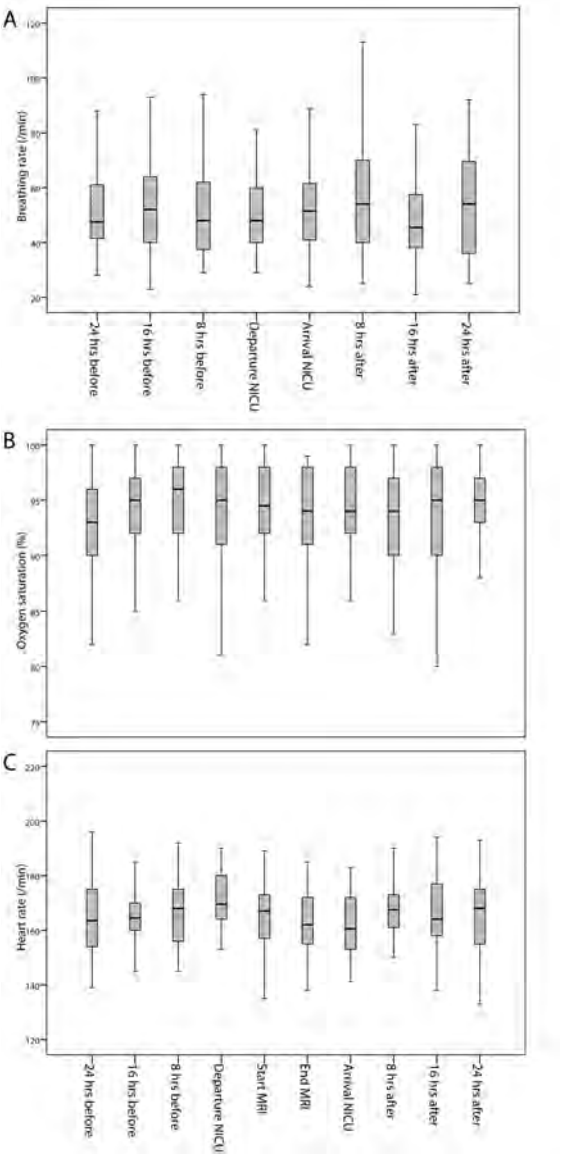

Figure 2 – Vital parameters during the MRI procedure. **A**, breathing rate (breathing rate was not measured during the MRI scan); **B**, trend of oxygen saturation, and **C**, heart rate during the 48 hours surrounding the MRI scan. Note that, in general, these parameters remained stable.

Results

A total of 158 infants were eligible for inclusion in the study. Among these, 32 infants died before 30 weeks PMA, 36 infants were transferred to other hospitals before the MRI scan could be performed and in 38 infants, the MRI scan was postponed because they were not hemodynamically stable enough for MRI scanning at 30 weeks PMA. Therefore, 52 infants (30 boys) underwent a cerebral MRI scan. Patient characteristics are listed in Table 2.

Adverse events

Generally, vital parameters (heart rate, breathing rate and oxygen saturation) remained stable in the 24 hours after the scan with regard to the 24 hours before the MRI scan (Fig 2). Increased hemodynamic instability occurred in 14 infants (26.9%) (Table 3).

Table 2: Patient characteristics

Gestational age at birth, mean ± SD (weeks)	26.8 ± 1.4	
Birth weight, mean ± SD (grams)	967 ± 247	
Postmenstrual age at MR acquisition, mean ± SD (weeks)	30.1 ± 0.3	
Weight at MR acquisition, mean ± SD (grams)	1133 ± 197	
Male gender, *n* (%)	30 (57.7)	
Mode of respiratory support during MRI, *n* (%)		
Mild respiratory support, *n* (%)		
Nasal prongs		10 (19.2)
CPAP		27 (51.9)
Moderate respiratory support, *n* (%)		
Non-invasive ventilation		11 (21.2)
Mechanical ventilation		4 (7.7)
Total acquisition time, mean ± SD (minutes)	39 ± 13	

Note: SD indicates standard deviation, and CPAP, continuous positive airway pressure.

Table 3: Minor adverse events related to MRI procedure

	n **(%)**
Increased hemodynamic instability	14 (26.9)
Cancellation of MRI because of respiratory instability	3 (5.8)
Obstruction of central venous catheter after MRI	1 (1.9)
Increased respiratory support necessary within 24 hours after MRI	12 (23.1)
Hypothermia (<36.0˚) after MRI	9 (17.3)
Total number of adverse events	39

Even though vital parameters remained generally stable during the MRI scan itself and no adverse events occurred in 26 infants (50%), increased hemodynamic instability was frequently encountered within the following 24 hours in some infants. Furthermore, in 26 infants, (preventable) incidents and minor adverse events occurred (Table 3). The MRI scan was cancelled in three infants (5.8%) because of respiratory instability. In another infant, obstruction of the central venous catheter occurred after the scan, although its cause is unclear. Twelve infants (23.1%) needed increased respiratory support within 24 hours after the MRI. In one infant, this might have been due to being transported twice to the MR scanning room because of technical problems with the magnet. Only two infants needed an increased mode of respiratory support: from continuous positive airway pressure to non-invasive ventilation.

Table 4: Comparisons of increased respiratory support with other variables

Parameter	**Need for increased respiratory support**		
	No	**Yes**	***P*-value**
Gestational age at birth, mean ± SD (weeks)	27.1 ± 1.3	25.8 ± 1.4	<0.01[a]
Birth weight, mean ± SD (grams)	1007 ± 244	831 ± 210	0.03[a]
Weight at MR acquisition, mean ± SD (grams)	1146 ± 210	1091 ± 148	NS[a]
Temperature drop after MRI procedure, mean ± SD (degrees Celsius)	0.5 ± 0.6	0.5 ± 0.5	NS[a]
Male gender, *n*	21	9	NS[b]
Mode of respiratory support during MRI, *n*			0.03[b]
Mild respiratory support	32	5	
Moderate respiratory support	8	7	

Note: SD indicates standard deviation, and NS, not significant

[a] Pearson's T-test

[b] Fisher's Exact test

Infants that required increased respiratory support after the scan were born at a significantly lower GA, were born with lower birth weight and/or more frequently received moderate respiratory support during the scan (Table 4). Hypothermia occurred in 9 infants (17.3%). On average, the infants' core temperature dropped 0.5 degrees after the MRI scan. Temperature was significantly decreased after MRI scanning (Fig 3).

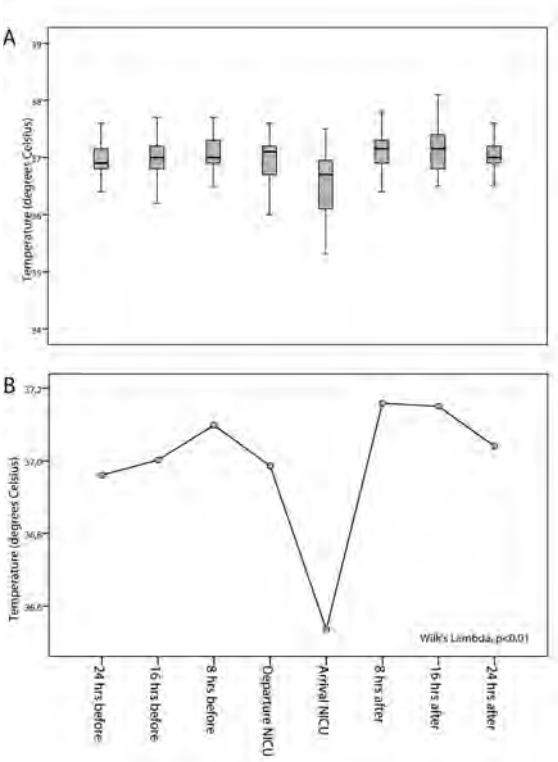

Figure 3 – Temperature measurements during the MRI procedure. **A**, trend of temperature during the 48 hours surrounding the MRI scan, and **B**, repeated measures ANOVA shows that temperature dropped significantly after the MRI scan.

Discussion

Our study stresses the importance of providing a controlled environment for early MRI procedures for preterm infants. Despite the presence of a multidisciplinary guideline specifically designed for preterm infants, minor adverse events, such as hypothermia and the need for increased respiratory support after the scan, were encountered frequently; these events occurred in 26 infants, 50% of our study population. In total, 39 minor adverse events occurred. Therefore, caution needs to be taken regarding the safety of VLBW infants during MRI procedures. Critical incident review and continuous re-evaluation of the guidelines are essential in this process.

MRI is becoming increasingly important for accurately evaluating brain injury and consequent effects on neurodevelopment in preterm infants[9, 11, 21, 22]. Compared with cranial ultrasonography, MRI has proven to be more sensitive for the detection of diffuse non-cystic white matter injury[3, 23, 24] and allows objective quantification of brain injury at a microstructural level[4, 25]. MRI is considered a safe imaging technique, independent of ionizing radiation and enables high-resolution neuroimaging in a non-invasive manner[26].

The use of MRI scanning is limited in preterm infants because of their cardio-respiratory instability and predisposition to hypothermia[17, 26-28]. Performing an MRI scan in this vulnerable population requires a comprehensive guideline that includes all essential elements: good preparation, optimal monitoring of vital parameters, open communication between the involved parties, individualized care and continuous efforts to improve quality of care.

Neonatal intensive care must obviously be maintained throughout the procedure, which requires the use of MR-compatible equipment that ensures optimal monitoring of vital parameters without causing injuries, such as burning or image degradation as a result of radiofrequency interference with the static magnetic field.

Because of the increased risk of respiratory and circulatory compromise, no sedation was used in this study. To reduce motion artifacts, we use other strategies to comfort the infant, such as those according to the principles of the Newborn Individualized Developmental Care and Assessment Program[29, 30].

Safety incidents in (neonatal) healthcare are generally related to poor preparation, equipment failure and human error[31, 32]. Studies on interventions to improve healthcare quality, such as staff training, implementation of a time out procedure (TOP) and the use of checklists and tailored guidelines, have shown that such preventable incidents can be reduced[33-35]. In addition, adverse events should always be reported in order for the guideline to be adjusted[31]. Comparable to operative procedures, a systematic pre-procedural briefing, such as a TOP, can be implemented for MR procedures as well. A pre-procedural TOP ensures that all involved caregivers agree that the correct procedure is being carried out properly for the correct patient.

We have shown that adverse events related to MRI scans in this vulnerable population are common. This is in contrast to other studies[17-19], in which no significant adverse events were found. However, these studies primarily investigated serious adverse events that occurred during the scan itself and the MRI scans had short acquisition times[17] or study population consisted of patients with a wide range of gestational age[17, 18]. In contrast, the results of our study only include data on VLBW infants with mean PMA of 30 weeks ± 4 days at MR acquisition. In addition, we collected data of the 48 hours surrounding the MRI procedure and total acquisition time was approximately 39 minutes. Although it is reasonable and logical to assume that a longer total acquisition time is likely to increase the number of adverse events, we were unable to demonstrate this relationship in our study, this might possibly be explained by the small sample size.

The limitations of this study include selection bias, as our data consist only of infants considered hemodynamically stable enough for a MRI scan. In our setting, the medical team decided whether the infants were hemodynamically stable enough to undergo an MRI scan. Perhaps, if more strict criteria for hemodynamic stability were applied, the incidence of adverse

events might be less frequent. In contrast, the incidence of adverse events might increase if more critically ill preterm infants are scanned, emphasizing the importance of a comprehensive guideline with strict contraindications and staff training to ensure the safe execution of MR procedures.

Another limitation could be the retrospective design and the lack of temperature measurement during MRI scanning. Despite using a MR compatible incubator, which provides controlled temperature and humidity, we encountered an increased incidence of hypothermia after the MRI scan. This could be explained by the mode of respiratory support; infants were supported with cold air or oxygen during the procedure, which is in contrast to the setting at our wards, where infants are supported with pre-heated (40˚C) air or oxygen. In order to decrease the high incidence of hypothermia after the MRI scan, we propose using an optical temperature probe to measure temperature continuously during the scan.

Although minor adverse events were encountered more frequently after the MRI scan, it is not with certainty established that this in fact can be attributed to having undergone a MRI scan. Being transported from the NICU alone could in fact be stressful enough. However, due to the lack of evidence regarding causality and in the context of patient safety, we argue that each adverse event should be considered as a complication of the procedure. Moreover, in order to avoid this possible bias, vital parameters, mode of respiratory support and number of episodes of bradycardia, apnea or oxygen desaturation that occurred within 24 hours before the MRI scan were compared with those that occurred within 24 hours following the MRI scan of each infant individually.

Logistic regression to weigh GA, birth weight and mode of respiratory support with the increased need for respiratory support was not performed given the small sample size (n = 12) in that group.

Finally, no serious adverse events occurred during the procedures, but clinical significance of minor adverse events for future neurodevelopmental outcome remains unclear. Until empirical evidence shows that these events do not adversely affect neurodevelopment, we argue that adverse events should always be considered potentially harmful and maximal efforts to prevent them must be undertaken.

In conclusion, adverse events within 24 hours after routine MRI procedures in VLBW infants at 30 weeks PMA are common, 50% of the MRI procedures in this study were complicated by a minor adverse event. Our findings illustrate the importance of providing a safe environment for early MRI procedures in preterm infants. Considering the increased application of MR imaging as part of standard clinical care for preterm infants, a multidisciplinary-based approach with continuous re-evaluation of the guidelines is necessary to ensure optimal safety for this population.

Attachment : tailored guideline for MRI procedures in preterm infants

Preparation

The medical team (attending neonatologist, pediatric radiologist and nursing staff) decides whether the infant is medically stable enough to undergo an MRI scan and whether the scan is indicated.

A multidisciplinary approach with close communication is essential.

A checklist is used to prepare the infant and equipment for the procedure, this checklist ensures a minimal risk of adverse events related to incorrect execution of the procedure.

An MR-compatible incubator is used, which provides controlled temperature and humidity as well as MR-compatible pulse oximetry and ventilation. The MR-compatible incubator is checked as follows: the temperature is set as it is set on the infant's own incubator; nonmagnetic air and oxygen tanks are present with sufficient capacity; and equipment for ventilation support is available and working.

A resuscitation bag with all necessary equipment for acute interventions is checked and available during the procedure.

All devices attached to the infant and implants (e.g., ECG leads, pulse oximetry probe, temperature probe, intravascular catheters, ductus arteriosus clips and ventriculo-peritoneal shunts as well as metal-containing infant clothing and bracelets) are checked for MR compatibility (http://www.mrisafety.com). MR-compatible ECG electrodes and pulse oximetry probe are attached to the infant to monitor heart rate and oxygen saturation during the scan.

The infant is protected against acoustic noise with moldable earplugs and neonatal earmuffs (Minimufs, provide around 7 Db attenuation).

Infusion lines are sufficiently extended such that the infant can undergo an MRI scan while the infusion pumps remain outside the scanning room, or MR-compatible infusion pumps can be used.

The infant is placed in the MR incubator in a comfortable and secure way with small cushions to encourage sleep and reduce movement. As sedation can cause respiratory and circulatory compromise, we do not use sedation in preterm infants.

Transport

A time out procedure is performed before leaving the NICU such that a quick re-check is conducted and all involved parties agree on the following: the correct infant has been properly prepared, the MR incubator is set correctly, the infant is stable and comfortable and the MR department is ready to scan the infant.

Transport is accompanied by trained staff and physiological stability is monitored during transport.

During the acquisition

Staff trained in neonatal life support remains present throughout the MRI scan.

A room near the MR suite with equipment, supplies and guidelines for neonatal resuscitation is checked and available during the MRI scan.

The technician at the MR suite performs a metal check on the infant, incubator, oxygen and air tanks and accompanying staff before entering the MR suite. Because of the potential hazards associated with the strong electromagnetic field, MR safety training for all accompanying staff is recommended and provided in our setting.

Before the actual MR procedure starts, the presence of adequate respiratory support, hemodynamic stability and the infant's comfort are verified.

Hemodynamic stability is closely monitored from the MRI incubator's screen, which can be seen from the console room. The MRI procedure should be interrupted if hemodynamic stability is compromised or if there is any doubt about it.

After the MRI scan

After the acquisition, the infant's hemodynamic stability and respiratory support are checked again before returning to the NICU.

Upon arrival to the NICU, a handover of the procedure to medical and nursing staff takes place and possible adverse events are noted.

The MR-compatible incubator and accessories are cleaned and the resuscitation bag is refilled if necessary.

During the subsequent 24 hours, the infant's vital parameters and hemodynamic stability are monitored continuously.

References

1. Dyet LE, Kennea N, Counsell SJ, Maalouf EF, Ajayi-Obe M, Duggan PJ, Harrison M, Allsop JM, Hajnal J, Herlihy AH, Edwards B, Laroche S, Cowan FM, Rutherford MA, Edwards AD. Natural history of brain lesions in extremely preterm infants studied with serial magnetic resonance imaging from birth and neurodevelopmental assessment. *Pediatrics* 2006;118:536-48.
2. Debillon T, N'Guyen S, Muet A, Quere MP, Moussaly F, Roze JC. Limitations of ultrasonography for diagnosing white matter damage in preterm infants. *Arch Dis Child Fetal Neonatal Ed* 2003;88:F275-9.
3. Inder TE, Anderson NJ, Spencer C, Wells S, Volpe JJ. White matter injury in the premature infant: a comparison between serial cranial sonographic and MR findings at term. *AJNR Am J Neuroradiol* 2003;24:805-9.
4. Huppi PS, Murphy B, Maier SE, Zientara GP, Inder TE, Barnes PD, Kikinis R, Jolesz FA, Volpe JJ. Microstructural brain development after perinatal cerebral white matter injury assessed by diffusion tensor magnetic resonance imaging. *Pediatrics* 2001;107:455-60.
5. Dudink J, Kerr JL, Paterson K, Counsell SJ. Connecting the developing preterm brain. *Early Hum Dev* 2008;84:777-82.
6. Ment LR, Hirtz D, Huppi PS. Imaging biomarkers of outcome in the developing preterm brain. *Lancet Neurol* 2009;8:1042-55.
7. Boardman JP, Craven C, Valappil S, Counsell SJ, Dyet LE, Rueckert D, Aljabar P, Rutherford MA, Chew AT, Allsop JM, Cowan F, Edwards AD. A common neonatal image phenotype predicts adverse neurodevelopmental outcome in children born preterm. *Neuroimage* 2010;52:409-14.
8. Dubois J, Benders M, Borradori-Tolsa C, Cachia A, Lazeyras F, Ha-Vinh Leuchter R, Sizonenko SV, Warfield SK, Mangin JF, Huppi PS. Primary cortical folding in the human newborn: an early marker of later functional development. *Brain* 2008;131:2028-41.
9. Rutherford MA, Supramaniam V, Ederies A, Chew A, Bassi L, Groppo M, Anjari M, Counsell S, Ramenghi LA. Magnetic resonance imaging of white matter diseases of prematurity. *Neuroradiology* 2010;52:505-21.
10. Seghier ML, Lazeyras F, Huppi PS. Functional MRI of the newborn. *Semin Fetal Neonatal Med* 2006;11:479-88.
11. Ramenghi LA, Rutherford M, Fumagalli M, Bassi L, Messner H, Counsell S, Mosca F. Neonatal neuroimaging: going beyond the pictures. *Early Hum Dev* 2009;85:S75-7.
12. Dudink J, Lequin M, van Pul C, Buijs J, Conneman N, van Goudoever J, Govaert P. Fractional anisotropy in white matter tracts of very-low-birth-weight infants. *Pediatr Radiol* 2007;37:1216-23.
13. Schenck JF. Safety of strong, static magnetic fields. *J Magn Reson Imaging* 2000;12:2-19.
14. Schenck JF. Physical interactions of static magnetic fields with living tissues. *Prog Biophys Mol Biol* 2005;87:185-204.
15. Collins CM, Wang Z. Calculation of radiofrequency electromagnetic fields and their effects in MRI of human subjects. *Magn Reson Med* 2011;65:1470-82.
16. McJury M, Shellock FG. Auditory noise associated with MR procedures: a review. *J Magn Reson Imaging* 2000;12:37-45.
17. Benavente-Fernandez I, Lubian-Lopez PS, Zuazo-Ojeda MA, Jimenez-Gomez G, Lechuga-Sancho AM. Safety of magnetic resonance imaging in preterm infants. *Acta Paediatr* 2010;99:850-3.

18. Merchant N, Groves A, Larkman DJ, Counsell SJ, Thomson MA, Doria V, Groppo M, Arichi T, Foreman S, Herlihy DJ, Hajnal JV, Srinivasan L, Foran A, Rutherford M, Edwards AD, Boardman JP. A patient care system for early 3.0 Tesla magnetic resonance imaging of very low birth weight infants. *Early Hum Dev* 2009;85:779-83.
19. Battin M, Maalouf EF, Counsell S, Herlihy A, Hall A, Azzopardi D, Edwards AD. Physiological stability of preterm infants during magnetic resonance imaging. *Early Hum Dev* 1998;52:101-10.
20. Speroff T, O'Connor GT. Study designs for PDSA quality improvement research. *Qual Manag Health Care* 2004;13:17-32.
21. Arthur R. Magnetic resonance imaging in preterm infants. *Pediatr Radiol* 2006;36:593-607.
22. Counsell SJ, Rutherford MA, Cowan FM, Edwards AD. Magnetic resonance imaging of preterm brain injury. *Arch Dis Child Fetal Neonatal Ed* 2003;88:F269-74.
23. Maalouf EF, Duggan PJ, Counsell SJ, Rutherford MA, Cowan F, Azzopardi D, Edwards AD. Comparison of findings on cranial ultrasound and magnetic resonance imaging in preterm infants. *Pediatrics* 2001;107:719-27.
24. Roelants-van Rijn AM, Nikkels PG, Groenendaal F, van Der Grond J, Barth PG, Snoeck I, Beek FJ, de Vries LS. Neonatal diffusion-weighted MR imaging: relation with histopathology or follow-up MR examination. *Neuropediatrics* 2001;32:286-94.
25. Counsell SJ, Edwards AD, Chew AT, Anjari M, Dyet LE, Srinivasan L, Boardman JP, Allsop JM, Hajnal JV, Rutherford MA, Cowan FM. Specific relations between neurodevelopmental abilities and white matter microstructure in children born preterm. *Brain* 2008;131:3201-8.
26. Stokowski LA. Ensuring safety for infants undergoing magnetic resonance imaging. *Adv Neonatal Care* 2005;5:14-27; quiz 52-4.
27. Mathur AM, Neil JJ, McKinstry RC, Inder TE. Transport, monitoring, and successful brain MR imaging in unsedated neonates. *Pediatr Radiol* 2008;38:260-4.
28. van Wezel-Meijler G, Leijser LM, de Bruine FT, Steggerda SJ, van der Grond J, Walther FJ. Magnetic resonance imaging of the brain in newborn infants: practical aspects. *Early Hum Dev* 2009;85:85-92.
29. Als H. NIDCAP: testing the effectiveness of a relationship-based comprehensive intervention. *Pediatrics* 2009;124:1208-10.
30. Legendre V, Burtner PA, Martinez KL, Crowe TK. The Evolving Practice of Developmental Care in the Neonatal Unit: A Systematic Review. *Phys Occup Ther Pediatr* 2011;31:315-38.
31. Moss SJ, Embleton ND, Fenton AC. Towards safer neonatal transfer: the importance of critical incident review. *Arch Dis Child* 2005;90:729-32.
32. Lim MT, Ratnavel N. A prospective review of adverse events during interhospital transfers of neonates by a dedicated neonatal transfer service. *Pediatr Crit Care Med* 2008;9:289-93.
33. Nguyen YL, Wunsch H, Angus DC. Critical care: the impact of organization and management on outcomes. *Curr Opin Crit Care* 2010;16:487-92.
34. Schlack WS, Boermeester MA. Patient safety during anaesthesia: incorporation of the WHO safe surgery guidelines into clinical practice. *Curr Opin Anaesthesiol* 2010;23:754-8.
35. Chassin MR, Loeb JM. The ongoing quality improvement journey: next stop, high reliability. *Health Aff (Millwood)* 2011;30:559-68.

CHAPTER 4

Acquisition Guidelines and Quality Assessment Tools for Analyzing Neonatal Diffusion Tensor MRI Data

A.M. Heemskerk
A. Leemans
A. Plaisier
K. Pieterman
M.H. Lequin
J. Dudink

American Journal of Neuroradiology, 2013; 34:1496-505

Abstract

Diffusion tensor imaging (DTI) is a valuable measure in clinical settings to assess diagnosis and prognosis of neonatal brain development. However, obtaining reliable images is not straightforward because of tissue characteristics of the neonatal brain and high likelihood of motion artifacts.

In this review, we present guidelines on how to acquire DTI data of the neonatal brain and recommend high-quality data acquisition and processing as an essential means to obtain accurate and robust parametric maps. Sudden head movements are problematic for DTI in neonates and these may lead to incorrect values. We describe strategies to minimize the corrupting effects both in terms of acquisition (e.g., more gradient directions) and post processing (e.g., tensor estimation methods). In addition, tools are described that can help assess whether a dataset is of sufficient quality for further assessment.

Introduction

Both premature birth and complications around term birth are risk factors for brain injury and subsequent neurodevelopmental impairment. However, this injury often remains "silent" long after the threshold of irreversible injury has been crossed. The most important challenge is to define early proxy measurements of long term neurodevelopmental outcome that will enable to intervene in the early stages of the still adaptive developing human brain. Magnetic resonance imaging (MRI) is widely used to monitor development and injury of the newborn brain and to predict neurodevelopmental outcome[1-6] (Fig 1). Advanced, quantitative MRI techniques, such as DTI[7-11] can detect subtle differences between normal and abnormal tissue. DTI has become invaluable for the assessment of brain development in preterm infants as it enables detection of white matter (WM) maturation during premyelination[1, 3, 12-14]. Several DTI studies have revealed that abnormal WM maturation is correlated to neuromotor and neurocognitive performances in childhood[15-18]. DTI measurements can therefore provide early biomarkers to be targeted in for neuroprotective intervention trials.

Although diffusion MRI of the neonatal brain is gaining popularity, time constraints often impede acquisition of high quality data. Total time in the scanner should be kept to a minimum, not only for ethical reasons but also to prevent hemodynamic instability. Moreover, a longer acquisition time increases the chance of motion. The feasibility of an MRI study and the optimal settings for the MRI scan are determined by the available time in combination with MRI hardware and requirements for obtaining reliable and meaningful data.

From the above, it may be clear that acquisition, processing and interpretation of the images with this advanced MRI technique is not as straightforward as with the conventional MRI sequences. Recent reviews have covered the general concerns within the DTI pipeline that can severely influence the measured results and therefore study outcome[11, 19, 20]. Many of the specifics of diffusion MRI acquisitions in adult brains are also applicable to imaging the neonatal brain. However, the latter presents challenges related to size, tissue composition and motion and therefore requires specific acquisition settings. Targeted acquisition schemes and post processing methods are necessary to account for motion and to obtain reliable DTI parameter maps.

In this review, we present guidelines on how to acquire diffusion MRI data of the neonatal brain. Furthermore, we recommend high-quality data acquisition and processing as an essential means to obtain accurate and robust parametric maps. We will first describe some general topics related to DTI acquisition. Next, we broadly describe the specific concerns and acquisition settings related to DTI in the neonate. Finally, we discuss the main steps related to DTI acquisition and processing and the ways they influence neonatal DTI data quality.

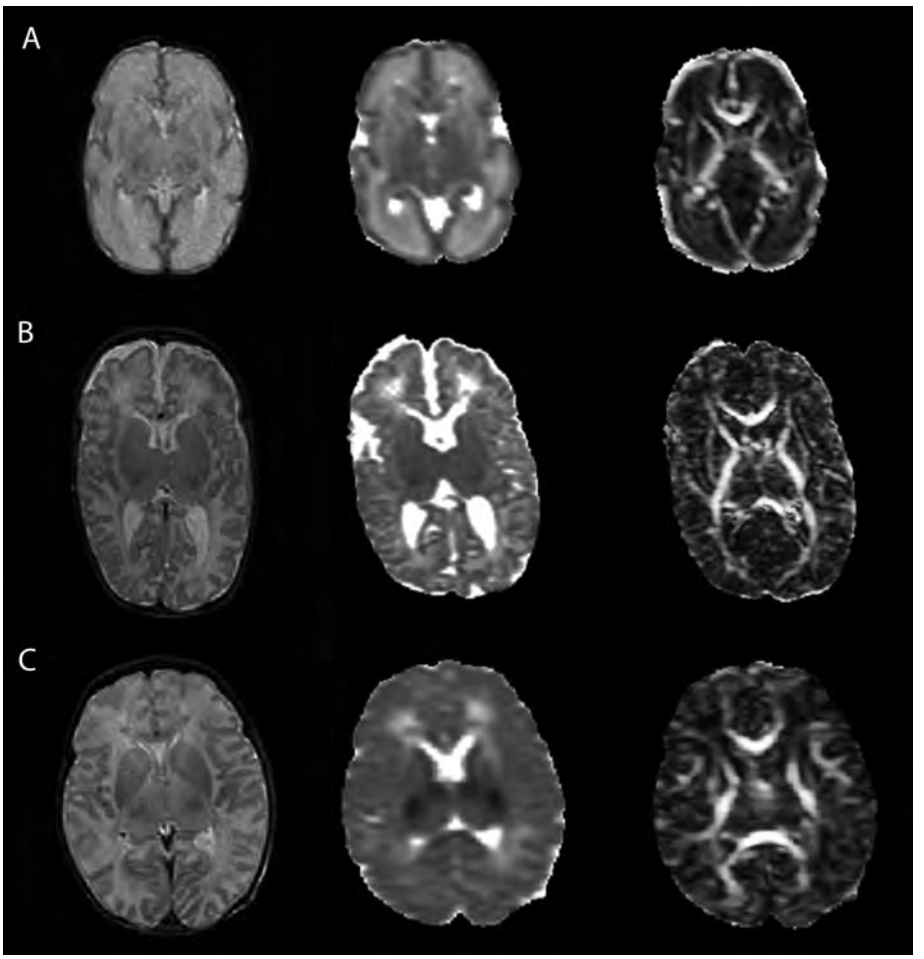

Figure 1 – Anatomical, mean diffusivity (MD) and fractional anisotropy (FA) map of a neonate. **A**, At 30 weeks' postmenstrual age; **B**, at term-equivalent age; and **C**, after perinatal asphyxia scanned on day four, with abnormal low signal intensity in the central gray matter on the MD map. Notice the decrease in MD values and increase in FA values between the preterm and term brain. The MD and FA maps are equally scaled for the three subjects, respectively 0–2 x 10^{-3} mm^2/s and 0–1.

Neonatal DTI

Imaging the neonatal brain is more difficult than imaging the adult brain. The neonate's head is much smaller and the brain is developing at a fast rate, has a high water content and is unmyelinated[21]. MRI acquisition settings therefore must be adjusted to neonatal MRI relaxation times and diffusion coefficients. Additionally, there is a greater likelihood of motion artifacts in the images because neonates have higher heart and breathing rates and will not lie motionless as sedation is usually not given in this situation. Fig 2 shows examples of motion artifacts. Thus, the optimal acquisition strategies established for the adult brain[22] are not nec-

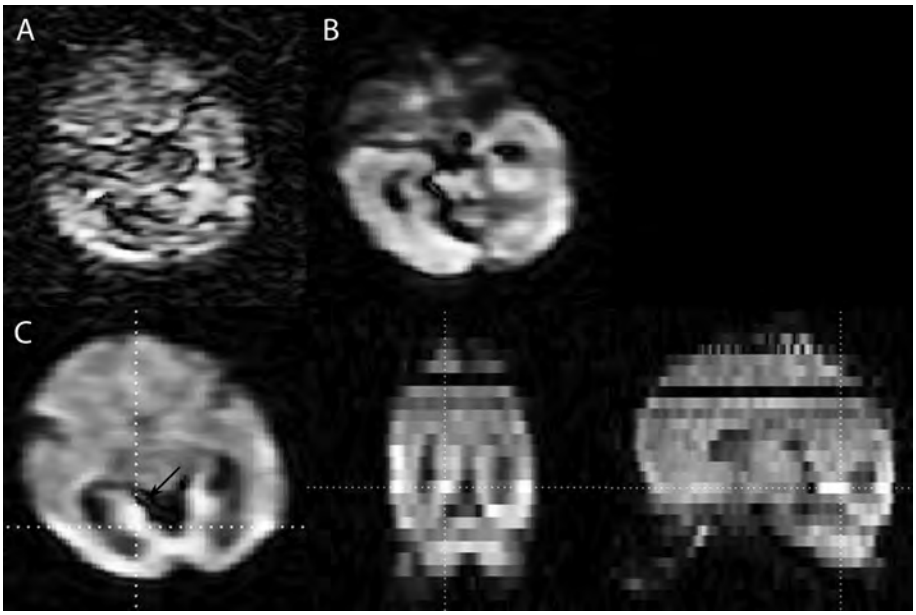

Figure 2 – Effects of motion and pulsation. **A**, Almost complete signal loss caused by head motion; **B**, signal drop-out caused by pulsation, and **C**, 3-plane view in which the effects of pulsation (*arrow*) and motion (*arrowhead*) are visible.

essarily applicable to the neonatal brain as diffusivities, anisotropy, T2 and signal to noise ratio (SNR) will differ. Additionally, optimal acquisition depends on multiple, interrelated parameters, including but not limited to, repetition time (TR), echo time (TE), acquisition matrix, field of view, section thickness, acquisition time, number of averages, maximum *b*-value, number of *b*-values, number of non-diffusion weighted images (DWI) and number of gradient directions.

Setup for neonatal imaging

Neonatal MRI is challenging as many neonates are on respiratory support and are vulnerable to hemodynamic instability[23-25]. A recent study showed that, despite of the use of a dedicated guideline, adverse events during neonatal MRI scanning are common[26]. Because of the increased application of neonatal MRI, provision of a safe environment during the MRI procedures is of great concern. An MR-compatible incubator with a specialized neonatal head coil allows to keep infants stable and safe during transport and scanning procedure. A small-size neonatal head coil typically offers better SNR than larger adult head coils[27]. With improved SNR, scan time can be reduced and/or spatial resolution for conventional scans can be improved.

Table 1: Published DTI acquisition settings for neonates from different groups

PMA	FS	neon. coil	TR	TE	FOV	thk	image resolution	*b*-value	no. *b* = 0	no. dir	Sedation	Reference
40–45	3	–	7745	48	180	2	1.41	800	1	32	+	van Pul et al[67]
Term	3	–	8400	84	220	2.2	2.20	750	?	?	±	Wintermark et al[68]
31–41	1.5	+	4000	60	210	3.0	0.82	1000	1	?	–	Arrigoni et al[69]
38–41	3	–	>3000	71	150	1.9	1.88	700	5	30	–	Oishi et al[70]
Term	3		7680	82		2.0	2.00	1000	7	42	–	Wang et al[71]
37 –43	1.5		6000	88	200	2.5	1.56	1000	1	15	+	Hasegawa et al[72]
40–44	3		7465	54		2.0	1.40	1000	1	32	+	de Bruine et al[73]
Term	1.5	+	4047	59	210	3.0	0.82	1000	1	6	–	Righini et al[74]
24–33/Term	1.5	+	7000	100		3.0	1.40	600	1	6	–	Bonifacio et al[75]
24–33/Term	1.5	+	4900	104	160	3.0	1.30	600/700	1	12	–	Bonifacio et al[75]
Term	3		5200	73		2.0	2.00	1000	1	6	–	Gillmore et al[76]
25–32	1.5	+	9150	98	200	3.0	0.78	1000	1	25	–	Dudink et al[77]
35–42	1.5	–	5888	92	220	2.3	2.00	600	1	32	–	Liu et al[78]
39–41	1.5	–	7000	74	180	2.2	1.40	700	1	15	+	Skiold et al[5]
Term	1.5	–	8000	100	240	3.0	1.88	700	1	10	–	Malik et al[79]
Term	1.5	–	6000	106	230	2.5	0.90	1100	16	44	–	Rose et al[80]
38–45	3	–	8000	79	224	2.0	1.75	750	1	15	±	Anjari et al[13]
30	1.5	+	11725	90.5	220	3.0	0.86	750	3	25	–	Erasmus MC – Sophia
Term	1.5	+	11725	85.6	220	3.0	0.66	1000	3	25	–	Erasmus MC – Sophia

Note: image resolution is all squared (mm); b-values are s/mm^2
PMA indicates postmenstrual age at image acquisition (weeks); TEA, term equivalent age; FS, Field strength (T); neon. coil, neonatal head coil; TR, repetition time (ms); TE, echo time (ms); FOV, field of view (mm); thk: section thickness (mm); no. *b* = 0, number of non-diffusion weighted images; no. dir, number of diffusion encoding directions; +, used and; –, not used.

Two common strategies are used to limit motion. One is sedation, which in neonates can compromise breathing and therefore must be performed with great caution. The second strategy is promoting sleep by placing infants in the incubator in a comfortable and secure way[28]. This will generally help, but it takes some practice to comfort the child and prevent it from waking up when imaging starts[29]. The infant's perception of acquisition noise can be reduced with the use of moldable earplugs, neonatal earmuffs and/or an acoustic hood[30].

Resolution, repetition time and echo time

A striking difference between the neonatal and adult brain is the inverse contrast between white and gray matter on both the T1- and T2-weighted images[31]. This is caused by the high water content and unmyelinated WM of the neonate. T1 and T2 relaxation times quickly decrease over the first year of life and the exact pattern is different for different brain structures. Typical T2 relaxation times are around 300 ms at <30 weeks' gestational age, approximately 200 ms at term age[32] and approximately 100 ms at adulthood[33]. T1 relaxation times for WM are approximately 1600 ms at term age and approximately 500 ms at 2 years of age[31]. For DTI measurements, a longer TR can be needed to reduce the effect of the high T1 relaxation time (e.g., saturation and therefore reduced SNR and/or bias to other proton pools). Fortunately, the long T2 relaxation time does favor the DTI measurement as there is more signal left at a similar TE. However, the DTI estimates for different ages or brain structures must be interpreted carefully as they can be influenced by the varying T1 and T2 relaxation times, possibly caused by altered relative contributions of the different water compartments (e.g., intracellular versus extracellular).

All structures in the neonatal brain are smaller than in the adult brain, thereby requiring a higher resolution. Typical in-plane resolutions range from 0.6 x 0.6 mm^2 to 2 x 2 mm^2, with a section thickness of 1.9–3.0 mm (Table 1). Which is still relatively large, therefore images should be interpreted cautiously[34]. Additionally, the in-plane resolution is often obtained with a low acquisition matrix that is zero-filled to a higher matrix, images therefore are smoother and boundaries are less sharp. Imaging resolution and partial volume effects determine what structures can be resolved. For fiber tracking purposes, the resolution is ideally isotropic and contiguous sections are needed without section gap. The use of isotropic voxels prevents preferential averaging of fiber orientation along a certain axis[11].

In addition, the resolution and SNR are related because higher resolution means lower SNR. Therefore, SNR constraints can limit the resolution. Higher resolutions are obtained by decreasing the field of view or increasing the matrix size. However, both options have their limitations as the field of view needs to fit the whole image volume and higher matrix size introduces artifacts and increases scan time.

General DTI acquisition considerations

Generally, a single-shot echo planar imaging (EPI) sequence allows fast acquisition, but unfortunately, is prone to artifacts that effect data acquisition and processing[11, 19, 20, 35]. The most critical artifacts are image distortions caused by magnetic susceptibility effects and eddy currents. Among the solutions proposed to reduce susceptibility artifacts are parallel imaging and $b = 0$ field correction. Eddy currents can be reduced by applying bipolar gradients and dual echo or twice refocused sequences[36]. For a more comprehensive and detailed description of these artifacts and other problems, we recommend the recent review by Jones and Cergignani[19] or other reviews regarding DTI[11, 20, 35].

Diffusion MRI is intrinsically a low SNR technique and SNR can significantly influence reliability of each tensor estimate. For example, in adult brains, low SNR levels reduce accuracy of diffusion estimates (e.g., increased fractional anisotropy (FA)) and decrease precision (e.g., larger standard deviations)[37]. The SNR dependence is influenced by underlying diffusivities, FA values and by acquisition settings, such as the *b*-value[37, 38].

The magnetic field strength affects quality of images both positively and negatively. At 3-T, the SNR is generally higher than at 1.5-T. However, images acquired at 3-T are more sensitive to susceptibility artifacts, which are prone around air-tissue boundaries. Therefore, the field strength must be considered carefully when setting up a protocol.

The performance of gradient systems is an important determinant of DTI image quality. Stronger gradients allow for higher diffusion weighting within a shorter time, thereby reducing TE, improving SNR and reducing artifacts. Gradient systems with advanced eddy-current compensation are preferred as these limit image distortions.

Hardware and software of MRI systems differ between manufactures and are constantly being upgraded. Therefore, imaging protocols cannot always be exchanged between sites and what is achievable at one scanner might not be possible at another. Additionally, even equally equipped MRI systems can introduce a bias[39]. The coil should adequately cover the volume of interest and exhibit sufficient SNR. Preferably, a multichannel coil should be used with the option to use parallel imaging. Parallel imaging techniques can shorten the EPI readout, thereby reducing imaging artifacts and TE[40].

Diffusion weighting

The *b*-value indicates the amount of diffusion weighting that is applied. The optimal *b*-value depends on the tensor information of interest but is generally around 1.09/apparent diffusion coefficient (ADC)[22]. For clinical adult brain DTI, a *b*-value of 1000 s/mm^2 is common practice, which is a concession between a longer optimal *b*-value and the need for shorter echo times to ensure enough SNR. As mentioned, the neonatal brain contains more water and

is less myelineated than the adult brain. Therefore, the neonatal mean diffusivity (MD) is higher than the adult MD (2.0 x10^{-3} mm^2/s vs. 0.7 x10^{-3} mm^2/s) and the optimal *b*-value should be lower to accurately estimate the diffusion tensor. Currently, there is no consensus on *b*-value in neonates and *b*-values range between 600 and 1100 s/mm^2 (Table 1). Simulation studies are needed to determine the optimal *b*-value, just as has been done for adult brains.

At least six diffusion gradient directions and one non-DWI are needed to estimate the diffusion tensor. However, more directions increase accuracy and precision of the diffusion estimates. Tensor estimates with 30 directions are statistically rotationally invariant[41]. Increasing the number of directions also entails increasing the number of $b = 0$ acquisitions as one $b = 0$ image is needed for every 8–10 DWI[22]. The optimal distribution of gradients is a uniform distribution along the surface of a sphere[22], which minimizes orientation dependency of tensor estimates. Additionally, the order of gradients ideally should be uniformly distributed in case of motion-induced corrupted or interrupted acquisition[42, 43]. Dubois et al[43] have proposed optimal diffusion gradient orientation schemes, that allow calculating the diffusion tensor estimates with the use of partial datasets. The higher likelihood of motion in neonates requires a higher number of gradient directions. The relative contribution of a corrupted image is less if more gradient directions are acquired. Therefore, it may be preferable to increase the number of gradient directions at the cost of reducing TR (and thereby SNR) to keep total scan time approximately equal. In addition, we recommend the use of extra $b = 0$ images because these images also can be affected by interslice and intraslice motion and good quality $b = 0$ images are needed to correctly calculate the tensor estimates.

Motion

Subject-related motion can impact the resulting parameters maps. Motion can be evident between images or within a single image. During long acquisition, adult subjects tend to slowly move their heads even if they are instructed to lay still and the head is secured by padding[44]. A slow displacement and/or rotation causes a misalignment between images. This can be adjusted for by image registration. The motion within a single image is caused by cardiac pulsation or sudden large amplitude subject-related motion. The latter occurs rarely in adults (1.4%)[45], but is a severe problem in neonates. Fig 2 shows the effects of severe motion, cardiac pulsation and the large differences in signal intensities throughout the image volume.

Cardiac pulsation causes both local deformation of tissue and additional signal loss. The tensor estimates are then less reliable. Because neonates have much faster heart rates than adults, the likelihood that the diffusion sensitization is obtained during a pulsation is higher, leading to a higher likelihood of artifacts. The effects of cardiac pulsation can be reduced by triggering the acquisition on the cardiac cycle. However, scan times become longer because the effective TR should be at least 5 times the T1 relaxation time of the tissue. For neonates, cardiac gating seems only possible by monitoring the ECG, because the delay time for the

pulse-wave on the pulse oximeter is too long (249 ms for adults[46]) compared with the heart beat (approximately every 350 ms).

Subject motion is a major concern for neonatal imaging as neonates tend to move about even when sedated. Intraslice motion from a sudden shake of the head may corrupt the image and result in miscalculation of DTI estimates. A typical motion-corrupted image is characterized by severe signal loss. This is caused by tissue displacement during the diffusion encoding, which also causes signal loss next to the dephasing caused by diffusion. This severe signal loss cannot be recovered and an apparent high displacement would be calculated. Improper dealing with motion artifacts may result in biased MD and high FA values.

Only a few studies have reported data rejection on the grounds of severe artifacts. Rejection was necessary in 15–60% of the subjects[15, 47-49] and the incidence of less noticeable artifacts will be larger. In a pilot study of 27 preterm neonates, we investigated statistical outliers of tensor regression (see "DTI Quality and Pathology" section) and showed that data of 60% of subjects were corrupted by motion (defined as >10 sections with >30% outliers) (Table 2)[50]. This high occurrence of motion can have devastating results. Unfortunately, the typical tensor regression method used by MRI vendors and commercial processing tools is insufficient with corrupted data and it appears that many DTI users are unaware of the motion-related problems.

Solutions to prevent corrupted images are limited. Obviously, movement should be minimized a priori by placing the child comfortably and supporting the head with pads. Acquisition strategies to reduce the signal loss are limited because the sudden gross motion occurs when diffusion encoding is performed. Therefore, navigator echoes or altered readout sequences appear not to be useful. However, shortening the diffusion time by stronger gradients or a lower *b*-value might reduce the effects. Fortunately, there are strategies to decrease detrimental effects of corrupted images. These include oversampling of gradient directions, removal of corrupted images and/or using more advanced tensor regression methods.

Temperature

Another issue one must be aware of is that diffusion is temperature-dependent. A one degree difference in temperature leads to a 2-3% difference in ADC[51, 52]. It will therefore be necessary to maintain the child at a constant temperature during scanning. Also, consistent core temperatures are necessary in studying group differences or performing a longitudinal study because the differences in MD or FA between ages, groups and therapies are small.

Table 2: Outliers in a small pilot study (27 preterms scanned at 30 weeks postmenstrual age)

	>10% outliers	>30% outliers	>50% outliers
No. of subjects >10 sections	27	15	10
No. of subjects >20 sections	26	10	1
Mean No. of sections with outliers	50	15	9
Range No. of sections with outliers	17–79	1–38	0–24
Mean percentage of sections with outliers	9.5	2.9	1.7
Range of percentage of sections with outliers	3.3–15.7	0.2–7.0	0.0–4.4

Post processing

The basic steps in data post processing are motion/distortion correction, estimation of the diffusion tensor and computation of parametric maps. Data should be inspected before and after each step to ensure good image quality and absence of artifacts. Post processing results in data reduction and it can be difficult to spot erroneous results on parametric maps.

Motion and distortion correction

Registration and correction of images is necessary to adjust for slight variation in brain position and to correct for eddy currents. A quick check for misregistration between images is to examine the FA maps for rims of high anisotropy at the edges of the brain or at the interface between cerebrospinal fluid and WM.

Because most available registration tools are optimized for the contrast in adult brains, one should check if the registration software is adequate for the neonatal brain, in view of its different contrast. In addition, most tools perform their registration on the whole image volume and it is therefore logical that section drop-outs caused by motion severely alter registration, especially in case of affine registration. A final step is to also correct the diffusion encoding gradients with the same rotational correction as the images[44]. Neglecting to do so will induce a mismatch between actual diffusion weighting and expected diffusion weighting and therefore result in errors in estimating the diffusion tensor and fiber orientation.

It is of paramount importance to ensure that motion correction, which is often necessary in neonatal scanning, does not negatively impact the DTI dataset. Interslice movement is problematic for volume registration and the $b = 0$ volume should be carefully checked on misalignment between sections. Large signal drop-outs are problematic with through-plane motion correction because thereafter, incorrect signal intensities affect two sections resulting in possible incorrect tensor estimations. Zhou et al[47] investigated the use of local texture fea-

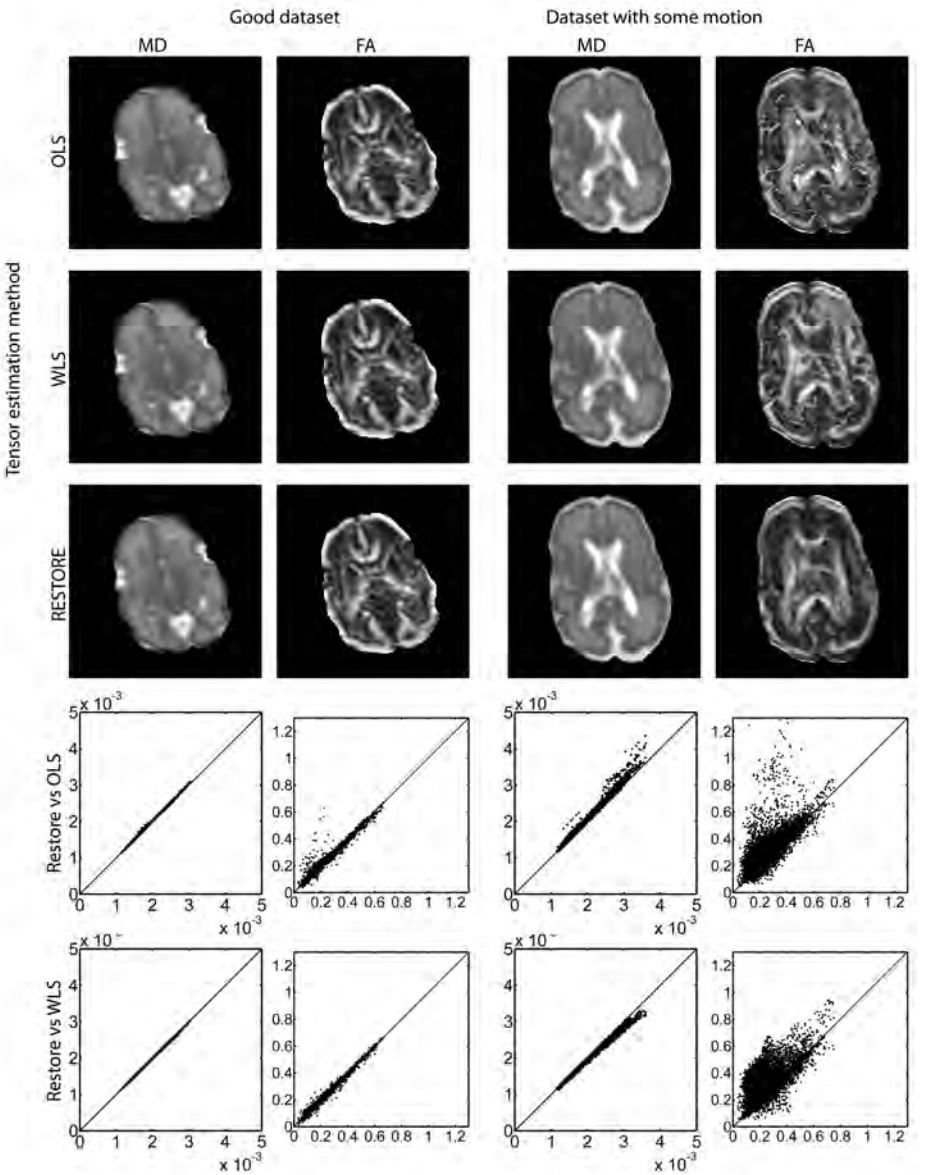

Figure 3 – Effects of different tensor estimation methods. Data of two datasets are displayed: on the left, data without gross motion artifacts, and on the right, data with gross motion artifacts for one of the gradient directions. Both MD and FA maps are depicted, showing no visible differences for the good dataset and clearly visible differences for the dataset with motion. Especially the FA maps show that the ordinary least-squares (OLS) estimation results in very high FA values that are not related to the known anatomy. In the graphs, the pixel value of the OLS or weighted least-squares (WLS) tensor estimation is plotted against the pixel value of the RESTORE tensor estimation (X-axis) and the line of identity is included. The spread around the line of identity is broader for the dataset with motion, indicating an effect of the tensor estimation method on the resulting FA or MD value. For the graphs, the images were eroded to exclude the outer rim, which contains poor-quality data caused by partial volume effects. Scaling: MD, 0–2 x 10^{-3} mm^2/s; FA, 0–1.

tures to identify and reject outlier images automatically before estimating the diffusion tensor. Their method is fast and removes sections that are corrupted and cannot be used for tensor estimation, resulting in more accurate data. Implementation of fast detection techniques based on image characteristics will improve data quality and might offer possibilities to repeat corrupted gradient directions while scanning[53].

Estimation of the diffusion tensor

Several tensor estimation methods have been developed to estimate the diffusion tensor. Each of these approaches is based on different principles. In general, speed and accuracy are inversely proportional: methods range from fast but less accurate, to slow but more accurate[9, 49, 54]. The main problem in estimating the tensor is presence of data outliers caused by motion, pulsation, artifacts, noise and so on. Depending on the method used, these outliers can have a significant impact on the resulting eigenvalues and eigenvectors. The linear least-squares method is commonly used by vendors and is the default setting for commonly used DTI post processing software such as FSL[55]. However, this method proved least appropriate to estimate the tensor because its assumptions are restrictive and physically implausible[56]. Fig 3 shows the effect of tensor estimation method on a dataset with few outliers and on a dataset with gross motion artifacts. The difference between the methods is clearly visible, with the ordinary least-squares method providing obviously erroneous results, whereas the weighted least-squares method, which only takes a fraction more computational time, providing more accurate results. Therefore, for neonatal DTI data with its high likelihood of corrupted data, we must use proper tensor estimation procedures to obtain reliable diagnostic images or research data. Robust estimation of tensors by outlier rejection (RESTORE)[54] is a method that detects and removes outlier data in the tensor estimation. This method requires additional gradient encoding directions to eliminate erroneous data. For neonatal DTI measurements, Morris et al[49] investigated the use of removing outliers based on the RESTORE algorithm before motion correction because the latter can result in averaging outliers with uncorrupted voxels. With this new method, they found an increased sensitivity to outliers, which is important as outliers correlated strongly with subject movement.

Quality assurance

It is of paramount importance to ensure that all steps from data acquisition to data analysis are correct and that parameter maps are of sufficient quality before analyzing data and drawing conclusions. Good-quality data are of paramount importance for the neonatal population, because chances of artifacts and corrupted data are larger than for the average adult population and artifacts will bias quantification and increase variation. Data of sufficient quality will provide quantitative measures with low variation.

Quality assurance begins by carefully checking the $b = 0$ images on accuracy, absence of artifacts and interslice movement. Interslice movement causes severe problems with the image registration resulting in erroneous results. Therefore, those image volumes must be excluded from further analysis and hence our previous suggestion to increase the number of $b = 0$ volumes. Thereafter, the DWI are inspected for large signal dropouts, which can be

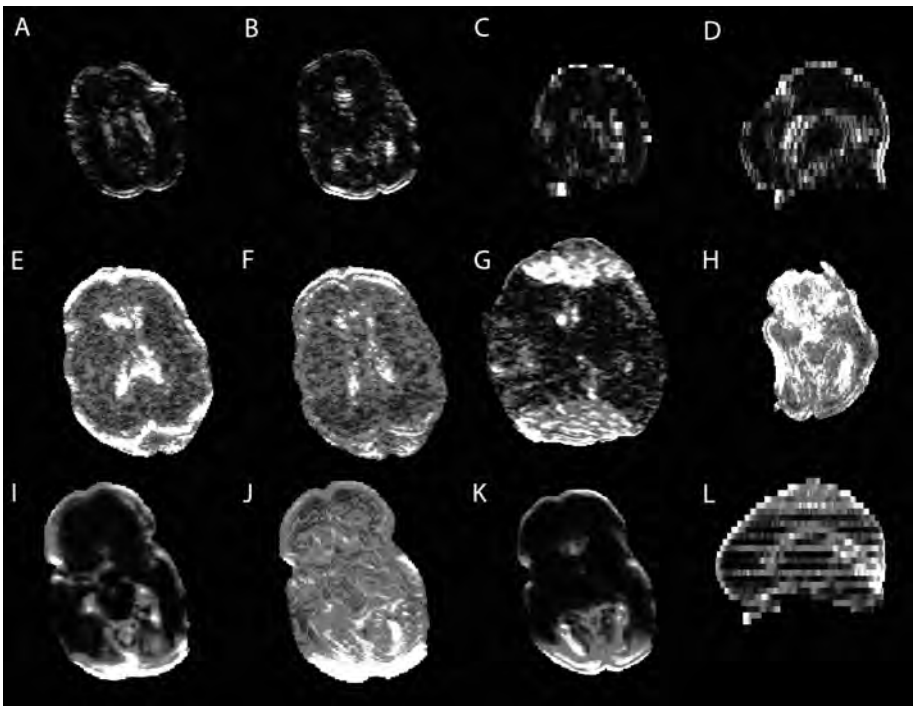

Figure 4 – Examples of residuals. **A** trough **D**, residuals from a subject with good data quality. Higher residuals are present at the border and in the ventricles. **A** and **B**, axial images; **C**, coronal view; and **D**, sagittal view. **E** and **F**, effects of motion and eddy current correction with higher residuals before correction and lower values after correction; **G**, higher residuals caused by ghosting; **H**, higher residuals caused to susceptibility artifacts; **I** through **L**, residuals from a subject with gross motion artifacts showing both sections with low (no motion) and high (motion) residuals. The sagittal view (**L**) shows a pattern with alternating sections of high and lower residuals. Each image is individually scaled. (A full color version of this illustration can be found in the color section).

easily observed by through plane projections (Fig 2c). Image misalignments caused by motion or eddy currents can be visualized by a high FA around the rim of the brain or by calculating standard deviations across the DWI, in which large standard deviations at the rims indicates misregistration. This is also a good method to check whether images were registered accurately, if registration issues persist or even are introduced. Artifacts in data can also be spotted by locating areas where FA is larger than one. By definition, this should not be plausible, but occurs when the diffusion weighted signal intensity is larger than the $b = 0$ signal intensity.

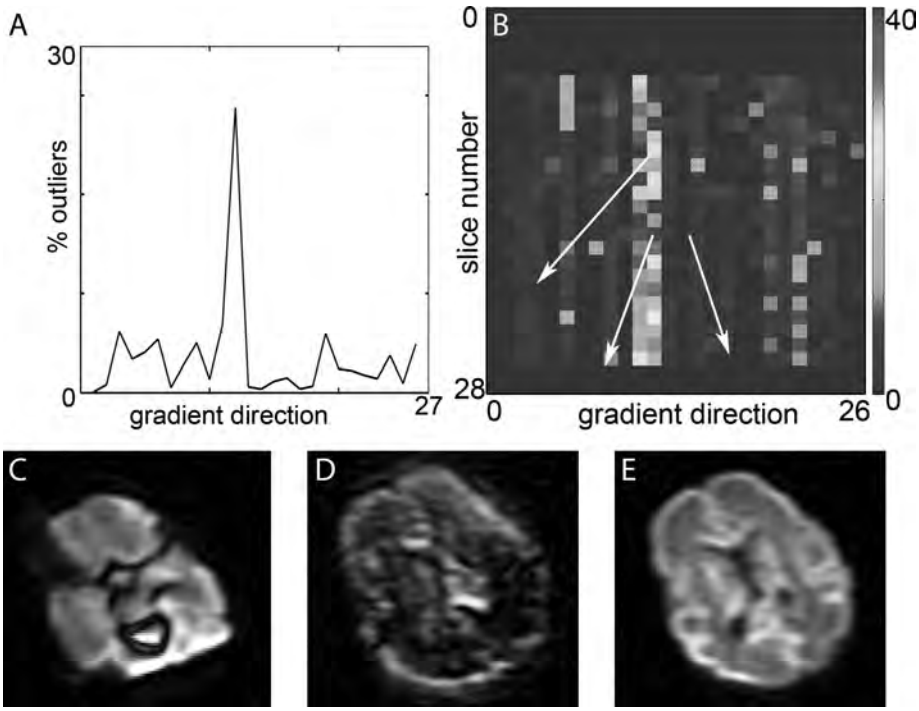

Figure 5 – Detection of outliers. **A**, percentage of outliers per DW image is a tool to indicate potential problems with the DTI dataset. In this case, DW images eleven and twelve have a high percentage of outliers. **B**, percentage outliers per section facilitate easy detection of the problematic sections. During the acquisition of gradient direction twelve, several sections are affected by movement of the infant. **C** and **D**, examples of the resulting images, and **E**, non-affected image. Because of the interleaved section acquisition, there is an alternating pattern for the odd and even sections. Scaling is similar for diffusion weighted images. (A full color version of this illustration can be found in the color section).

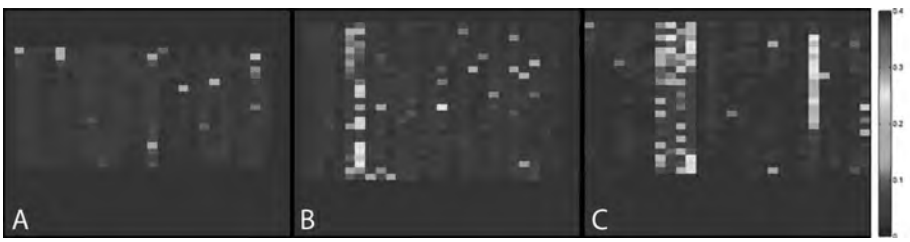

Figure 6 – Outlier profile for different datasets. Outliers are only depicted for those sections that contain >1000 voxels with signal intensity. **A**, dataset without gross motion artifacts; **B**, dataset with one corrupted gradient direction, and **C**, dataset with multiple corrupted gradient directions. Scaling is for 0–40% outliers. (A full color version of this illustration can be found in the color section).

The tensor estimation model also enables possibilities to spot artifacts by means of residuals of the tensor fit and calculation of data outliers. Residuals represent the difference between fit and data signal, with high residuals indicating either a poor estimation model or underlying data artifacts. The average residual maps as depicted in Fig 4 are helpful to detect and locate artifacts assuming that high residuals are caused by artifacts and that good image data result in an homogeneous residuals map[20]. High residuals are generally found in areas with partial volume effects (rims) and in regions with low signal intensities[20] and therefore one should extra carefully interpret results from those regions.

In addition, the residuals are used to detect signal outliers. The location and extent of outliers is a functional tool to investigate DTI quality. The example in Fig 5 shows that two DTI volumes have a high percentage of outliers, which corresponds to corrupted images. We have found that determining the volumes and sections with high percentage outliers is an excellent method to assess data corruption caused by gross motion[50]. However, labeling a point as an outlier also is dependent on the presence or absence of other (larger) outliers. Indeed, one expects a more or less even distribution of outliers with high-quality data, whereas corrupted sections cause a significant increase in outliers (Fig 6). Further research is needed to determine the relation between distribution of outliers and resulting parameter maps, the needed processing steps and suitability of a dataset for further analysis.

Data analysis

After computation of the tensor estimates, parametric maps can be used for further data analysis to assess WM integrity or structure. Commonly used techniques are region of interest selection, voxel-based analysis, tract-based spatial statistics (TBSS) and fiber tractography. Region of interest selection is used to compare WM properties within a specific region of the brain. The lower number of comparisons between subjects increases statistical power and small differences between subjects may be found. The technique is also independent of individual variations in shape and size of the brain. Major limitations include reliance on accuracy of the region of interest placement, the likelihood of missing differences in regions that are not included, its time-consuming nature when regions of interest are manually drawn and the observer dependency.

Whole-brain analysis can be performed with voxel-based analyses, in which all voxels are analyzed in terms of a tensor estimate. Because of individual variation in size and shape of the brain, all individual brains must first be aligned to a template (normalization) before they can be compared[57, 58]. Normalization is the main challenge in voxel-based analysis because inaccurate normalization results in incorrect comparison of individuals[59]. This is particularly problematic in patients with cerebral injuries where normalization results in distortion of the brains. TBSS overcomes this limitation by aligning the FA images from multiple subjects to a "mean FA skeleton". With this technique, only voxels are included that are at the center of

tracts common to all individuals in the population. Because voxels with poor alignment are excluded, one of the limitations of this strategy is that it may miss variations in the periphery of WM tracts. Other limitations and concerns related to TBSS have been addressed by others[60, 61].

Fiber tractography enables delineation and comparison of orientation and direction of a specific WM tract between individuals. This method is independent of variation in brain organization. In the deterministic approach[62], the algorithm moves in the direction of the principal eigenvector (ε_1); this is assumed to be parallel to the dominant fiber orientation in each voxel. The main limitation of deterministic tractography is uncertainty about the reliability of a reconstructed trajectory. Probabilistic tractography takes the uncertainty in ε_1 into account by propagating a distribution of possible orientations from the seed point[63]. Although probabilistic tractography seems more reliable, it remains dependent on the placement of seed points, which is manually done[3, 12, 35, 64-66].

Although these analytic measurements provide in vivo information about orientation, organization and microstructural properties of cerebral WM, DTI analysis remains a proxy technique and not a direct visualization of WM. Moreover, because tensor estimations are subject to error, we emphasize the importance of appropriate acquisition settings with regard to gestational age, a quality check before post processing, reliable post processing techniques and good knowledge of neuro-anatomy[35].

DTI quality and pathology

Investigating DTI results with pathology brings out the importance of accurate data acquisition, processing and data interpretation. Fig 7 shows two examples of DTI measurements: a patient with a middle cerebral artery infarct and a patient diagnosed with massive cerebral infarction, both scanned within days after injury. Large portions of the brain are affected and these consequently have lower MD values as a result of edema. These datasets appear to be of lesser quality in terms of outliers and residuals than the non-pathologic datasets without motion corruption. However, a closer look reveals that outliers are randomly distributed in time and that residuals are high in areas with low MD values. This is expected as diffusivities in the pathological areas are lower and therefore the *b*-value might not be optimal to accurately determine MD and FA values in these areas. Although data quality assurance is not directly a vital issue for clinical practice, in which the main goal is to visualize areas with altered MD and FA values, it is imperative for analysis of DTI values to exclude any bias in DTI indices.

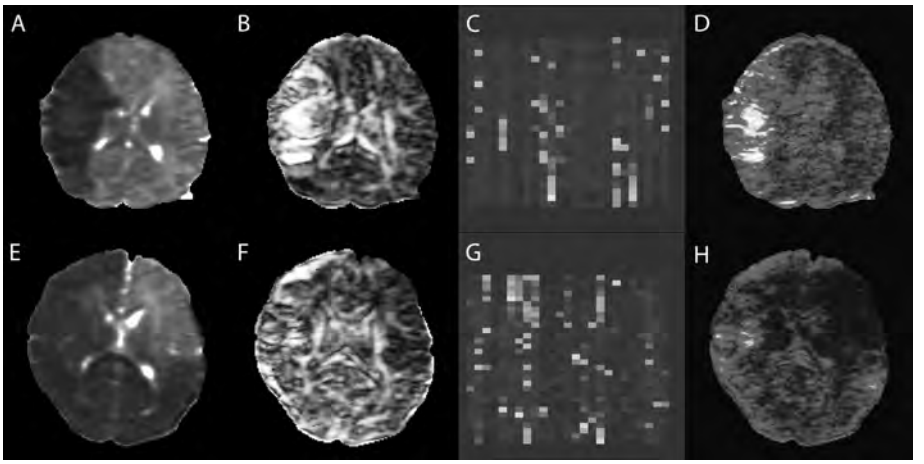

Figure 7 – Quality assessment in two term-born neonates with brain pathology. The damaged brain areas have much lower mean diffusivity (MD) (**A** and **E**) and apparent high fractional anisotropy (FA) (**B** and **F**) values. The percentage outliers (**C** and **G**) are low and are distributed uniformly. Because the residuals are also dependent on the underlying MD and FA values, they (**D** and **H**) are large in the damaged areas. Scaling: MD, 0–2 x 10^{-3} mm^2/s; FA, 0–1; outliers, 0–40%. (A full color version of this illustration can be found in the color section).

Conclusion

High-quality, quantitative data are essential to ensure reliable and meaningful imaging findings. Both data quality and analysis will improve with the use of protocols and image-processing tools specifically designed for neonatal imaging, seeing that tissue composition and occurrence of artifacts in neonates are significantly different from those in the adult population. Optimized acquisition and targeted processing will increase the diagnostic and prognostic value of scans but will also considerably improve intervention or outcome studies because a reduced data spread will lead to stronger correlations, less required study subjects and earlier determination of valuable intervention methods.

References

1. Counsell SJ, Rutherford MA, Cowan FM, Edwards AD. Magnetic resonance imaging of preterm brain injury. *Arch Dis Child Fetal Neonatal Ed* 2003;88:F269-74.
2. Huppi PS, Barnes PD. Magnetic resonance techniques in the evaluation of the newborn brain. *Clin Perinatol* 1997;24:693-723.
3. Ment LR, Hirtz D, Huppi PS. Imaging biomarkers of outcome in the developing preterm brain. *Lancet Neurol* 2009;8:1042-55.
4. Lequin MH, Dudink J, Tong KA, Obenaus A. Magnetic resonance imaging in neonatal stroke. *Semin Fetal Neonatal Med* 2009;14:299-310.
5. Skiold B, Horsch S, Hallberg B, Engstrom M, Nagy Z, Mosskin M, Blennow M, Aden U. White matter changes in extremely preterm infants, a population-based diffusion tensor imaging study. *Acta Paediatr* 2010;99:842-9.
6. Gimenez M, Miranda MJ, Born AP, Nagy Z, Rostrup E, Jernigan TL. Accelerated cerebral white matter development in preterm infants: a voxel-based morphometry study with diffusion tensor MR imaging. *Neuroimage* 2008;41:728-34.
7. Basser PJ, Mattiello J, LeBihan D. Estimation of the effective self-diffusion tensor from the NMR spin echo. *Journal of magnetic resonance* 1994;103:247-54.
8. Pierpaoli C, Jezzard P, Basser PJ, Barnett A, Di Chiro G. Diffusion tensor MR imaging of the human brain. *Radiology* 1996;201:637-48.
9. Le Bihan D, van Zijl P. From the diffusion coefficient to the diffusion tensor. *NMR in biomedicine* 2002;15:431-4.
10. Mori S, van Zijl PC. Fiber tracking: principles and strategies - a technical review. *NMR in biomedicine* 2002;15:468-80.
11. Jones DK, Leemans A. Diffusion tensor imaging. *Methods Mol Biol* 2011;711:127-44.
12. Dudink J, Kerr JL, Paterson K, Counsell SJ. Connecting the developing preterm brain. *Early Hum Dev* 2008;84:777-82.
13. Anjari M, Srinivasan L, Allsop JM, Hajnal JV, Rutherford MA, Edwards AD, Counsell SJ. Diffusion tensor imaging with tract-based spatial statistics reveals local white matter abnormalities in preterm infants. *Neuroimage* 2007;35:1021-7.
14. Bassi L, Chew A, Merchant N, Ball G, Ramenghi L, Boardman J, Allsop JM, Doria V, Arichi T, Mosca F, Edwards AD, Cowan FM, Rutherford MA, Counsell SJ. Diffusion tensor imaging in preterm infants with punctate white matter lesions. *Pediatr Res* 2011;69:561-6.
15. van Kooij BJ, van Pul C, Benders MJ, van Haastert IC, de Vries LS, Groenendaal F. Fiber tracking at term displays gender differences regarding cognitive and motor outcome at 2 years of age in preterm infants. *Pediatr Res* 2011;70:626-32.
16. Bassi L, Ricci D, Volzone A, Allsop JM, Srinivasan L, Pai A, Ribes C, Ramenghi LA, Mercuri E, Mosca F, Edwards AD, Cowan FM, Rutherford MA, Counsell SJ. Probabilistic diffusion tractography of the optic radiations and visual function in preterm infants at term equivalent age. *Brain* 2008;131:573-82.
17. Drobyshevsky A, Bregman J, Storey P, Meyer J, Prasad PV, Derrick M, MacKendrick W, Tan S. Serial diffusion tensor imaging detects white matter changes that correlate with motor outcome in premature infants. *Dev Neurosci* 2007;29:289-301.

18. van Kooij BJ, de Vries LS, Ball G, van Haastert IC, Benders MJ, Groenendaal F, Counsell SJ. Neonatal tract-based spatial statistics findings and outcome in preterm infants. *AJNR Am J Neuroradiol* 2012;33:188-94.
19. Jones DK, Cercignani M. Twenty-five pitfalls in the analysis of diffusion MRI data. *NMR in biomedicine* 2010;23:803-20.
20. Tournier JD, Mori S, Leemans A. Diffusion tensor imaging and beyond. *Magn Reson Med* 2011;65:1532-56.
21. Johansen-Berg H, Behrens TE, editors. Diffusion MRI: From quantitative measurement to in-vivo neuroanatomy 2009.
22. Jones DK, Horsfield MA, Simmons A. Optimal strategies for measuring diffusion in anisotropic systems by magnetic resonance imaging. *Magn Reson Med* 1999;42:515-25.
23. Battin M, Maalouf EF, Counsell S, Herlihy A, Hall A, Azzopardi D, Edwards AD. Physiological stability of preterm infants during magnetic resonance imaging. *Early Hum Dev* 1998;52:101-10.
24. Benavente-Fernandez I, Lubian-Lopez PS, Zuazo-Ojeda MA, Jimenez-Gomez G, Lechuga-Sancho AM. Safety of magnetic resonance imaging in preterm infants. *Acta Paediatr* 2010;99:850-3.
25. Merchant N, Groves A, Larkman DJ, Counsell SJ, Thomson MA, Doria V, Groppo M, Arichi T, Foreman S, Herlihy DJ, Hajnal JV, Srinivasan L, Foran A, Rutherford M, Edwards AD, Boardman JP. A patient care system for early 3.0 Tesla magnetic resonance imaging of very low birth weight infants. *Early Hum Dev* 2009;85:779-83.
26. Plaisier A, Raets MM, van der Starre C, Feijen-Roon M, Govaert P, Lequin MH, Heemskerk AM, Dudink J. Safety of routine early MRI in preterm infants. *Pediatr Radiol* 2012;42:1205-11.
27. Keil B, Alagappan V, Mareyam A, McNab JA, Fujimoto K, Tountcheva V, Triantafyllou C, Dilks DD, Kanwisher N, Lin W, Grant PE, Wald LL. Size-optimized 32-channel brain arrays for 3 T pediatric imaging. *Magn Reson Med* 2011;66:1777-87.
28. Legendre V, Burtner PA, Martinez KL, Crowe TK. The Evolving Practice of Developmental Care in the Neonatal Unit: A Systematic Review. *Phys Occup Ther Pediatr* 2011;31:315-38.
29. Neubauer V, Griesmaier E, Baumgartner K, Mallouhi A, Keller M, Kiechl-Kohlendorfer U. Feasibility of cerebral MRI in non-sedated preterm-born infants at term-equivalent age: report of a single centre. *Acta Paediatr* 2011;100:1544-7.
30. Nordell A, Lundh M, Horsch S, Hallberg B, Aden U, Nordell B, Blennow M. The acoustic hood: a patient-independent device improving acoustic noise protection during neonatal magnetic resonance imaging. *Acta Paediatr* 2009;98:1278-83.
31. Holland BA, Haas DK, Norman D, Brant-Zawadzki M, Newton TH. MRI of normal brain maturation. *AJNR Am J Neuroradiol* 1986;7:201-8.
32. Counsell SJ, Kennea NL, Herlihy AH, Allsop JM, Harrison MC, Cowan FM, Hajnal JV, Edwards B, Edwards AD, Rutherford MA. T2 relaxation values in the developing preterm brain. *AJNR Am J Neuroradiol* 2003;24:1654-60.
33. Kumar R, Delshad S, Macey PM, Woo MA, Harper RM. Development of T2-relaxation values in regional brain sites during adolescence. *Magn Reson Imaging* 2011;29:185-93.
34. Vos SB, Jones DK, Viergever MA, Leemans A. Partial volume effect as a hidden covariate in DTI analyses. *Neuroimage* 2011;55:1566-76.
35. Mukherjee P, Chung SW, Berman JI, Hess CP, Henry RG. Diffusion tensor MR imaging and fiber tractography: technical considerations. *AJNR Am J Neuroradiol* 2008;29:843-52.

36. Reese TG, Heid O, Weisskoff RM, Wedeen VJ. Reduction of eddy-current-induced distortion in diffusion MRI using a twice-refocused spin echo. *Magn Reson Med* 2003;49:177-82.
37. Pierpaoli C, Basser PJ. Toward a quantitative assessment of diffusion anisotropy. *Magn Reson Med* 1996;36:893-906.
38. Damon BM. Effects of image noise in muscle diffusion tensor (DT)-MRI assessed using numerical simulations. *Magn Reson Med* 2008;60:934-44.
39. Chenevert TL, Galban CJ, Ivancevic MK, Rohrer SE, Londy FJ, Kwee TC, Meyer CR, Johnson TD, Rehemtulla A, Ross BD. Diffusion coefficient measurement using a temperature-controlled fluid for quality control in multicenter studies. *J Magn Reson Imaging* 2011;34:983-7.
40. Bammer R, Schoenberg SO. Current concepts and advances in clinical parallel magnetic resonance imaging. *Top Magn Reson Imaging* 2004;15:129-58.
41. Jones DK. The effect of gradient sampling schemes on measures derived from diffusion tensor MRI: a Monte Carlo study. *Magn Reson Med* 2004;51:807-15.
42. Cook PA, Symms M, Boulby PA, Alexander DC. Optimal acquisition orders of diffusion-weighted MRI measurements. *J Magn Reson Imaging* 2007;25:1051-8.
43. Dubois J, Poupon C, Lethimonnier F, Le Bihan D. Optimized diffusion gradient orientation schemes for corrupted clinical DTI data sets. *MAGMA* 2006;19:134-43.
44. Leemans A, Jones DK. The B-matrix must be rotated when correcting for subject motion in DTI data. *Magn Reson Med* 2009;61:1336-49.
45. Ling J, Merideth F, Caprihan A, Pena A, Teshiba T, Mayer AR. Head injury or head motion? Assessment and quantification of motion artifacts in diffusion tensor imaging studies. *Hum Brain Mapp* 2012;33:50-62.
46. Pierpaoli C, Marenco S, Rohde G, Jones DK, Barnett AS. Analyzing the contribution of cardiac pulsation to the variability of quantities derived from the diffusion tensor. ISMRM; 2003; Toronto, Canada; 2003. p. 70.
47. Zhou Z, Liu W, Cui J, Wang X, Arias D, Wen Y, Bansal R, Hao X, Wang Z, Peterson BS, Xu D. Automated artifact detection and removal for improved tensor estimation in motion-corrupted DTI data sets using the combination of local binary patterns and 2D partial least squares. *Magn Reson Imaging* 2011;29:230-42.
48. Dudink J, Lequin M, van Pul C, Buijs J, Conneman N, van Goudoever J, Govaert P. Fractional anisotropy in white matter tracts of very-low-birth-weight infants. *Pediatr Radiol* 2007;37:1216-23.
49. Morris D, Nossin-Manor R, Taylor MJ, Sled JG. Preterm neonatal diffusion processing using detection and replacement of outliers prior to resampling. *Magn Reson Med* 2011;66:92-101.
50. Heemskerk AM, Plaisier A, Reiss I, Lequin M, Leemans A, Dudink J. DTI in neonates: data corruption due to motion. ISMRM; 2012; Melbourne; 2012.
51. Tofts PS, Lloyd D, Clark CA, Barker GJ, Parker GJ, McConville P, Baldock C, Pope JM. Test liquids for quantitative MRI measurements of self-diffusion coefficient in vivo. *Magn Reson Med* 2000;43:368-74.
52. Kozak LR, Bango M, Szabo M, Rudas G, Vidnyanszky Z, Nagy Z. Using diffusion MRI for measuring the temperature of cerebrospinal fluid within the lateral ventricles. *Acta Paediatr* 2010;99:237-43.
53. Aksoy M, Forman C, Straka M, Skare S, Holdsworth S, Hornegger J, Bammer R. Real-time optical motion correction for diffusion tensor imaging. *Magn Reson Med* 2011;66:366-78.
54. Chang LC, Jones DK, Pierpaoli C. RESTORE: robust estimation of tensors by outlier rejection. *Magn Reson Med* 2005;53:1088-95.

55. Smith SM, Jenkinson M, Woolrich MW, Beckmann CF, Behrens TE, Johansen-Berg H, Bannister PR, De Luca M, Drobnjak I, Flitney DE, Niazy RK, Saunders J, Vickers J, Zhang Y, De Stefano N, Brady JM, Matthews PM. Advances in functional and structural MR image analysis and implementation as FSL. *Neuroimage* 2004;23 Suppl 1:S208-19.
56. Koay CG, Chang LC, Carew JD, Pierpaoli C, Basser PJ. A unifying theoretical and algorithmic framework for least squares methods of estimation in diffusion tensor imaging. *J Magn Reson* 2006;182:115-25.
57. Van Hecke W, Leemans A, D'Agostino E, De Backer S, Vandervliet E, Parizel PM, Sijbers J. Nonrigid coregistration of diffusion tensor images using a viscous fluid model and mutual information. *IEEE Trans Med Imaging* 2007;26:1598-612.
58. Van Hecke W, Sijbers J, D'Agostino E, Maes F, De Backer S, Vandervliet E, Parizel PM, Leemans A. On the construction of an inter-subject diffusion tensor magnetic resonance atlas of the healthy human brain. *Neuroimage* 2008;43:69-80.
59. Van Hecke W, Leemans A, Sage CA, Emsell L, Veraart J, Sijbers J, Sunaert S, Parizel PM. The effect of template selection on diffusion tensor voxel-based analysis results. *Neuroimage* 2011;55:566-73.
60. Edden RA, Jones DK. Spatial and orientational heterogeneity in the statistical sensitivity of skeleton-based analyses of diffusion tensor MR imaging data. *J Neurosci Methods* 2011;201:213-9.
61. Van Hecke W, Leemans A, De Backer S, Jeurissen B, Parizel PM, Sijbers J. Comparing isotropic and anisotropic smoothing for voxel-based DTI analyses: A simulation study. *Hum Brain Mapp* 2010;31:98-114.
62. Basser PJ, Pajevic S, Pierpaoli C, Duda J, Aldroubi A. In vivo fiber tractography using DT-MRI data. *Magn Reson Med* 2000;44:625-32.
63. Jones DK. Tractography gone wild: probabilistic fibre tracking using the wild bootstrap with diffusion tensor MRI. *IEEE Trans Med Imaging* 2008;27:1268-74.
64. Feldman HM, Yeatman JD, Lee ES, Barde LH, Gaman-Bean S. Diffusion tensor imaging: a review for pediatric researchers and clinicians. *J Dev Behav Pediatr* 2010;31:346-56.
65. Jones DK. Studying connections in the living human brain with diffusion MRI. *Cortex* 2008;44:936-52.
66. Huppi PS, Dubois J. Diffusion tensor imaging of brain development. *Semin Fetal Neonatal Med* 2006;11:489-97.

CHAPTER 5

Choice of Diffusion Tensor Estimation Approach Affects Fiber Tractography of the Fornix in the Preterm Brain

A. Plaisier
K. Pieterman
M.H. Lequin
P. Govaert
A.M. Heemskerk
I.K.M. Reiss
G.P. Krestin
A. Leemans
J. Dudink

American Journal of Neuroradiology, January 2014

Abstract

Background

Neonatal diffusion tensor imaging (DTI) enables quantitative assessment of microstructural brain properties. Although its use is increasing, it is not widely known that vast differences in tractography results can occur, depending on the used diffusion tensor estimation methodology. Current clinical work seems insufficiently focused on data quality and processing of neonatal DTI. To raise awareness about this important processing step, we investigated tractography reconstructions of the fornix using several estimation techniques. We hypothesized that the method of tensor estimation significantly affects DTI tractography results.

Methods

28 DTI scans of infants born <29 weeks' of gestation, acquired at 30 weeks' postmenstrual age and without intracranial injury observed, were prospectively collected. This study was approved by the institutional review board and informed consent was obtained. Four diffusion tensor estimation methods were applied: 1) linear least squares (LLS); 2) weighted linear least squares (WLLS); 3) non-linear least squares (NLLS), and 4) robust estimation of tensors by outlier rejection (RESTORE). Quality of DTI data and tractography results were evaluated for each method.

Results

With NLLS and RESTORE, significantly lower mean FA values were obtained than with LLS and WLLS. Visualized quality of tract reconstruction was significantly higher using RESTORE and correlated with quality of DTI data.

Conclusion

Quality assessment and choice of processing methodology have considerable impact on neonatal DTI analysis. Dedicated acquisition, quality assessment and advanced processing of neonatal DTI data must be assured prior to performing clinical analyses, such as associating microstructural brain properties with patient outcome.

Introduction

Diffusion tensor imaging (DTI) enables in vivo assessment of white matter (WM) microstructure and has become essential for quantification of brain abnormalities as it has been suggested to provide early biomarkers of neurodevelopment[1]. Fiber tractography has the unique property to delineate specific WM pathways and is rapidly gaining in popularity because it may reveal substantial insights into disturbed brain connectivity and functionality of infants born preterm[2-4].

There are many technical issues that may complicate the analysis of DTI data, including scanner type, hardware setup, acquisition parameters and processing methodology[5, 6]. In addition, DTI applied in preterm infants is especially challenging because of specific clinical factors, such as the increased risk of subject motion, hemodynamic vulnerability, smaller head sizes and higher heart and breathing rates compared to healthy adults. Therefore, before associations between tractography results and neurodevelopmental outcome can be established, it is of paramount importance that acquisition and processing of DTI data are performed with the highest standards possible[7, 8]. For example, different algorithms to estimate the diffusion tensor have been developed. These methods differ considerably in processing speed and dealing with data outliers. For instance, the linear least squares (LLS) method is widely used to estimate diffusion parameters, but may lead to inaccuracy as it incorrectly assumes that data outliers are homogeneously distributed. Furthermore, there seems no consensus on how to practically define and handle data outliers.

Awareness of these matters is essential because improper use may lead to inaccuracy, especially if data are compared when different estimation methods have been used. Unfortunately, however, the majority of studies using preterm brain DTI data have hardly focused on these important aspects, calling for a thorough investigation.

In this study, trajectories of the fornix were reconstructed with fiber tractography for 28 preterm infants and compared when different diffusion tensor estimation approaches were used. Our hypothesis was that the chosen tensor estimation methodology significantly affects results of fiber tractography. This would demonstrate that an informed choice of diffusion tensor estimation is crucial for a reliable tractography analysis, which is especially relevant when artifact-sensitive DTI data of the preterm brain are involved.

Methods

This study was approved by the institutional review board. Written informed parental consent was obtained for all subjects.

Subjects

Between February 2011 and December 2012, preterm infants born before a gestational age of 29 weeks were recruited prospectively. Magnetic resonance imaging (MRI) data were acquired at a postmenstrual age of 30 weeks (29 4/7 – 30 4/7 weeks). In order to avoid unnecessary data heterogeneity, infants with evidence of intracranial injury (intraventricular or cerebellar hemorrhage, WM abnormalities) observed with conventional MRI (see T1- and T2-weighted imaging protocols below) were excluded.

Of the 217 eligible infants, 36 died before 30 weeks postmenstrual age. In 82 infants, the MRI scan could not be performed at 30 weeks postmenstrual age because of hemodynamic instability or logistic circumstances and informed parental consent was not obtained for 20 infants. Of the remaining 79 infants, 36 had intracranial abnormalities and 15 others were excluded from further analysis because different DTI acquisition settings were applied. This eventually resulted in 28 usable data sets.

Imaging

MRI procedures were carried out according to protocol[9]: all infants were accompanied by trained staff only and were positioned in an MRI-compatible incubator (Lammers Medical Technology GmbH, Luebeck, Germany) that provided controlled temperature and humidity, MR-compatible pulse oximetry and MR-compatible ventilation. Moldable earplugs and neonatal earmuffs protected the infants from auditory noise, no sedation was given.

Imaging data were acquired with a 1.5-T GE EchoSpeed scanner (GE Healthcare Technologies, Waukesha, USA). Axial T2-weigthed fast spin-echo was obtained with the following parameter settings: repetition time (TR): 13100 ms; echo time (TE): 139 ms; flip angle: 90°; slice thickness: 1.2 mm; field of view (FOV): 190 x 190 mm^2; acquisition matrix: 256 x 224; reconstruction matrix: 256 x 256 (voxel size: 0.74 x 0.74 x 1.23 mm^3), acquisition time was 2:58 minutes. Axial 3D T1-SPGR MRI data were acquired using: TR: 9 ms; TE: 3 ms; flip angle: 15°; slice thickness: 1.6 mm; FOV: 150 x 150 mm^2; acquisition matrix: 224 x 224; reconstruction matrix 256 x 256 (voxel size: 0.59 x 0.59 x 1.6 mm^3), acquisition time was 3:10 minutes. DTI was performed using a single-shot echo planar imaging (EPI) sequence with diffusion gradients in 25 non-collinear directions, TR: 11725 ms; TE: 85.6 ms; slice thickness: 3 mm; FOV: 220 x 220 mm^2; acquisition matrix: 128 x 64; reconstruction matrix 256 x 256 (voxel size: 0.86 x 0.86 x 3 mm^3);

b value: 750 s/mm^2; number of non-diffusion weighted images: 3, acquisition time was 5:17 minutes.

Data processing

DTI data were analyzed with *ExploreDTI* (http://www.exploredti.com)[10] version 4.8.3. The diffusion weighted images were first corrected for eddy currents, EPI distortion and patient movement[11, 12]. The diffusion tensor was then estimated according to four different methods: 1) LLS; 2) weighted linear least squares (WLLS); 3) nonlinear least squares (NLLS), and 4) robust estimation of tensors by outlier rejection (RESTORE)[13-15]. Next, whole-brain tractography was performed for all data sets with the following parameters: fractional anisotropy (FA) threshold: 0.08; fiber length range: 15–500 mm; angle threshold 30˚ and step size: 1 mm[16].

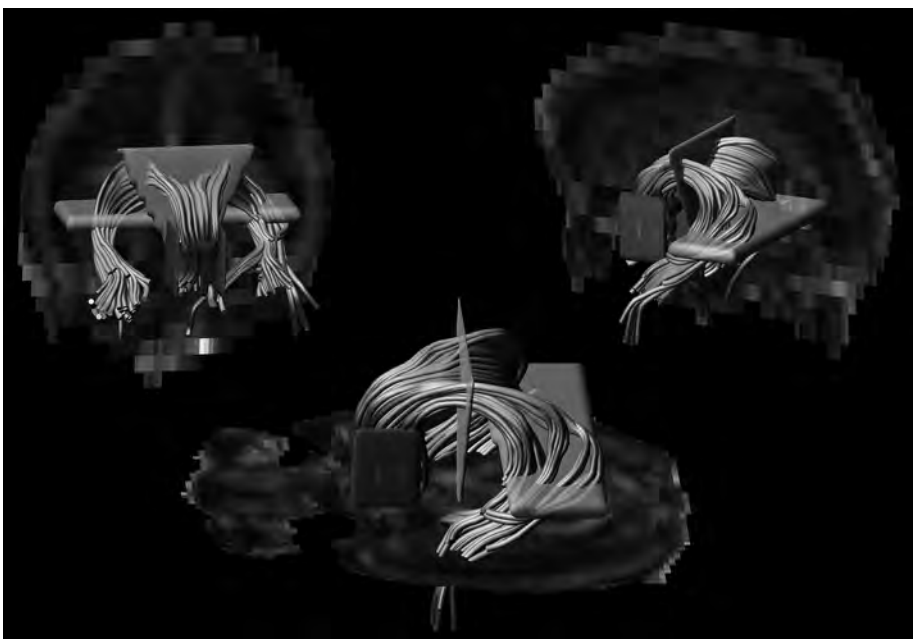

Figure 1 – Placement of regions of interests (ROIs). Tractography of the fornix was performed by placing one "OR" ROI (in blue), two "AND" ROIs (in green) and two "NOT" ROIs (in red) on color-coded fractional anisotropy maps. (A full color version of this illustration can be found in the color section).

Without loss of generality of this work, a single WM structure was investigated. Because of its important relation to cognition[17, 18] and high tracking reproducibility due to its unique shape, we performed tractography of the fornix. Region of interest (ROI) placement was done on the color-coded FA maps[19]: 1) one "OR" ROI was placed in the axial plane at the level of the bilateral columns of the fornix, above the mammillary bodies; 2) two "AND" ROIs were placed:

a) in the coronal plane to encompass the corpus of the fornix, and b) in the axial plane to include both crura of the fornix in the same slice where the "OR" ROI was placed, and 3) two "NOT" ROIs were placed in the sagittal plane laterally to the seed region to exclude fibers from the anterior commissure[20] (Fig 1). For each subject, tractography was repeated for each method of tensor estimation while using the same subject-specific ROIs.

Data analysis

Quality of the diffusion weighted images was assessed with the outlier profiles of each data set, after diffusion tensor estimation using RESTORE (see Fig 2). The mean percentage of outliers per data set was calculated by averaging the percentage artifacted voxels across the diffusion gradient orientation[6]. In addition, tract parameters, including mean FA, mean diffusivity, mean fiber trajectory length (in mm) and number of fiber trajectories were computed for each dataset.

Quality of tractography was visually and systematically evaluated by two authors independently. Both reviewers were blinded to the method of tensor estimation. Final score was the average of both total scores and ranged from 0 to 10 (Table 1).

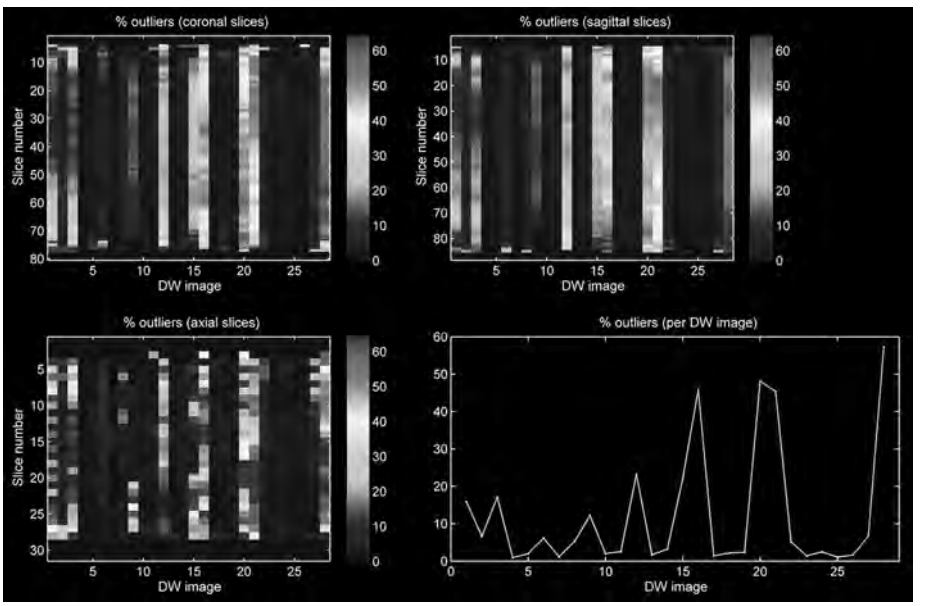

Figure 2 – Outlier profile of DTI data with high percentage of outliers. (A full color version of this illustration can be found in the color section).

Statistical analysis was performed using SPSS version 20.0.0.1 (IBM SPSS Statistics, New York, USA). Intraclass correlation between both observers were calculated using two-way mixed model. Coefficients <0 were considered as no agreement; 0–0.20 as slight; 0.21–0.40 as fair; 0.41–0.60 as moderate; 0.61–0.80 as substantial, and 0.81–1 as almost perfect agreement[21]. Spearman's correlation coefficient was used to investigate the correlation between the visualized quality of tract reconstruction and the mean outlier percentage per data set. Independent sample T-tests served to test differences in visualized quality of tract reconstruction between data with <10% and >10% data outliers. Repeated measures ANOVA served to test differences in tract parameters between the diffusion tensor estimation methods respectively. Difference in variability of tract parameters between the estimation techniques was tested with Levene's test for equality of variances. A *p*-value of <0.05 (two-sided) was considered statistically significant.

Table 1: Scoring system for visual evaluation of tract reconstruction of the fornix

	0 points	**1 points**	**2 points**
Shape of the fornix*	No recognition of shape	Partially abnormal shape	Normal shape
Orientation of fibers*	Complete disorientation	Partially abnormal orientation	Normal orientation
Symmetry of crura	One missing crus	Partially asymmetric	Normal symmetry
Presence of non-realistic fibers*	Outweighing total number of fibers	Less than number of realistic fibers	None
Number of fiber trajectories	< 10	10-100	>100

Note: – * Shape, orientation and presence of non-realistic fibers with regard to description of anatomy by Nieuwenhuys et al., The human central nervous system, 2008.

Results

Patient characteristics

28 infants (15 boys) were included in this study. Mean gestational age and birth weight were 27.7 weeks (SD: 1.1 weeks) and 1053 grams (SD: 256 grams) respectively. Mean postmenstrual age at image acquisition was 30.0 weeks (SD: 0.3 weeks). The mean percentage of outliers per data set was 10.1% (SD: 1.3%).

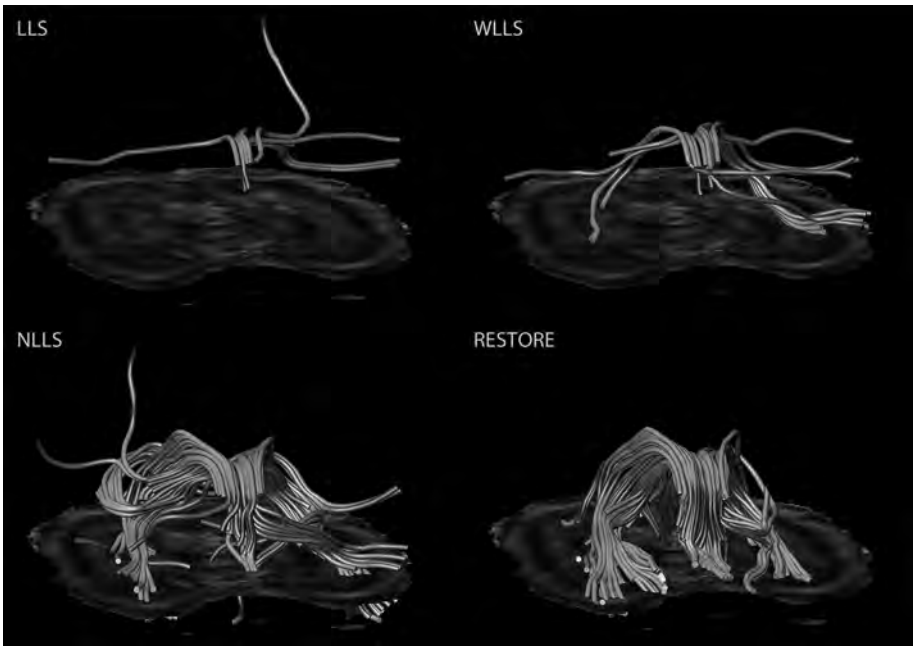

Figure 3 – Impact of diffusion tensor estimation method on tract reconstruction of poor-quality DTI data. Characteristic representations to illustrate the effect of tensor estimation methodology on reconstruction of the fornix with high percentage of data outliers (>10%). Note that reconstruction is not possible using the linear least squares (LLS) and weighted linear least squares (WLLS) methods, seems slightly possible with non-linear least squares (NLLS), but is very well performed if the robust estimation of tensors by outlier rejection (RESTORE) approach is used. (A full color version of this illustration can be found in the color section).

Outlier evaluation

Figure 3 and 4 are characteristic representations of data with poor and good quality of data, respectively.

Interclass correlation between observers showed excellent agreement with high significance (intraclass correlation coefficient: 0.87, 95% confidence interval: 0.82–0.91, p-value <0.01). Although there was some overlap among the methods of tensor estimation, visualized quality of reconstruction of the fornix was significantly higher using the RESTORE algorithm, particularly in data sets with high percentage (>10%, n = 13) of data outliers (Fig 5).

Visualized quality of tract reconstruction across all tensor estimation methods depended also on the presence of data artifacts as tract quality was significantly correlated to the mean outlier percentage per data set (Spearman's correlation coefficient: -0.46; *p*-value: <0.01). This correlation was also tested for each tensor estimation method separately. The following Spearman's coefficients were found: LLS: -0.48 (*p*-value: 0.01); WLLS: -0.47 (*p*-value: 0.01); NLLS: -0.57 (*p*-value: <0.01), and RESTORE: -0.36 (*p*-value: 0.06).

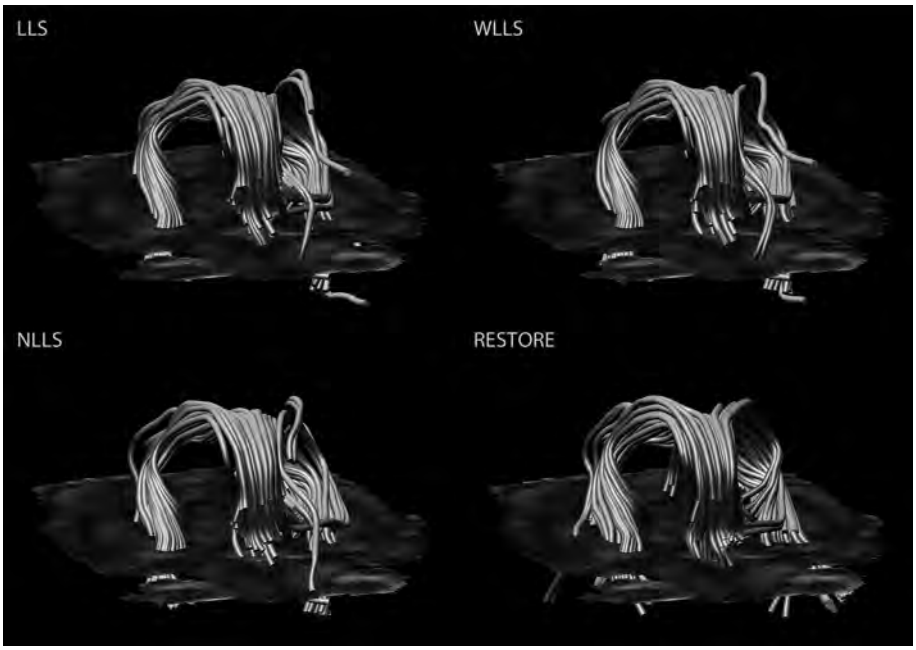

Figure 4 – Impact of diffusion tensor estimation method on tract reconstruction of good quality DTI data. Characteristic representations to illustrate the effect of the tensor estimation on fiber tracking of the fornix with low percentage of data outliers (<10%). Note the more accurate tract reconstruction using the RESTORE approach. (A full color version of this illustration can be found in the color section).

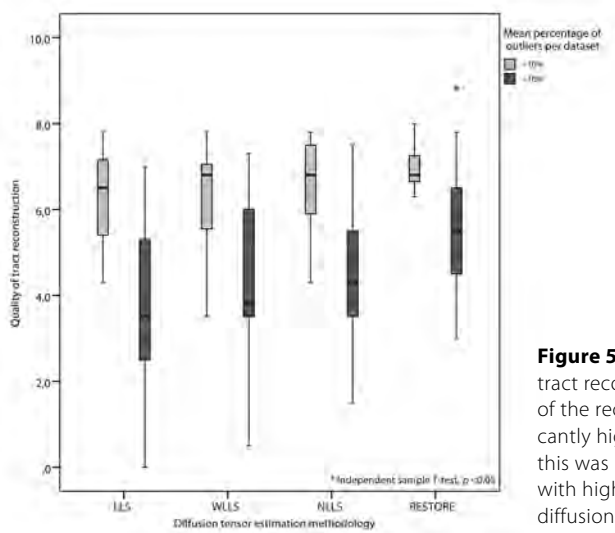

Figure 5 – Impact of DTI data quality on tract reconstruction of the fornix. Quality of the reconstructed fornix was significantly higher by the RESTORE technique, this was particular evident for data sets with high percentage of outliers in the diffusion weighted images (>10%).

Tract parameters

The impact of the used diffusion tensor estimation method on tract parameters is shown in Figure 6. There was a significant difference in mean FA value using different diffusion estimation algorithms. Significantly lower mean FA values were obtained with NLLS and RESTORE than with LLS and WLLS. Furthermore, application of the RESTORE approach resulted in the lowest standard deviation of the mean FA value; LLS: 0.059; WLLS: 0.054; NLLS: 0.052; RESTORE: 0.051 (Repeated measures ANOVA, *p*-values <.05). Although not statistically significant, there was a trend towards an increased number of fiber trajectories in the following order of tensor estimation approaches: LLS, WLLS, NLLS and RESTORE (Spearman's correlation coefficient: 0.10; *p*-value: 0.32).

Using LLS, variability of mean FA-values was significantly higher in data sets with more than 10% outliers compared to data sets with less than 10% outliers. With WLLS, NLLS or RESTORE, there was no difference in variability of mean FA-values with regard to the quality of the diffusion weighted images (Fig 7).

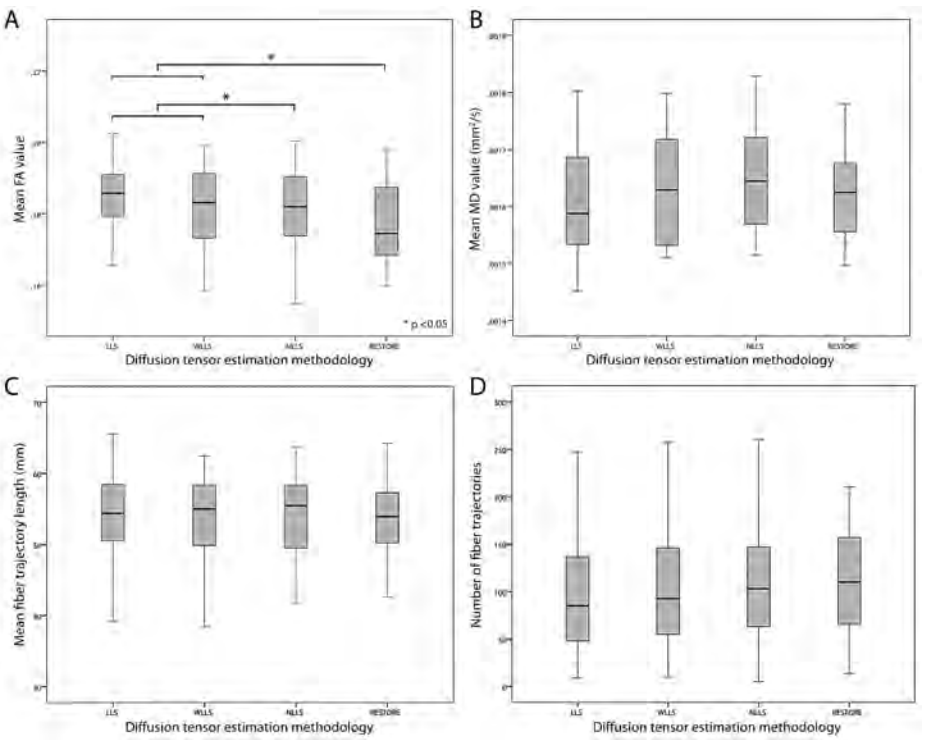

Figure 6 – Impact of diffusion tensor estimation method on tract parameters. Tract parameters, such as fractional anisotropy (A); mean diffusivity (B); mean fiber trajectory length (C), and number of fiber trajectories (D) were affected by the tensor estimation method. Mean FA value was significantly lower with the NLLS and RESTORE techniques (Paired sample T-test, p<0.05).

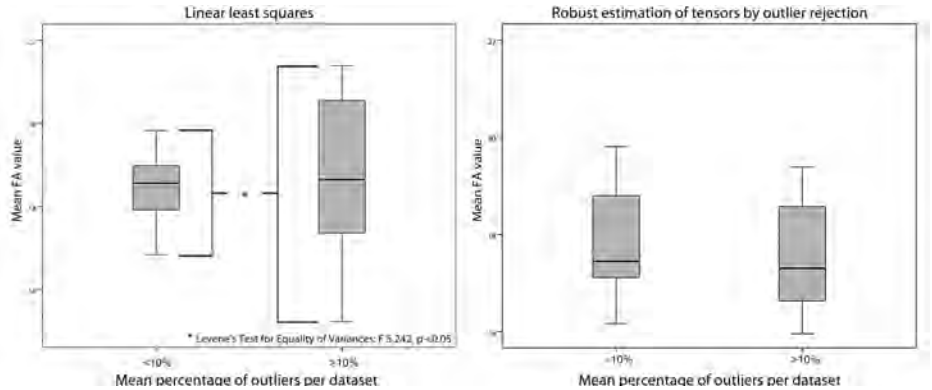

Figure 7 – Impact of data quality on variability of tract parameters. Diffusion weighted images with high outlier percentage (>10%) resulted in a significantly increased variability of mean fractional anisotropy values compared with data with fewer data outliers (<10%) is LLS was used (Levene's test for equality of variances, $p<0.05$). With application of RESTORE, there was no difference in variability with regard to data quality.

Discussion

This study emphasizes the paramount importance of quality assessment and dedicated use of processing methodology of neonatal DTI data prior to performing analysis. With our work, we demonstrated that: 1) tract parameters are significantly affected by the chosen tensor estimation method and are estimated more reliably if data outliers are handled carefully; 2) robust estimation of the diffusion tensor results in significantly improved visualized quality of fiber reconstruction; 3) the mean percentage of data outliers of the diffusion weighted images correlates significantly to visualized quality of tract reconstruction, and 4) data outliers are common and significantly affect subsequent DTI analysis if they are not taken into account.

Although the incidence of destructive types of brain injury with subsequent serious deficits is decreasing, preterm infants remain at considerable risk to develop cognitive and socio-emotional disabilities that persist into adolescence[22, 23]. Advanced MRI techniques, such as DTI, have already provided important valuable insights into WM microstructural properties of these "subtle" types of brain injury[1]. Still, the neuropathological correlates show high variation and inconsistency[23] and their workings are not completely understood[24]. Moreover, preterm infants are vulnerable to respiratory and hemodynamic instability and movement artifacts[7, 9]. So acquisition and processing of DTI data must be handled with dedicated care, which is essential to avoid misinterpretation. This is appropriately described in technical DTI papers[5-7, 25, 26], but, paradoxically, such work receives little attention in clinical research. This could be because of their emphasis on clinical results or more importantly, because of the lack of awareness that the choice of diffusion tensor estimation approach may affect subsequent reconstruction of fiber pathways.

As shown in this study, the choice of tensor estimation algorithms can significantly affect DTI tractography results, which may complicate interpretation of specific findings. In this context, study populations can only be compared reliably when identical processing pipelines have been applied, necessitating the use of standardized guidelines before drawing conclusions with regard to outcome.

Thus, strategies to limit image corruption should be incorporated into setups to acquire neonatal DTI data[27], this includes: 1) prevention of motion by comforting the infant and promoting natural sleep[28]; 2) adjustment of parameter settings, by shortening diffusion time, applying stronger gradients or by using lower b-values[7]; 3) oversampling gradient-sensitizing directions and removing corrupted diffusion weighted images[6], and 4) applying more advanced tensor estimation methods[5].

Because diffusion tensor estimation techniques differ considerably in principle, speed and accuracy[29], awareness of benefits and pitfalls is essential: the LLS method is fast and mostly used, but assumes that errors are identically distributed, which can result in inaccurate estimation of the tensor[30]. The WLLS method is slightly slower, but provides more accurate results as it considers errors to be heterogeneously distributed[31]. NLLS iteratively minimizes errors and results in more reliable estimation, but needs considerably longer processing time and may get stuck in local optima during optimization[5, 14]. The RESTORE approach automatically detects and removes outliers prior to tensor estimation. This avoids manual and subjective identification of corrupted diffusion weighted images and seems particularly valuable for data with frequent motion corruption[13, 26].

In summary, the reliability of DTI analyses is drastically improved when handling data outliers in an appropriate way. However, additional research is needed to determine what types of data processing can reliably be performed without affecting data quality. This paper presses the need for careful data handling as corrupted data can significantly impact final results. Although this will take longer processing time and perhaps the necessity to remove datasets completely, it will most likely decrease the spread in final analysis and therefore improve statistical significance and reduce sample size.

Limitations of this study are important to be addressed. First, only data sets without evidence of injury were used and this may have resulted in a selection bias. Although this policy provided a homogeneous study population, we did not investigate the impact of processing data sets with brain injury. Second, we applied an arbitrary boundary to define "good-quality" and "poor-quality" data: 10% data outliers. We used this threshold solely to illustrate the impact of poor data quality on DTI analysis. Hence, we do not suggest that this 10% level should be used as a threshold for future studies to define poor data quality.

In conclusion, as demonstrated with our tractography analysis of the fornix in the preterm brain, it is clear that the choice of diffusion tensor estimation methodology is crucial

and that it has a considerable impact on subsequent analyses for studying microstructural brain properties. Given the insufficient attention in the majority of clinical studies to date, this work raises the urgency to comply with the requirements to include state-of-the-art standardized research methodology wherever and whenever possible. Future studies should apply dedicated acquisition setups, standardized evaluation of data quality and reliable processing of neonatal DTI data prior to performing analyses, such as associating microstructural brain properties with outcome.

References

1. Ment LR, Hirtz D, Huppi PS. Imaging biomarkers of outcome in the developing preterm brain. *Lancet Neurol* 2009;8:1042-55.
2. Bassi L, Ricci D, Volzone A, Allsop JM, Srinivasan L, Pai A, Ribes C, Ramenghi LA, Mercuri E, Mosca F, Edwards AD, Cowan FM, Rutherford MA, Counsell SJ. Probabilistic diffusion tractography of the optic radiations and visual function in preterm infants at term equivalent age. *Brain* 2008;131:573-82.
3. Ball G, Boardman JP, Aljabar P, Pandit A, Arichi T, Merchant N, Rueckert D, Edwards AD, Counsell SJ. The influence of preterm birth on the developing thalamocortical connectome. *Cortex* 2013;34:1124-26.
4. van der Aa NE, Leemans A, Northington FJ, van Straaten HL, van Haastert IC, Groenendaal F, Benders MJ, de Vries LS. Does diffusion tensor imaging-based tractography at 3 months of age contribute to the prediction of motor outcome after perinatal arterial ischemic stroke? *Stroke* 2011;42:3410-4.
5. Jones DK, Cercignani M. Twenty-five pitfalls in the analysis of diffusion MRI data. *NMR Biomed* 2010;23:803-20.
6. Tournier JD, Mori S, Leemans A. Diffusion tensor imaging and beyond. *Magn Reson Med* 2011;65:1532-56.
7. Heemskerk AM, Leemans A, Plaisier A, Pieterman K, Lequin MH, Dudink J. Acquisition Guidelines and Quality Assessment Tools for Analyzing Neonatal Diffusion Tensor MRI Data. *AJNR Am J Neuroradiol* 2013;34:1496-505.
8. Kozak LR, David S, Rudas G, Vidnyanszky Z, Leemans A, Nagy Z. Investigating the need of triggering the acquisition for infant diffusion MRI: a quantitative study including bootstrap statistics. *Neuroimage* 2013;69:198-205.
9. Plaisier A, Raets MM, van der Starre C, Feijen-Roon M, Govaert P, Lequin MH, Heemskerk AM, Dudink J. Safety of routine early MRI in preterm infants. *Pediatr Radiol* 2012;42:1205-11.
10. Leemans A, Jeurissen B, Sijbers J, Jones DK. ExploreDTI: a graphical toolbox for processing, analyzing, and visualizing diffusion MR data. 17th Annual Meeting of Intl Soc Mag Reson Med. Honolulu, Hawaii, USA; 2009. p. 3537.
11. Leemans A, Jones DK. The B-matrix must be rotated when correcting for subject motion in DTI data. *Magn Reson Med* 2009;61:1336-49.
12. Irfanoglu MO, Walker L, Sarlls J, Marenco S, Pierpaoli C. Effects of image distortions originating from susceptibility variations and concomitant fields on diffusion MRI tractography results. *Neuroimage* 2012;61:275-88.
13. Chang LC, Jones DK, Pierpaoli C. RESTORE: robust estimation of tensors by outlier rejection. *Magn Reson Med* 2005;53:1088-95.
14. Jones DK, Basser PJ. "Squashing peanuts and smashing pumpkins": how noise distorts diffusion-weighted MR data. *Magn Reson Med* 2004;52:979-93.
15. Veraart J, Sijbers J, Sunaert S, Leemans A, Jeurissen B. Weighted linear least squares estimation of diffusion MRI parameters: strengths, limitations, and pitfalls. *Neuroimage* 2013;81C:335-46.
16. Basser PJ, Pajevic S, Pierpaoli C, Duda J, Aldroubi A. In vivo fiber tractography using DT-MRI data. *Magn Reson Med* 2000;44:625-32.
17. Nagy Z, Ashburner J, Andersson J, Jbabdi S, Draganski B, Skare S, Bohm B, Smedler AC, Forssberg H, Lagercrantz H. Structural correlates of preterm birth in the adolescent brain. *Pediatrics* 2009;124:e964-72.

18. Zhuang L, Sachdev PS, Trollor JN, Reppermund S, Kochan NA, Brodaty H, Wen W. Microstructural white matter changes, not hippocampal atrophy, detect early amnestic mild cognitive impairment. *PLoS One* 2013;8:e58887.
19. Catani M, Thiebaut de Schotten M. A diffusion tensor imaging tractography atlas for virtual in vivo dissections. *Cortex* 2008;44:1105-32.
20. Nieuwenhuys R, Voogd J, van Huijzen C. *The human central nervous system.* Fourth ed. Berlin: Springer-Verlag; 2008.
21. Landis JR, Koch GG. The measurement of observer agreement for categorical data. *Biometrics* 1977;33:159-74.
22. Volpe JJ. Brain injury in premature infants: a complex amalgam of destructive and developmental disturbances. *Lancet Neurol* 2009;8:110-24.
23. Plaisier A, Govaert P, Lequin MH, Dudink J. Optimal Timing of Cerebral MRI in Preterm Infants to Predict Long-Term Neurodevelopmental Outcome: A Systematic Review. *AJNR Am J Neuroradiol* 2013.
24. Dyet LE, Kennea N, Counsell SJ, Maalouf EF, Ajayi-Obe M, Duggan PJ, Harrison M, Allsop JM, Hajnal J, Herlihy AH, Edwards B, Laroche S, Cowan FM, Rutherford MA, Edwards AD. Natural history of brain lesions in extremely preterm infants studied with serial magnetic resonance imaging from birth and neurodevelopmental assessment. *Pediatrics* 2006;118:536-48.
25. Mukherjee P, Chung SW, Berman JI, Hess CP, Henry RG. Diffusion tensor MR imaging and fiber tractography: technical considerations. *AJNR Am J Neuroradiol* 2008;29:843-52.
26. Morris D, Nossin-Manor R, Taylor MJ, Sled JG. Preterm neonatal diffusion processing using detection and replacement of outliers prior to resampling. *Magn Reson Med* 2011;66:92-101.
27. Malamateniou C, Malik SJ, Counsell SJ, Allsop JM, McGuinness AK, Hayat T, Broadhouse K, Nunes RG, Ederies AM, Hajnal JV, Rutherford MA. Motion-Compensation Techniques in Neonatal and Fetal MR Imaging. *AJNR Am J Neuroradiol* 2013;34:1124-36.
28. Mathur AM, Neil JJ, McKinstry RC, Inder TE. Transport, monitoring, and successful brain MR imaging in unsedated neonates. *Pediatr Radiol* 2008;38:260-4.
29. Veraart J, Rajan J, Peeters RR, Leemans A, Sunaert S, Sijbers J. Comprehensive framework for accurate diffusion MRI parameter estimation. *Magn Reson Med* 2012.
30. Koay CG, Chang LC, Carew JD, Pierpaoli C, Basser PJ. A unifying theoretical and algorithmic framework for least squares methods of estimation in diffusion tensor imaging. *J Magn Reson* 2006;182:115-25.
31. Salvador R, Pena A, Menon DK, Carpenter TA, Pickard JD, Bullmore ET. Formal characterization and extension of the linearized diffusion tensor model. *Hum Brain Mapp* 2005;24:144-55.

CHAPTER 6

Standardized Workflow for Constructing a Site-Specific DTI Template of the Preterm Brain

A. Plaisier
H. Achterberg
M. de Groot
A. Leemans
I.K.M. Reiss
W.J. Niessen
G.P. Krestin
J. Dudink
S. Klein

In preparation

Abstract

Background

Prematurity is of major concern because of the increased risk of brain injury and subsequent neurodevelopmental impairment. Therefore, there is a growing interest in non-invasive methods for early detection and quantification of (ab-) normal brain development. Diffusion tensor imaging (DTI) is promising as it seems well-suited to provide such quantitative measurements. However, DTI parameters are center, scanner and population specific and can typically not be exchanged with other centers. Clinical relevance of normal DTI values provided by current available online brain templates seems therefore limited. Creating a site-specific neonatal DTI brain template would overcome many of these problems. To this end, we propose a standardized practical workflow for the construction of site-specific DTI templates of the preterm brain. We will also illustrate its application to our own data.

Methods

DTI data of 24 preterm infants, scanned at 30 weeks' postmenstrual age, without brain injury on conventional magnetic resonance imaging, were prospectively collected. Informed consent was obtained. An experienced observer performed manual segmentation of different brain regions. Robust estimation of diffusion tensors was performed using nonlinear least squares fitting with outlier rejection. A nonrigid group wise registration technique was used to bring all scans to a common template space, in which mean and standard deviation maps of extracted DTI parameters were computed for different brain regions. Finally, in order to test practicality of the template, new data of infants either with or without injury were evaluated using the template.

Results

In a proof of concept study, it was shown that mean diffusivity in white matter (z-score: 4.15) and basal ganglia (z-score 11.18) in severe brain injury deviated from template values.

Conclusion

The novel workflow to construct a site-specific DTI template could effectively be applied in identifying severe preterm brain injury. The software that is part of this workflow will be made available in *ExploreDTI* to guide other imaging centers to perform similar work.

Introduction

Preterm infants are born in the most critical period of brain maturation and consequently at risk for maturational disturbances and irreversible brain injury. Because of subsequent neurodevelopmental impairment; prematurity is considered an increasing concern for global healthcare[1-3]. Neuropathological correlates of these impairments have extensively been investigated with the use of magnetic resonance imaging (MRI) and include germinal matrix – intraventricular hemorrhage and a wide spectrum of white matter injury[4, 5]. Conventional structural MRI offers excellent detection of overt brain damage, but seems less sensitive to detect microstructural abnormalities in diffuse non-cystic types of white matter injury, which are considered today's most important predictors of disturbed brain growth, connectivity and functionality in preterm infants[2].

Consequently, there is a growing interest in assessing (ab-)normal brain development using diffusion tensor imaging (DTI)[6, 7]. DTI enables in vivo assessment of microstructural brain properties by measuring diffusion of water molecules. A large body of scientific work has been dedicated to reveal important insights in pathophysiology of brain injury using DTI[8, 9]. However, for clinical individual profit from DTI scans, quantitative measurements of normal brain development are needed. Such reference values can be derived from normal brain DTI templates[10-12]. If their correlation to long term neurodevelopmental outcome has been validated, these measurements might improve our abilities to predict outcome of individual preterm infants without clear evidence of brain injury[13]. Neonatal brain atlases have recently been developed to provide such biomarkers of long term outcome of preterm infants (Table 1)[14-19].

Table 1: Characteristics of published neonatal brain atlases

Reference	PMA	*n*	MRI data	Registration method	Online available
Kazemi et al., 2007[14]	39 – 42	7	3D T1-W	Affine	Yes
Kuklisova-Murgasova et al., 2011[15]	28.6 – 47.7	142	T2-W	Kernel based	Yes
Oishi et al., 2011[16]	38 – 41	25	T1-W/T2-W/DTI	Affine	Yes
Shi et al., 2010[19]	46	10	T1-W/T2-W	Nonlinear	No
Rose et al., 2013[18]	36	45	DTI	Nonlinear	No
Wang et al., 2013[17]	38.6	20	T2-W	Nonlinear	No

Note: – PMA indicates postmenstrual age at image acquisition (weeks) and *n*, number of included subjects.

Creating neonatal brain atlases and templates from MR brain images is challenging, owing to different factors, such as: spatial variations of contrasts, intensity inhomogeneity, low signal to noise ratio, partial volume effects and neuro-anatomical variability. These are a result of constant maturational processes, such as myelination and cortical folding[17, 20, 21]. In addition, many other factors (hardware setup, acquisition settings and processing methodology) may affect neonatal DTI data, resulting in complicated interpretation of analysis[22-24]. Reproducibility of DTI measurements across different imaging centers is therefore low and exchange of DTI measurements between different institutions seems infeasible[25]. Because this also accounts for references values from DTI templates, these limitations impede the clinical individual profit from online brain templates. Improved standardization of DTI acquisition and processing pipelines across centers could solve these problems. Using a site- and population-specific brain DTI template to obtain reference values from brain templates might be another solution.

In this paper, we propose a novel workflow for constructing a practical, site-specific DTI template of the preterm brain. To evaluate the method, we performed a proof of concept study, in which our method is tested using patient data, acquired at 30 weeks postmenstrual age (PMA). In order to enable other centers to create site-specific templates in a similar manner, the method will be integrated in *ExploreDTI* [26].

Methods

Subjects

Data for template construction were acquired from a prospective cohort study, in which preterm infants born <29 weeks gestational age were recruited. According to protocol, MRI data were acquired at a postmenstrual age of 30 weeks (29 4/7 – 30 4/7 weeks). 19 Infants (11 boys) without evidence of intracranial injury (intraventricular or cerebellar hemorrhage, white matter abnormalities) on conventional MRI, were included for template construction. Another 17 infants (9 boys), either with or without brain injury, were included to test template efficacy. The institutional review board approved this study. Written informed parental consent was obtained for all subjects. Patient characteristics and patterns of brain injury are listed in Table 2.

Imaging

MRI procedures were carried out according to protocol as previously described[27]: all infants were accompanied by trained staff only and were positioned in an MRI-compatible incubator (Lammers Medical Technology GmbH, Luebeck, Germany) that provided controlled temperature and humidity, MR-compatible pulse oximetry and MR-compatible ventilation. Moldable earplugs and neonatal earmuffs (Natus MiniMuffs; Natus Medical Inc., San Carlos, USA) protected the infants from auditory noise, no sedation was given.

Table 2: Patient characteristics and brain injury patterns

	Template set	Evaluation set	
		No brain injury	**With brain injury**
Number of subjects	19	5	12
Gestational age in weeks, median (iqr)	28.1 (1.7)	28.1 (1.9)	27.7 (2.0)
Birth weight in grams, median (iqr)	1150 (410)	795 (433)	990 (244)
Postmenstrual age at MRI acquisition in weeks, median (iqr)	30.0 (0.3)	30.0 (0.5)	30.1 (0.5)
Germinal matrix hemorrhage (*n*)	-	-	6
Intraventricular hemorrhage grade II (*n*)	-	-	3
Diffuse non-cystic white matter injury (*n*)	-	-	1
Cystic periventricular leukomalacia (*n*)	-	-	1
Periventricular hemorrhagic infarction (*n*)	-	-	1

Note: – iqr indicates interquartile range and *n*, number of subjects.

Imaging data were acquired with a 1.5-T GE EchoSpeed scanner (GE Healthcare Technologies, Waukesha, USA). Axial T2-weighted fast spin-echo MRI data were obtained with the following parameter settings: repetition time (TR): 13100 ms; echo time (TE): 139 ms; flip angle: 90˚; slice thickness: 1.2 mm; field of view: 190 x 190 mm^2; acquisition matrix: 256 x 224; reconstruction matrix: 256 x 256 (voxel size: 0.74 x 0.74 x 1.23 mm^3). DTI was performed using a single-shot echo planar imaging (EPI) sequence with diffusion gradients in 25 non-collinear directions, TR: 11725 ms; TE: 85.6 ms; slice thickness: 3 mm; field of view: 220 x 220 mm^2; acquisition matrix: 128 x 64; reconstruction matrix 256 x 256 (voxel size: 0.86 x 0.86 x 3 mm^3); b value: 750 s/mm^2; number of non-diffusion weighted images: 3.

Data processing

Post processing of diffusion weighted images was performed using *ExploreDTI* (http://www.exploredti.com)[26]. Diffusion weighted data were first corrected for Eddy currents, EPI distortion and patient movement[26, 28]. Subsequently, robust estimation of tensors by outlier rejection (RESTORE) was performed[29, 30]. Mean diffusivity (MD) and fractional anisotropy (FA) were derived from the estimated diffusion tensors.

Manual segmentation was performed in FSLView[31]. An experienced observer delineated brain regions on three axial T2-weighted scans, with identical tresholding of signal intensities. A second observer inspected the segmented images. The following regions were manually

segmented: cortical and deep gray matter, white matter, intracranial cerebrospinal fluid, mesencephalon, cerebellum and brain stem. Cortical gray matter was further subdivided in frontal, parietal, temporal, occipital and insular cortex (Fig 1).

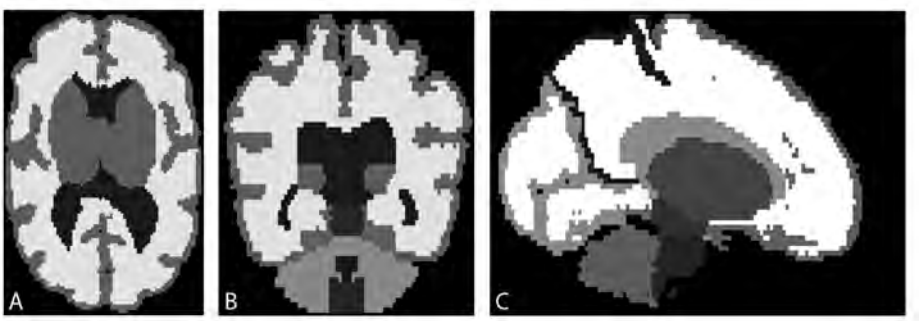

Figure 1 – Manually segmented brain regions in axial (**A**) and coronal (**B**) plane: cortical (orange) and deep (green) gray matter, white matter (yellow), intracranial cerebrospinal fluid (blue), mesencephalon (red), cerebellum (pink) and brain stem (gray). **C**, subdivision of cortical gray matter was further in frontal (orange), parietal (blue), temporal (green) and occipital (pink) cortex. Note that the insular cortex is not shown. (A full color version of this illustration can be found in the color section).

Template construction

For the creation of the template, a common space was defined into which all scans were transformed. The common space was defined in a way that avoids bias towards any of the individual scans[15], using a nonlinear B-spline registration method as implemented in the Elastix software[32]. Briefly, the common template space was defined by registering each subject to all other subjects, averaging the resulting transformations and applying this average transformation to the subject. All T2-weighted images were thus transformed into the common space, creating a structural template. MD images were then affinely registered with their corresponding T2-weighted image. MD and FA images were subsequently brought into the common space, resulting in the average MD and FA templates. Registered images were manually inspected for proper alignment prior to generating parameter maps. In common space, regional mean MD and FA values and standard deviations were computed using regions of interest obtained by transforming the manual segmented scans to the template space. The template construction process is shown schematically in Figure 2 and described in detail in the attachment of this chapter.

Proof of concept study; reference template

The purpose of the DTI template is to serve as a reference to evaluate new scans. Regional MD/FA values of a new scan can be compared with the template mean and standard deviation in the corresponding region, to detect possible abnormal brain development.

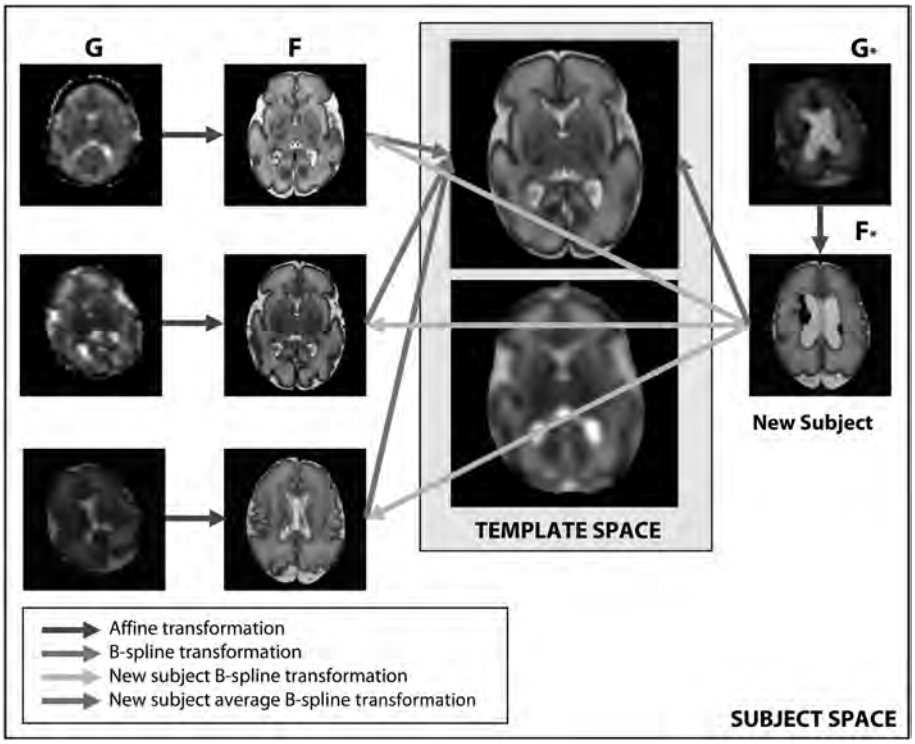

Figure 2 – Schematic representation of image transformation template construction.
F indicates T2-weighted images; **G**, MD/FA maps; $\mathbf{F}_*$, T2-weighted image from new patients, and $\mathbf{G}_*$ MD/FA maps from new patients. (A full color version of this illustration can be found in the color section).

Alignment of new images to the template space was performed with a method similar to the template construction process (see schematic view in Fig 2 and detailed description in the attachment). Subsequently, z-scores were calculated using region-wise analysis regarding MD/FA differences between new image and template measurements.

Results

Template

T2-weighted, mean MD and mean FA template images are shown in Figure 3. Table 3 and 4 present the region-based z-scores for MD and FA of the test subjects respectively.

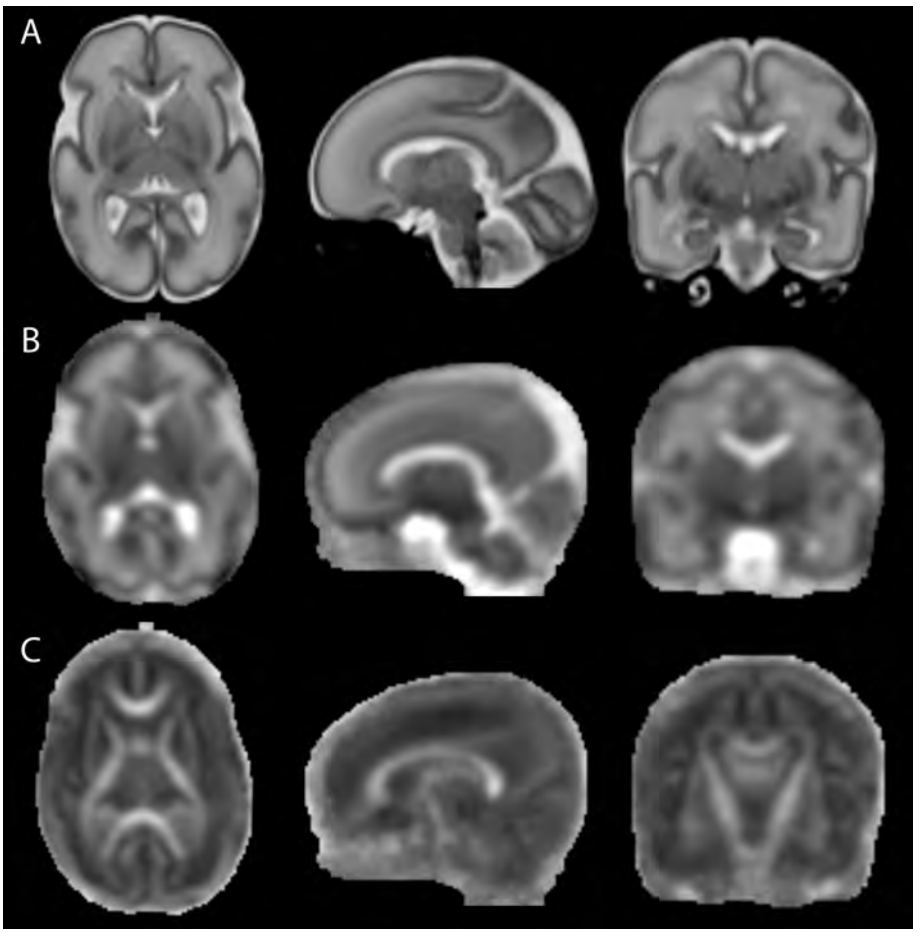

Figure 3 – T2-weighted (**A**), mean MD (**B**) and mean FA (**C**) templates.

Table 3: Region-based z-scores for mean diffusivity of the test subjects

	GMH	GMH	GMH	GMH	GMH	GMH	IVH	IVH	IVH	DWMI	PVL	PVHI	no	no	no	no	no
Total brain volume	0.71	-0.48	0.24	2.60	1.90	1.34	-0.17	0.26	-1.57	-0.01	1.05	3.76	-1.63	-0.62	0.69	-2.41	-1.18
White matter	0.99	-0.53	0.07	2.34	2.46	2.20	0.21	0.96	-2.10	-0.18	0.31	4.15	-1.47	-0.84	1.37	-1.43	-1.78
Deep gray matter	1.66	-1.09	-0.60	2.25	0.41	1.35	0.70	1.13	0.20	-1.00	0.55	11.18	-2.36	-0.79	2.41	2.84	-1.55
Brainstem	0.79	0.54	0.15	0.82	1.13	0.53	-0.65	0.06	-0.08	1.58	0.48	2.03	-1.28	0.29	-1.09	-3.04	0.47
Cerebellum	0.55	-0.50	-0.28	-0.16	-0.64	-0.28	-1.07	0.20	-0.39	0.34	0.53	0.70	-2.37	0.02	-0.98	-3.52	-0.74
Mesencephalon	0.14	-0.09	-1.47	0.15	0.04	0.20	-0.92	-0.09	1.11	0.45	3.08	1.99	-3.24	-0.32	-0.28	1.91	0.05
Cortical gray matter	-0.07	-0.07	0.30	2.12	0.85	-0.37	-0.94	-1.19	-1.13	0.26	1.42	0.84	-1.16	-0.21	0.49	-2.23	-0.09
Frontal cortex	-0.42	-0.08	0.92	2.51	0.93	-0.45	-1.12	-0.77	-1.37	0.00	2.13	0.80	-0.93	-0.01	0.40	-2.02	-0.09
Occipital cortex	-0.13	0.21	-0.15	0.89	-0.39	-1.07	-0.59	-1.46	-0.80	-0.47	1.47	0.66	-1.54	-1.26	-0.74	-1.92	-0.33
Parietal cortex	0.09	0.12	0.52	2.61	1.19	0.20	-0.67	-0.98	-1.03	0.47	0.83	1.13	-0.42	-0.06	0.80	-1.79	0.17
Temporal cortex	0.28	-0.46	-0.47	1.07	1.03	-0.14	-0.83	-1.46	-0.66	1.10	0.41	0.42	-1.42	0.21	1.11	-2.49	-0.27
Insular cortex	0.60	-0.15	-1.85	2.00	0.80	-0.44	-0.50	-0.72	-0.56	-0.68	0.37	0.62	-2.51	0.25	0.51	-1.32	0.97

Note: - GMH indicates germinal matrix hemorrhage; IVH, intraventricular hemorrhage; DWMI, diffuse non-cystic white matter injury; PVL, cystic periventricular leukomalacia; PVHI, Periventricular hemorrhagic infarction, and no: no brain abnormalities.

Table 4: Region-based z-scores for fractional anisotropy of the test subjects

	GMH	GMH	GMH	GMH	GMH	GMH	IVH	IVH	IVH	DWMI	PVL	PVHI	no	no	no	no	no
Total brain volume	-0.15	0.22	-0.78	-0.81	-0.65	-0.69	1.27	-0.07	1.75	-0.37	1.01	-0.81	-0.45	-0.05	-0.61	3.50	0.33
White matter	-0.16	0.16	-0.82	-1.00	-1.01	-1.20	0.84	-0.32	1.68	-0.56	0.93	-1.00	-0.43	-0.11	-0.57	3.63	0.40
Deep gray matter	-0.78	0.73	0.71	-1.10	0.05	-0.67	3.70	1.90	1.03	-1.10	-0.47	1.54	1.64	-0.17	0.34	3.49	0.30
Brainstem	-0.49	-0.08	-0.55	-0.73	-0.01	-0.40	1.08	0.24	0.90	-0.40	1.87	-0.45	-0.25	-0.47	0.07	2.28	-0.30
Cerebellum	-0.61	0.39	-0.37	-0.12	-0.16	-0.20	1.48	0.30	1.18	0.23	1.18	-0.25	-0.21	0.51	0.96	3.64	-0.03
Mesencephalon	0.07	0.32	0.16	-0.16	0.69	0.03	2.76	0.73	1.53	-1.85	1.21	1.14	1.18	-1.05	-0.81	3.37	-1.33
Cortical gray matter	0.00	0.12	-0.78	-0.67	-0.41	-0.14	1.25	0.05	1.65	-0.12	1.10	-0.70	-0.56	0.00	-0.97	2.72	0.26
Frontal cortex	0.09	0.41	-0.81	-1.01	-0.55	-0.47	1.14	-0.47	1.77	0.05	1.22	-0.82	-0.52	-0.05	-0.95	2.58	0.32
Occipital cortex	0.75	-0.23	-1.44	0.13	-0.27	1.15	1.05	0.34	1.50	0.09	0.21	-0.07	-0.79	0.48	-1.51	2.53	-0.07
Parietal cortex	-0.55	-0.04	-0.87	-0.74	-0.41	-0.42	0.64	-0.24	1.16	-0.39	1.15	-0.98	-0.73	0.16	-0.63	2.51	0.27
Temporal cortex	-0.19	-0.03	-0.02	-0.37	-0.23	-0.20	1.73	0.94	1.55	-0.35	1.04	-0.32	-0.19	-0.37	-0.70	2.52	0.26
Insular cortex	-0.21	-0.20	-0.47	-0.78	0.58	-0.06	3.29	1.25	1.80	0.42	2.08	-0.71	-0.69	-0.48	-1.00	2.01	0.37

Note: - GMH indicates germinal matrix hemorrhage; IVH, intraventricular hemorrhage; DWMI, diffuse non-cystic white matter injury; PVL, cystic periventricular leukomalacia; PVHI, Periventricular hemorrhagic infarction, and no: no brain abnormalities.

Comparison with brain injury

From Table 3 and 4, it can be seen that infants without evident brain damage had similar or even further developed microstructure, compared with the average brain template, evidenced by similar or smaller MD and similar or larger FA. Contrary, less organized microstructure was found predominantly in the white matter and basal ganglia of the infant with severe brain injury (periventricular hemorrhagic infarction).

Discussion

Because of the lack of standardization in diffusion tensor MRI, quantitative measures of brain maturation cannot effectively be compared between different imaging sites. Therefore, we propose a method to construct site- and population-specific brain DTI templates that can be used as a reference to evaluate new scans. By making our workflow and software available, we facilitate other sites to construct similar brain templates.

DTI performed in preterm infants has great potentials to provide unique objective details of brain development. Because these markers are highly needed to design tailored intervention strategies to prevent effects of brain injury, DTI could become even more essential in neonatal clinical care. Clinical applicability of DTI in the neonatal brain is currently limited due to the lack of standardization of acquisition and processing pipelines of DTI data. Due to specific characteristics with respect to brain size, changes in tissue composition during maturation and the higher likelihood of motion, scanning preterm infants is especially challenging[23]. However, current clinical literature seems little focused on these matters. Therefore, awareness regarding the importance of standardization of diffusion tensor MR data is crucial. Furthermore, developments aimed to implement high-quality standardized procedures in clinical neonatal neuroimaging centers need to be prioritized.

Meanwhile, issues that arise due the inability to generalize DTI data across sites could be avoided by the constructing of site- and population specific brain templates[11]. Accordingly, this paper introduces a robust novel workflow for developing such a template. To minimize data corruption due to DTI data outliers, tensor estimation was performed according to the RESTORE approach, which automatically detects and removes outliers prior to tensor estimation[29, 30]. This methods seems particularly valuable for data with frequent motion corruption. Also, the used registration method to align brain images ensures minimized bias from spatial image misalignment due to inter-subject variability[10, 33]. Finally, region-wise analysis of DTI measurements in the proof of concept study demonstrates that our method may be effectively used to identify severe preterm brain injury.

Limitations of this study include: 1) The inclusion of 'normal brain images' in this study cannot be established with certainty. In this study, presence of brain injury was assessed on

conventional MRI images. However, because microstructural abnormalities are demonstrated even in the absence of clear signs of injury, selection bias may be involved. 2) Data regarding long term neurodevelopmental outcome is not available. Following the previous limitation, the lack of outcome data may have led to incorrect selection of 'normal' brain scans. 3) Segmentation of brain regions was performed manually in this study. Current robust automatic segmentation tools are suggested to be effective for accurate neonatal brain segmentation[34-36]. Using an automatic segmentation tool may therefore improve precision of assigning brain regions. And, 4) although the proof of concept study demonstrates that our method seems effective to identify severe brain injury, it still needs some refinements: MD and FA values in subjects with normal conventional MRI scans are also deviated from template measurements. This can be explained by microstructural brain abnormalities that are undetectable by conventional MRI sequences[13] or improper identification of brain regions due to suboptimal segmentation, as discussed previously. In order to optimize the presented method, these limitations need proper clarification. Hence, future work will focus on these matters.

Nevertheless, this paper should be considered as a conceptual adjustment of workflow that demonstrates the value of site-specific DTI templates for clinical use as standardization of DTI seems currently infeasible. Future work is necessary and will be focused on improving accuracy by reducing selection bias and by using advanced automatic image processing tools.

Attachment: template construction

In the following subsections, F is used to denote a T2-weighted scan and G is used to denote both MD and FA.

Structural template

Given a set of n T2-weighted images F the goal is to create a template image, which is defined as the average image in a common space Ω_c:

$$\overline{F}(x) = \frac{1}{N}\sum_{i=1}^{N} F_i(T_i(x)), \tag{1}$$

With $T_i(x) : \Omega_c \rightarrow \Omega_{Fi}$ denoting the coordinate transformation from the common space to the subject space Ω_{Fi} and $F_i(T_i(x))$ representing the deformed image.

The transformations $T_i(x)$ are derived from pairwise image registrations. To compute T_i, image F_i is registered to all images F_i resulting in a set of transformations $S_{i,j}(x)$. When image F_i is used as a fixed image, we define the transformations $S_{i,j}(x) : \Omega_{Fi} \rightarrow \Omega_{Fj}$, where Ω_{Fj} represents the image space of F_j. By averaging the transformations $S_{i,j}$ the mean transformation of image F_i, $S_i(x) : \Omega_{Fi} \rightarrow \Omega_c$, is calculated:

$$S_i(x) = \frac{1}{N}\sum_{j=1}^{N} S_{i,j}(x), \tag{2}$$

The transformation $T_i(x)$ is then calculated by inverting, $T_i(x) = S^{-1}(x)$. Note that the identity transformation $S_{i,i}$ is also taken into account in equation (2).

MD and FA template

For MD and FA, the procedures are identical. Let G_i denote the MD/FA image corresponding to the T2-weighted image F_i. We compute mean ($\overline{G}$) and standard deviation ($\widetilde{G}$) template images as follows:

$$\overline{G}(x) = \frac{1}{N}\sum_{i=1}^{N} G_i(R_i(T_i(x))), \tag{3}$$

$$\widetilde{G}(x) = \frac{1}{N-1}\sum_{i=1}^{N} (G_i(R_i(T_i(x))) - \overline{G}(x))^2, \tag{4}$$

Where $R_i(x) : \Omega_{Fi} \rightarrow \Omega_{Gi}$ is the transformation that relates the MD/FA images to the corresponding T2-weighted image.

Region-wise statistics

For region-based analysis, the various structures of interest in the template image must be defined. To this end, a manual segmentation is made on the T2-weighted image of one subject that is not used to construct the template. This segmentation is deformed to the template space following a similar procedure as described previously: registering the T2-weighted image to all, F_i used for constructing the template, averaging the resulting transformations, inverting the average transformation and applying it to the manual segmentation.

Region-wise statistics of the MD and FA values can then be calculated. In each image $G_i(R_i(T_i(x)))$, the mean MD/FA is calculated over each region j ($H_{i,j}$). The population mean and standard deviation of these region-based diffusion parameters are defined by:

$$\overline{H}_j = \frac{1}{N}\sum_{i=1}^{N} H_{i,j} \quad \text{and} \quad \widetilde{H}_j = \sqrt{\frac{1}{N-1}\sum_{i=1}^{N}(H_{i,j} - \overline{H}_j)^2}$$

Comparison with new images

We denote new subjects' scans as F_* and G_*. For the comparison, these images must be brought to the template space. We apply a similar procedure: register the T2-weighted scan to all F_i used for constructing the template, average the resulting transformations, invert the average transformation and apply it to F_*, followed by transformation of G_*.

In template space, a z-score map $(G_* - \overline{G})/\widetilde{G}$ is presented for voxel-wise analysis and per region $(H_{*,j} - \overline{H}_j)/\widetilde{H}_j$ for region-wise analysis.

Registration settings

To compute $S_{i,j}$, a three stage (rigid, affine and B-spline) registration procedure was performed. For R_i, only rigid and affine registrations were used, since the images are from the same subject. Instead of computing R_i directly, with F_i as fixed image, we performed the registration in the other direction, with G_i as the fixed image and subsequently inverted the transformation. Preliminary experiments indicated that this approach is slightly more robust.

We used mutual information, in a Parzen windowing based implementation[37], as the similarity metric and adaptive stochastic gradient descent[38] as the optimization method. Three resolution levels were used, with the B-spline grid spacing changing from 28 mm, to 14 mm, to 7 mm. All registrations were done with Elastix[32].

References

1. Gulland A. Fifteen million and rising--the number of premature births every year. *BMJ* 2012;344:e3084.
2. Volpe JJ. Brain injury in premature infants: a complex amalgam of destructive and developmental disturbances. *Lancet Neurol* 2009;8:110-24.
3. Beck S, Wojdyla D, Say L, Betran AP, Merialdi M, Requejo JH, Rubens C, Menon R, Van Look PF. The worldwide incidence of preterm birth: a systematic review of maternal mortality and morbidity. *Bull World Health Organ* 2010;88:31-8.
4. Rutherford MA, Supramaniam V, Ederies A, Chew A, Bassi L, Groppo M, Anjari M, Counsell S, Ramenghi LA. Magnetic resonance imaging of white matter diseases of prematurity. *Neuroradiology* 2010;52:505-21.
5. Inder TE, Tao J, Neil JJ. Common lesions in the newborn brain. *Top Magn Reson Imaging* 2011;22:25-32.
6. Ment LR, Hirtz D, Huppi PS. Imaging biomarkers of outcome in the developing preterm brain. *Lancet Neurol* 2009;8:1042-55.
7. Jones DK. Studying connections in the living human brain with diffusion MRI. *Cortex* 2008;44:936-52.
8. Huppi PS, Dubois J. Diffusion tensor imaging of brain development. *Semin Fetal Neonatal Med* 2006;11:489-97.
9. Pandit AS, Ball G, Edwards AD, Counsell SJ. Diffusion magnetic resonance imaging in preterm brain injury. *Neuroradiology* 2013;55:65-95.
10. Van Hecke W, Sijbers J, D'Agostino E, Maes F, De Backer S, Vandervliet E, Parizel PM, Leemans A. On the construction of an inter-subject diffusion tensor magnetic resonance atlas of the healthy human brain. *Neuroimage* 2008;43:69-80.
11. Oishi K, Faria AV, Mori S. Advanced neonatal NeuroMRI. *Magn Reson Imaging Clin N Am* 2012;20:81-91.
12. Verhoeven JS, Sage CA, Leemans A, Van Hecke W, Callaert D, Peeters R, De Cock P, Lagae L, Sunaert S. Construction of a stereotaxic DTI atlas with full diffusion tensor information for studying white matter maturation from childhood to adolescence using tractography-based segmentations. *Hum Brain Mapp* 2010;31:470-86.
13. Counsell SJ, Edwards AD, Chew AT, Anjari M, Dyet LE, Srinivasan L, Boardman JP, Allsop JM, Hajnal JV, Rutherford MA, Cowan FM. Specific relations between neurodevelopmental abilities and white matter microstructure in children born preterm. *Brain* 2008;131:3201-8.
14. Kazemi K, Moghaddam HA, Grebe R, Gondry-Jouet C, Wallois F. A neonatal atlas template for spatial normalization of whole-brain magnetic resonance images of newborns: preliminary results. *Neuroimage* 2007;37:463-73.
15. Kuklisova-Murgasova M, Aljabar P, Srinivasan L, Counsell SJ, Doria V, Serag A, Gousias IS, Boardman JP, Rutherford MA, Edwards AD, Hajnal JV, Rueckert D. A dynamic 4D probabilistic atlas of the developing brain. *Neuroimage* 2011;54:2750-63.
16. Oishi K, Mori S, Donohue PK, Ernst T, Anderson L, Buchthal S, Faria A, Jiang H, Li X, Miller MI, van Zijl PC, Chang L. Multi-contrast human neonatal brain atlas: application to normal neonate development analysis. *Neuroimage* 2011;56:8-20.
17. Wang L, Shi F, Li G, Gao Y, Lin W, Gilmore JH, Shen D. Segmentation of neonatal brain MR images using patch-driven level sets. *Neuroimage* 2013.

18. Rose J, Vassar R, Cahill-Rowley K, Guzman XS, Stevenson DK, Barnea-Goraly N. Brain microstructural development at near-term age in very-low-birth-weight preterm infants: An atlas-based diffusion imaging study. *Neuroimage* 2013.
19. Shi F, Fan Y, Tang S, Gilmore JH, Lin W, Shen D. Neonatal brain image segmentation in longitudinal MRI studies. *Neuroimage* 2010;49:391-400.
20. Cabezas M, Oliver A, Llado X, Freixenet J, Cuadra MB. A review of atlas-based segmentation for magnetic resonance brain images. *Comput Methods Programs Biomed* 2011;104:e158-77.
21. Oishi K, Faria AV, Yoshida S, Chang L, Mori S. Quantitative evaluation of brain development using anatomical MRI and diffusion tensor imaging. *Int J Dev Neurosci* 2013;31:512-24.
22. Mukherjee P, Chung SW, Berman JI, Hess CP, Henry RG. Diffusion tensor MR imaging and fiber tractography: technical considerations. *AJNR Am J Neuroradiol* 2008;29:843-52.
23. Heemskerk AM, Leemans A, Plaisier A, Pieterman K, Lequin MH, Dudink J. Acquisition Guidelines and Quality Assessment Tools for Analyzing Neonatal Diffusion Tensor MRI Data. *AJNR Am J Neuroradiol* 2013;34:in press.
24. Jones DK, Cercignani M. Twenty-five pitfalls in the analysis of diffusion MRI data. *NMR Biomed* 2010;23:803-20.
25. Sled JG, Nossin-Manor R. Quantitative MRI for studying neonatal brain development. *Neuroradiology* 2013;55:97-104.
26. Leemans A, Jeurissen B, Sijbers J, Jones DK. ExploreDTI: a graphical toolbox for processing, analyzing, and visualizing diffusion MR data. 17th Annual Meeting of Intl Soc Mag Reson Med. Hawaii, USA; 2009. p. 3537.
27. Plaisier A, Raets MM, van der Starre C, Feijen-Roon M, Govaert P, Lequin MH, Heemskerk AM, Dudink J. Safety of routine early MRI in preterm infants. *Pediatr Radiol* 2012;42:1205-11.
28. Irfanoglu MO, Walker L, Sarlls J, Marenco S, Pierpaoli C. Effects of image distortions originating from susceptibility variations and concomitant fields on diffusion MRI tractography results. *Neuroimage* 2012;61:275-88.
29. Chang LC, Jones DK, Pierpaoli C. RESTORE: robust estimation of tensors by outlier rejection. *Magn Reson Med* 2005;53:1088-95.
30. Morris D, Nossin-Manor R, Taylor MJ, Sled JG. Preterm neonatal diffusion processing using detection and replacement of outliers prior to resampling. *Magn Reson Med* 2011;66:92-101.
31. Smith SM, Jenkinson M, Woolrich MW, Beckmann CF, Behrens TE, Johansen-Berg H, Bannister PR, De Luca M, Drobnjak I, Flitney DE, Niazy RK, Saunders J, Vickers J, Zhang Y, De Stefano N, Brady JM, Matthews PM. Advances in functional and structural MR image analysis and implementation as FSL. *Neuroimage* 2004;23 Suppl 1:S208-19.
32. Klein S, Staring M, Murphy K, Viergever MA, Pluim JP. elastix: a toolbox for intensity-based medical image registration. *IEEE Trans Med Imaging* 2010;29:196-205.
33. Van Hecke W, Leemans A, Sage CA, Emsell L, Veraart J, Sijbers J, Sunaert S, Parizel PM. The effect of template selection on diffusion tensor voxel-based analysis results. *Neuroimage* 2011;55:566-73.
34. Cardoso MJ, Melbourne A, Kendall GS, Modat M, Robertson NJ, Marlow N, Ourselin S. AdaPT: An adaptive preterm segmentation algorithm for neonatal brain MRI. *Neuroimage* 2013;65:97-108.
35. Gui L, Lisowski R, Faundez T, Huppi PS, Lazeyras F, Kocher M. Morphology-driven automatic segmentation of MR images of the neonatal brain. *Med Image Anal* 2012;16:1565-79.

36. Wang L, Shi F, Lin W, Gilmore JH, Shen D. Automatic segmentation of neonatal images using convex optimization and coupled level sets. *Neuroimage* 2011;58:805-17.
37. Thevenaz P, Unser M. Optimization of mutual information for multiresolution image registration. *IEEE Trans Image Process* 2000;9:2083-99.
38. Klein S, Pluim JP, Staring M, Viergever MA. Adaptive stochastic gradient descent optimisation for image registration. *International Journal of Computer Vision* 2009;81:227-39.

CHAPTER 7

Serial Cranial Ultrasonography and Early MRI are Complementary in Detecting Preterm Brain Injury

A. Plaisier
M.M.A. Raets
G.M. Ecury - Goossen
P. Govaert
M. Feijen – Roon
I.K.M. Reiss
L.S. Smit
M.H. Lequin
J. Dudink

Submitted

Abstract

Background

Magnetic resonance imaging (MRI) is considered superior in detecting preterm brain injury, but its clinical use is challenged. Advanced serial cranial ultrasonography (CUS) has acquired great clinical value. We hypothesized that dedicated serial CUS is equally effective in diagnosing preterm brain damage as a routine MRI scan at 30 weeks postmenstrual age and excels in clinical feasibility.

Methods

We prospectively collected data of 307 infants born <29 weeks gestational age. Serial CUS and MRI were performed according to standard clinical protocol. In case of instability, MRI was postponed or canceled. Brain images were assessed by independent experts and compared between modalities.

Results

Serial CUS was performed in all infants, MRI was often postponed (n = 58) or canceled (n = 127). Injury was found in 146 infants (47.6%). Clinical characteristics differed significantly between groups that were subdivided according to timing of MRI. 61 discrepant imaging findings were found. MRI was superior in identifying cerebellar hemorrhages; CUS in detection of acute intraventricular hemorrhage and cerebral sinovenous thrombosis.

Conclusion

Advanced serial CUS seems highly effective in diagnosing preterm brain injury, but may miss cerebellar abnormalities. Although MRI does identify these lesions, clinical additional value is limited. Improved safety, better availability and tailored procedures are essential for MRI to increase its value in clinical care.

Introduction

With the World Health Organization reporting increasing numbers of infants born preterm (over 15 million/year) and increased survival rates, there is a growing recognition that many of these infants may develop long term neurodevelopmental problems[1, 2]. Not surprisingly, preterm birth is rapidly becoming the leading cause of neurodevelopmental impairment in childhood[3]. Early objective diagnosis of brain injury in preterm infants is important for prognostication and decision making in neonatal intensive care.

Current neuroimaging tools are suited for quantitative assessment of preterm brain injury and thus can provide insight into pathogenesis of brain injury in preterm infants[4]. Magnetic resonance imaging (MRI) is a powerful, non-ionizing neuroimaging tool with several advanced techniques to evaluate preterm brains: diffusion tensor imaging (DTI), functional MRI, volumetric MRI and proton magnetic resonance spectroscopy allow quantification of disturbances in brain maturation and elucidate brain connectivity and functionality of infants born preterm. Therefore, quantitative MRI promises to provide early proxy biomarkers of long term outcome[4, 5]. MRI is considered the best method to detect and quantify diffuse non-cystic white matter (WM) injury[6] and is increasingly performed at preterm age to provide early diagnosis of lesions[2]. However, MRI is expensive, time consuming and challenging for critically ill infants. Furthermore, technical background of advanced MRI modalities is a complex matter and imaging accuracy depends on many aspects, including acquisition and processing methodology[7-10]. MRI seems therefore limited as a practical clinical tool to detect most common reported preterm brain lesions on which outcome data are available.

Cranial ultrasonography (CUS) is relatively cheap, directly available and allows serial bedside scanning with limited disturbance for the infant. Color Doppler imaging enables sequential monitoring of intracranial hemodynamic adaptation after birth. Traditionally, CUS is used to detect lesions, such as germinal matrix and intraventricular hemorrhage (GMH-IVH), post-hemorrhagic ventricular dilatation and periventricular leukomalacia (PVL). Its value to detect brain lesions is increasing, owing to technical developments such as high-resolution ultrasound (<200 micron), quantitative measurements (linear, volumetric, raw data and texture analysis) and use of supplemental acoustic windows (mastoid and posterior fontanel)[11-17]. Limitations of CUS include observer-dependency[18], problems to detect posterior fossa abnormalities and cerebral cortical changes and the challenge of reproducible objective measurement[15].

Based on comparative studies between MRI and CUS regarding abilities to predict outcome, MRI is proposed as imaging method of choice for high risk preterm infants[19-21]. However, these studies did not use additional acoustic windows, high-resolution ultrasound and Doppler imaging – as recommended by others[11, 22-24]. And, most importantly, the limitations of MRI in clinical context are often not fully considered.

In order to raise awareness regarding feasibility of routine, clinical MRI scanning in a vulnerable population, we performed this prospective study. Our aims were to investigate detection accuracy and clinical feasibility of serial CUS from birth until discharge, compared with a routine MRI scan obtained from 30 weeks' postmenstrual age (PMA) onwards in infants born <29 weeks' gestational age (GA). We hypothesized that dedicated advanced serial CUS is equally effective as a single routine MRI scan at 30 weeks PMA to diagnose most common brain lesions in infants born very preterm and has greater clinical value due to higher availability for critically ill preterm infants.

Methods

Subjects

Between May 2010 and January 2013, preterm infants born below 29 weeks GA were recruited prospectively. Standard clinical neuroimaging included serial CUS from birth until discharge and MRI at 30 weeks PMA (29 4/7 – 30 4/7 weeks). Of the 336 eligible infants, 29 were excluded because of congenital malformation ($n = 18$), uncertainty regarding gestational age ($n = 5$) or refusal of parental informed consent ($n = 6$). The institutional review board approved this study and parental consent was obtained for all participants.

Imaging

Cranial ultrasonography

Serial CUS was performed by an experienced observer using an Esaote MyLab 70 (Genova, Italy). According to standard clinical protocol, images were obtained in standard sections; six coronal and five sagittal / parasagittal planes through the anterior fontanel, at days 0, 1, 2 and 7 and subsequently, once a week until discharge. Additional images of the cerebellum and transverse sinus were acquired through the mastoid fontanel. Serial color Doppler imaging was performed to assess the intracranial (sino-) venous and arterial system (Fig 1). Images were acquired with a convex, 8.5 MHz probe. To obtain higher resolution of superficially located areas, a high frequency linear probe (13 MHz) was used at the anterior and mastoid fontanel.

Magnetic resonance imaging

MRI procedures were carried out according to protocol[8]: MRI scanning was postponed if patients were hemodynamically and respiratory unstable, which was evaluated by the attending neonatologist and nursing staff. All infants were accompanied by trained staff and were placed in an MRI-compatible incubator, which allowed controlled temperature and humidity and MR-compatible pulse oximetry and ventilation. Moldable earplugs and neonatal earmuffs protected the infants from auditory noise; sedative drugs were not administered.

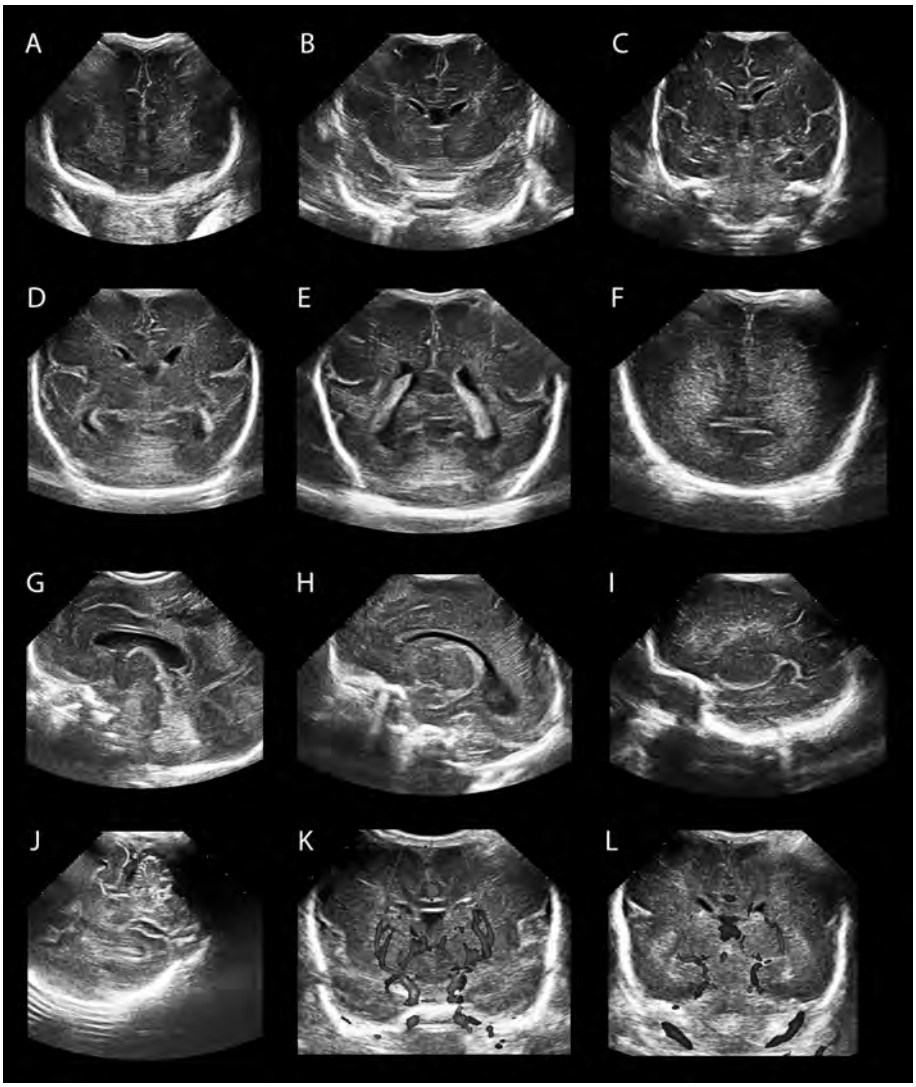

Figure 1 – Ultrasound images were obtained in six coronal (**A**-**F**) and five sagittal/parasagittal planes (**G**-**I**) through the anterior fontanel. Additional images were acquired through the mastoid fontanel (**J**) to visualize the cerebellum and color Doppler images (**K**-**L**) were acquired to assess arterial and (sino-) venous systems. (A full color version of this illustration can be found in the color section).

Imaging data were acquired with a 1.5-T GE EchoSpeed scanner (General Electrics Healthcare Technologies, Waukesha, USA) (Fig 2). Axial T2-weighted fast spin-echo MRI data were obtained with the following parameter settings: repetition time (TR): 13100 ms; echo time (TE): 139 ms; flip angle: 90˚; slice thickness: 1.2 mm; field of view: 190 x 190 mm^2. Axial 3D T1-SPGR MRI data were acquired using: TR: 9 ms; TE: 3 ms; flip angle: 15˚; slice thickness:

1.6 mm; field of view: 150 x 150 mm^2. DTI was performed using a single-shot echo planar imaging sequence with diffusion gradients in 25 non-collinear directions, TR: 11725 ms; TE: 85.6 ms; slice thickness: 3 mm; field of view: 220 x 220 mm^2; *b* value: 750 s/mm^2; number of non-diffusion weighted images: 3.

For the sake of optimization during the study, advanced sequences were added to scanning protocol: susceptibility weighted imaging (SWI) was performed using: TR: 75 ms; TE: 48 ms; flip angle: 20˚; slice thickness: 2.2 mm; field of view: 210 x 210 mm^2. Arterial spin labeling was executed using: TR: 4200 ms; TE: 10 ms; flip angle: 155˚; post label delay: 1025 ms; slice thickness: 4 mm; field of view: 220 x 220 mm^2.

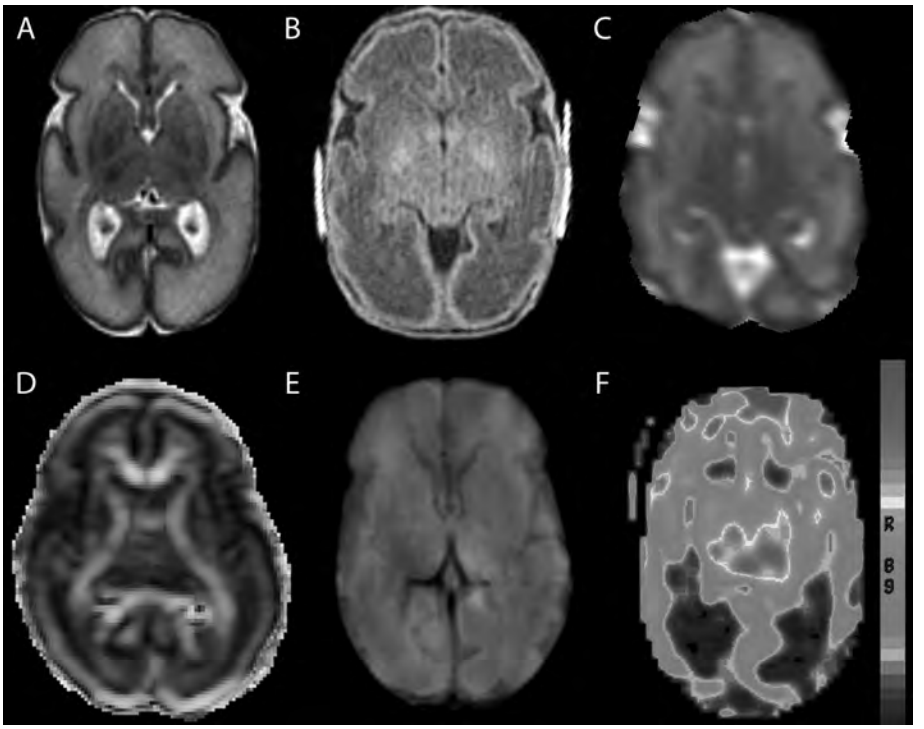

Figure 2 – Applied MRI sequences: **A**, axial T2-weighted fast spin-echo; **B**, axial 3D T1-SPGR; diffusion tensor imaging; **C**, mean diffusivity map; **D**, color-coded directionality map (red represents fibers in the left–right direction, blue represents fibers in the superior–inferior direction, and green represents fibers in the anterior–posterior direction); **E**, susceptibility weighted imaging, and **F**, arterial spin labeling. (A full color version of this illustration can be found in the color section).

Assessment of preterm brain injury

CUS and MRI data were assessed for signs of preterm brain injury by experienced authors independently (MR, PG for CUS and AP, ML for MRI) using a detailed classification system[25]. In all cases, consensus was reached between authors. IVH was graded according to Papile et al[26]. WM abnormalities were classified into cystic PVL and diffuse non-cystic WM injury; the latter were defined as periventricular inhomogeneous echodensities on CUS or diffuse WM lesions on MRI[6, 23]. Cerebellar hemorrhage was categorized into folial or lobar cerebellar hemorrhage[27].

Data analysis

Statistical analysis was performed using SPSS version 20.0.0.1 (IBM SPSS Statistics, New York, USA). Descriptive statistics were applied to patient characteristics and neonatal morbidities. GA was calculated from the first date of the last menstrual period; severity of illness was assessed with the score for neonatal acute physiology perinatal extension[28]; intrauterine growth restriction was defined as birth weight below two standard deviations; persistent ductus arteriosus was recorded if it required treatment and necrotizing enterocolitis was diagnosed by pneumatosis intestinalis, hepatobiliary gas or free intraperitoneal air on radiography. Proportional differences between imaging groups were investigated with Pearson's Chi-squared test. One-way ANOVA served to test differences between imaging group means. Combined sum of findings by CUS and MRI served as golden standard for calculation of sensitivity to detect injury patterns. A p-value of <0.05 (two-sided) was considered statistically significant.

Results

Patient characteristics

307 Infants (170 boys) were included in this study, with mean GA of 26 weeks, 5 days and birth weight of 922 grams. 28 infants (9.1%) did not receive prenatal steroid therapy. Additional clinical characteristics are listed in Table 1. All 307 infants were serially scanned using CUS. In contrast, MRI was not performed at all in 127 infants, as 57 died before 30 weeks PMA; 55 were transferred to other hospitals before the MRI scan could be performed and scanning was not performed in 15 due to logistic difficulties. At 30 weeks PMA, 73 infants were considered not stable enough for MRI scanning; 58 of them were eventually scanned at a later time. Thus, three different groups with regard to MRI scanning are distinguished: group I: MRI scanning at 30 weeks PMA (n = 122); group II: MRI scanning after 30 weeks PMA (n = 58), and group III: no MRI scanning (n =127) (Fig 3).

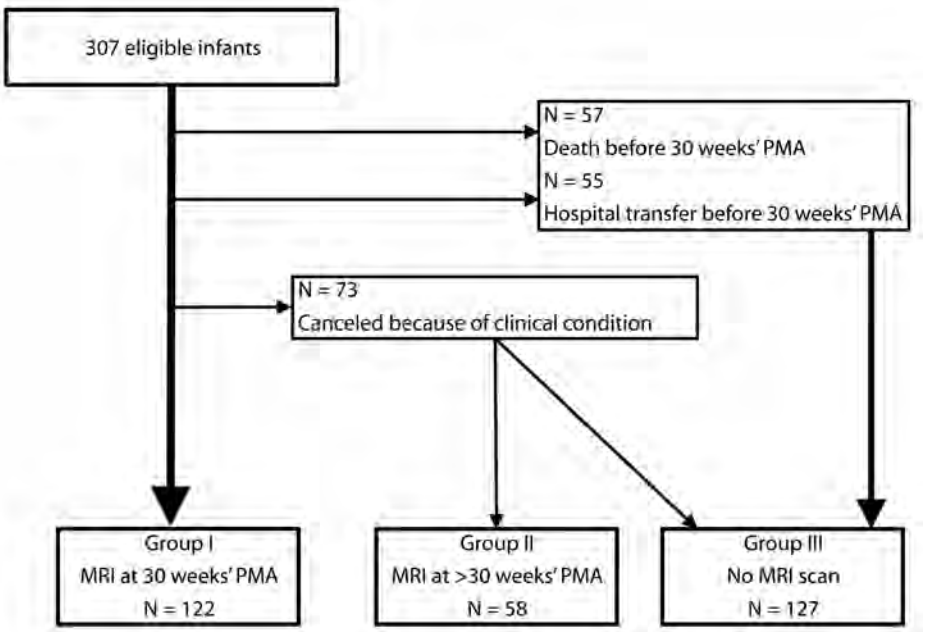

Figure 3 – Flowchart of formation of neuroimaging groups.

Patterns of preterm injury *(Fig 4)*

Combined imaging findings

Injury patterns found either with CUS or MRI are listed in Table 1. GMH-IVH was detected in 100 infants, WM injury in 10, cerebellar hemorrhage in 21, cerebral sinovenous thrombosis (CSVT) in 11 and perforator stroke in 4 infants.

Ultrasonographic findings

180 infants (58.6%) had normal CUS. GMH-IVH was seen in 80 infants (26.7%); in 23 this was limited to germinal matrix (7.5%), in 39 it was assigned IVH grade II (12.7%), in six IVH grade III (2.0%) and in 12 (3.9%), the hemorrhage was complicated by parenchymal infarction. WM injury was sonographically detected in seven infants (2.2%); in four of them (1.3%), it was diffuse non-cystic WM injury and in three (1.0%), cystic PVL was detected. Lobar cerebellar hemorrhage was identified in 10 infants (3.3%). Folial cerebellar hemorrhages were not recognized with CUS. CSVT was present in 11 infants; in all infants, the transverse sagittal sinus was involved, in one infant there was also almost complete thrombosis of the superior sagittal sinus. Four infants presented with a perforator stroke on CUS.

MRI findings

MRI was performed in 180 infants and did not show any injury in 112 infants (62.2%). GMH-IVH was present in 43 infants (23.8%): GMH in 20 (11.1%); IVH-II in 14 (7.7%) and periventricular

Table 1: Descriptive statistics

		Total (*n* = 307)
Gestational age, mean ± SD (weeks)		26.7 ± 1.5
Birth weight, mean ± SD (grams)		922 ± 256
Male gender, *n* (%)		170 (55.4%)
Apgar score at 5 minutes, mean ± SD		7 ± 2
Antenatal steroids	None	28 (9.1%)
	1 dose, *n* (%)	88 (28.7%)
	2 doses, *n* (%)	187 (60.9%)
Intrauterine growth restriction, *n* (%)		42 (13.7%)
Score for neonatal acute physiology perinatal extension-score, mean ± SD		26 ± 21
Postnatal steroids, *n* (%)		43 (14.0%)
Necrotizing enterocolitis, *n* (%)		45 (14.7%)
Persistent ductus arteriosus, *n* (%)		142 (46.3%)
Death, *n* (%)		61 (19.9%)
Postmenstrual age at MRI scan, mean ± SD (weeks)		31.03 ± 2.3
No signs of brain injury, *n* (%)		161 (52.4)
Germinal matrix and intraventricular hemorrhage (GMH-IVH), *n* (%)		100 (32.6%)
GMH, *n* (%)		39 (12.7%)
	Limited IVH grade II, *n* (%)	43 (14.0%)
	Extensive IVH grade III, *n* (%)	6 (2.0%)
	Periventricular hemorrhagic infarction, *n* (%)	12 (3.9%)
White matter injury, *n* (%)		10 (3.3%)
	Diffuse non-cystic white matter injury, *n* (%)	7 (2.3%)
	Cystic periventricular leukomalacia, *n* (%)	3 (1.0%)
Cerebellar hemorrhage, *n* (%)		21 (6.8%)
	Folial hemorrhage, *n* (%)	9 (2.9%)
	Lobar hemorrhage, *n* (%)	12 (3.9%)
Cerebral sinovenous thrombosis, *n* (%)		11 (3.6%)
Perforator stroke, *n* (%)		4 (1.3%)
Discrepant imaging findings on CUS and MRI, *n* (%)		61

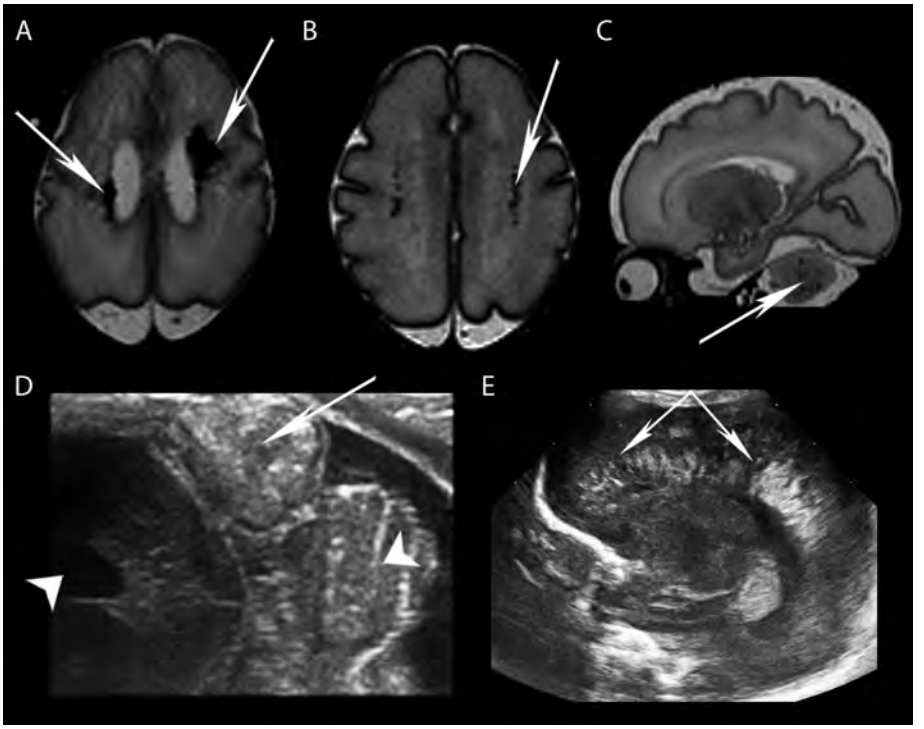

Figure 4 – Examples of brain injury patterns on MRI (**A**-**C**) and CUS (**D**-**E**): **A**, bilateral periventricular hemorrhagic infarction on axial T2-weighted image, note the ventricular dilatation caused by intraventricular hemorrhage; **B**, punctate white matter lesions on axial T2-weighted image; **C**, multiple folial cerebellar hemorrhages on sagittal T2-weighted image; **D**, cerebral sinovenous thrombosis in transverse sinus on cranial ultrasound, assessed through mastoid fontanel, note the large mass (arrow) between the lateral ventricle (left arrowhead) and cerebellum (right arrowhead), and **E**, periventricular leukomalacia on parasagittal cranial ultrasound, assessed through the anterior fontanel.

hemorrhagic infarction in nine infants (5.0%). WM injury was detected in eight infants (4.4%); in seven (3.9%) this was diffuse non-cystic WM injury and one infant had cystic PVL. Cerebellar hemorrhage was detected with MRI in 15 infants (8.3%); lobar in six and folial in nine. CSVT was identified on MRI in two infants; perforator stroke was not detected at all by MRI.

Differences between imaging groups

Clinical characteristics between the three MRI imaging groups differed significantly (Table 2). In general, infants in imaging group I were born with higher GA and birth weight and seemed to have fewer complications: intrauterine growth restriction, persistent ductus arteriosus, supplementation of postnatal steroids and death were significantly less common and score for severity of illness was significantly lower: 19 compared with 27 and 34 of groups

Table 2: Differences between imaging groups

		Group I (*n* = 122)	Group II (*n* = 58)	Group III (*n* = 127)	*p*-value
Gestational age, mean ± SD (weeks)		27.1 ± 1.3	26.5 ± 1.3	26.4 ± 1.6	**
Birth weight, mean ± SD (grams)		994 ± 224	864 ± 181	880 ± 297	**
Male gender, *n* (%)		58 (47.5%)	35 (60.3%)	77 (60.6%)	
Apgar score at 5 minutes, mean ± SD		8 ± 1	8 ± 2	7 ± 2	*
Antenatal steroids	None	12 (9.8%)	5 (8.6%)	11 (8.7%)	†
	1 dose, *n* (%)	35 (28.7%)	14 (24.1%)	39 (30.7%)	
	2 doses, *n* (%)	72 (59.0%)	39 (67.2%)	76 (59.8%)	
Intrauterine growth restriction, *n* (%)		9 (7.4%)	8 (13.8%)	25 (19.7%	*
SNAPPE-score, mean ± SD		19 ± 16	27 ± 16	34 ± 25	**
Postnatal steroids, *n* (%)		5 (4.1%)	12 (20.7%)	26 (20.5%)	**
Necrotizing enterocolitis, *n* (%)		11 (9.0%)	9 (15.5%)	25 (19.7%)	†
Persistent ductus arteriosus, *n* (%)		44 (36.1%)	41 (70.7%)	57 (44.9%)	**
Death, *n* (%)		2 (1.6%)	2 (3.4%)	57 (44.9%)	**
Postmenstrual age at MRI scan, mean ± SD (weeks)		30.1 ± 0.3	33.0 ± 3.3	-	-
No signs of brain injury, *n* (%)		58 (47.5)	27 (46.6)	76 (59.8)	†
Germinal matrix and intraventricular hemorrhage (GMH-IVH), *n* (%)		42 (34.4%)	19 (32.8%)	39 (30.7%)	†
	GMH, *n* (%)	18 (14.7%)	7 (12.1%)	14 (11.0%)	
	Limited IVH grade II, *n* (%)	19 (15.6%)	8 (13.8%)	16 (12.6%)	
	Extensive IVH grade III, *n* (%)	-	-	6 (4.7%)	
	Periventricular hemorrhagic infarction, *n* (%)	5 (4.1%)	4 (6.9%)	3 (2.4%)	
White matter injury, *n* (%)		8 (6.6%)	-	2 (1.6%)	†
	Diffuse non-cystic white matter injury, *n* (%)	7 (5.7%)	-	-	
	Cystic periventricular leukomalacia, *n* (%)	1 (0.8%)	-	2 (1.6%)	
Cerebellar hemorrhage, *n* (%)		9 (7.4%)	6 (10.3%)	6 (4.7%)	†
	Folial hemorrhage, *n* (%)	5 (4.1%)	4 (6.9%)	-	
	Lobar hemorrhage, *n* (%)	4 (3.3%)	2 (3.4%)	6 (4.7%)	
Cerebral sinovenous thrombosis, *n* (%)		5 (4.1%)	4 (6.9%)	2 (1.6%)	†
Perforator stroke, *n* (%)		-	2 (3.4%)	2 (1.6%)	†
Discrepant imaging findings on CUS and MRI, *n* (%)		41 (33.6%)	20 (34.5%)	-	†

Note: SNAPPE indicates score for neonatal acute physiology perinatal extension.

II and III respectively. Occurrence of necrotizing enterocolitis and pattern of preterm brain injury did not significantly differ between imaging groups (Table 2).

Table 3: Discrepant imaging findings on CUS and MRI

	Imaging findings			**Accuracy**	
	CUS	**MRI**		**Sensitivity CUS**	**Sensitivity MRI**
		+	**-**		
Germinal matrix hemorrhage, *n* = 25	**+**	4	5	36.0%	80.0%
	-	16	-		
Intraventricular hemorrhage, grade II-III, *n* = 27	**+**	10	13	85.2%	51.9%
	-	4	-		
Diffuse non-cystic white matter injury, *n* = 7	**+**	4	0	57.1%	100%
	-	3	-		
Folial cerebellar hemorrhage, *n* = 9	**+**	0	0	0%	100%
	-	9	-		
Lobar cerebellar hemorrhage, *n* = 6	**+**	4	0	66.7%	100%
	-	2	-		
Cerebral sinovenous thrombosis, *n* = 9	**+**	2	7	100%	22.2%
	-	0	-		
Perforator stroke, *n* = 2	**+**	0	2	100%	0%
	-	0	-		

Note: + indicates detected, and -, not detected.

Discrepant imaging findings on CUS and MRI

Table 3 compares imaging findings of CUS with MRI findings in the 180 infants who were scanned by both techniques. Inconsistencies were predominantly found for GMH-IVH in 38 infants, cerebellar hemorrhage in 11 and CSVT in seven infants. MRI had higher sensitivity to detect GMH and identified all posterior fossa abnormalities, but in 27 infants, CUS excelled in the acute detection of IVH grade II-III, perforator strokes and CSVT, as these lesions were no longer clearly visible on MRI at the time of scanning. Findings for WM injury were discrepant in three infants.

Discussion

This study demonstrates that many infants born very preterm suffer from brain injury and CUS effectively detects most common lesions. CUS has higher clinical feasibility than MRI, which cannot always be performed in severely ill infants. However, despite mastoid fontanel scanning, CUS remains inferior to identify small posterior fossa abnormalities. As MRI provides additional diagnostic information, we would recommend to optimize safety and feasibility of MRI procedures.

Comprehensive application of CUS, usage of supplemental acoustic windows, color Doppler imaging, higher transducer frequencies and careful interpretation of images by an experienced observer results in high accuracy to identify certain lesions. CUS provided better assessment of injury than MRI in 27 infants, mostly because of higher sensitivity to detect IVH grade II-III, perforator stroke and CSVT. These lesions seem to correlate with adverse long term outcome and would have been missed if serial CUS had not been performed, leading to less prognostic accuracy[29, 30].

The higher sensitivity of CUS to detect IVH grade II-III seems mainly attributable to the consecutive application of CUS. Conventional MRI was unable to detect intraventricular blood and/or ventricular dilatation, possibly due to the resolving nature of IVH. Parodi et al.[31] recently reported a lower sensitivity (60%) of CUS to detect grade I-II GMH-IVH compared with SWI. The authors point out the unique possibilities of SWI to detect subependymal and/or intraventricular hemosiderin depositions and accentuate that dedicated timing and application of advanced MRI sequences is quite valuable in assessing the preterm brain.

In the present study, CUS was insufficient to detect diffuse non-cystic WM injury in three infants only. All other diffuse WM lesions on MRI were already detected on CUS by inhomogeneous echodensities on CUS. This confirms the assumption that inhomogeneous hyperechogenicities are the CUS correlates of punctate WM lesions and stresses the value of sequential and advanced CUS to monitor and detect diffuse non-cystic WM injury[13, 15, 22-24]. However, MRI is needed to assess the extent and localization of WM injury for its full impact on long term outcome[32].

In correspondence with current literature[33, 34], MRI in the present study excelled in the detection of posterior fossa abnormalities: it confirmed all cerebellar hemorrhages detected with CUS and identified all folial and two lobar cerebellar hemorrhages that had been missed with CUS. Although cerebellar hemorrhages seen only on MRI seem to correlate with more optimistic outcomes than those visible on CUS[16], neurologic abnormalities are common. Tam et al.[34] reported abnormal neurologic examinations at age 3-6 years in 50% of infants with cerebellar hemorrhage seen only on MRI, compared with 16% of children without cerebellar hemorrhage. Furthermore, disrupted cerebellar development in preterm infants is suggested to contribute significantly to poor outcome[35].

In addition to the detection of limited cerebellar hemorrhage, neonatal care may clearly benefit from quantitative MRI sequences that could provide early objective biomarkers of outcome[4]. However, MRI is a complex technique with limitations in the very young. Our study design dictated MRI scanning at 30 weeks' PMA, but depending on clinical condition, scanning was postponed or canceled in 185 infants (60%). Inherently, infants scanned at 30 weeks' PMA may likely have been the most healthy ones. Postponement or cancelation seems rather worrying because especially preterm infants with severe illness are at risk of brain injury and may benefit most from early MRI scanning[36, 37]. Moreover, more premature babies are surviving than ever before and related brain injury is on the rise[1]. It would be essential, therefore, to considerably improve the applicability of MRI. This includes: 1) safety improvement: transfers and monitoring of critically ill infants to the MR suite should be optimized and MRI sequences can be shortened to reduce procedure times[10, 38]; 2) tailored MRI scanning: indications, usage of sequences and timing to scan should be established more individually. For instance, MRI may be unnecessary for infants with uncomplicated history and absence of brain injury on ultrasound scans, provided that CUS was performed serially, comprehensively and carefully by an experienced observer[22]. But MRI would be required, even in case of critical illness, when CUS is inconclusive on the need to continue intensive care. And 3) improved availability: a dedicated neonatal MRI scanner in the vicinity of the NICU would improve its accessibility and overcome logistic problems.

Important limitations of this study should be addressed: 1) imaging group III was heterogeneous because it included both deceased patients and infants transferred to other hospitals before the MRI could take place. Inclusion of deceased patients may have influenced clinical characteristics; 2) due to absence of correlation between injury patterns and long term neurodevelopmental outcome in our study population, we were not able to demonstrate clinical relevance of all findings; 3) because strategies were being optimized over the course of this study, SWI was not performed in all MRI procedures, which may have led to lower sensitivity to detect low-grade GMH-IVH compared with other studies[31]; 4) in this study, we observed imaging findings of routine, clinical MRI scans, as such, we were not able to perform post processing of advanced MRI sequences to obtain quantitative measurements of injury. We are aware that sophisticated use of MRI sequences, such as DTI, volumetric MRI and proton MR spectroscopy, which are usually performed in the context of research, would undoubtedly result in greater value of MRI. And, 5) due to logistic problems, our prospective study did not include term equivalent MRI scanning. As a result, we might not have been able to detect 'typical' characteristics of WM abnormality at term, such as thinning of corpus callosum, ventricular enlargements[32] and diffuse excessive high signal intensities[39]. Our results could therefore not be compared with other studies. However, MRI was performed at mean PMA of 31 weeks, but was still unable to detect some lesions that were previously detected with serial advanced CUS. We argue therefore that performance of CUS to detect acute brain lesions accurately would have been higher if MRI had been performed at term-equivalent age. Moreover, experienced use of CUS at term corrected age is well able to detect callosal thinning, ventricular enlargement and presence of small WM cysts[22].

In conclusion, serial advanced CUS is adequate to detect and monitor preterm brain injury and therefore deserves more appreciation in neonatal neurology. MRI is invaluable as it allows objective quantitative assessment of microstructural brain properties and is superior to detect posterior fossa abnormalities. However, clinical use in preterms is currently limited because of safety and logistic issues. These issues need to be addressed in view of the increasing demand for quantitative biomarkers of outcome. Furthermore, dual use of sequential CUS and MRI provides high sensitivity to detect common patterns of preterm brain injury. Future research should therefore focus on the improvement of their complementary applications.

References

1. Gulland A. Fifteen million and rising--the number of premature births every year. *BMJ* 2012;344:e3084.
2. Plaisier A, Govaert P, Lequin MH, Dudink J. Optimal Timing of Cerebral MRI in Preterm Infants to Predict Long-Term Neurodevelopmental Outcome: A Systematic Review. *AJNR Am J Neuroradiol* 2013.
3. Wood NS, Marlow N, Costeloe K, Gibson AT, Wilkinson AR. Neurologic and developmental disability after extremely preterm birth. EPICure Study Group. *N Engl J Med* 2000;343:378-84.
4. Ment LR, Hirtz D, Huppi PS. Imaging biomarkers of outcome in the developing preterm brain. *Lancet Neurol* 2009;8:1042-55.
5. Smyser CD, Snyder AZ, Shimony JS, Blazey TM, Inder TE, Neil JJ. Effects of white matter injury on resting state FMRI measures in prematurely born infants. *PLoS One* 2013;8:e68098.
6. Rutherford MA, Supramaniam V, Ederies A, Chew A, Bassi L, Groppo M, Anjari M, Counsell S, Ramenghi LA. Magnetic resonance imaging of white matter diseases of prematurity. *Neuroradiology* 2010;52:505-21.
7. Heemskerk AM, Leemans A, Plaisier A, Pieterman K, Lequin MH, Dudink J. Acquisition Guidelines and Quality Assessment Tools for Analyzing Neonatal Diffusion Tensor MRI Data. *AJNR Am J Neuroradiol* 2013;34:1496-505.
8. Plaisier A, Raets MM, van der Starre C, Feijen-Roon M, Govaert P, Lequin MH, Heemskerk AM, Dudink J. Safety of routine early MRI in preterm infants. *Pediatr Radiol* 2012;42:1205-11.
9. Mathur AM, Neil JJ, McKinstry RC, Inder TE. Transport, monitoring, and successful brain MR imaging in unsedated neonates. *Pediatr Radiol* 2008;38:260-4.
10. Rutherford M, Biarge MM, Allsop J, Counsell S, Cowan F. MRI of perinatal brain injury. *Pediatr Radiol* 2010;40:819-33.
11. Leijser LM, de Vries LS, Cowan FM. Using cerebral ultrasound effectively in the newborn infant. *Early Hum Dev* 2006;82:827-35.
12. Govaert P, De Vries LS. *An atlas of neonatal brain sonography.* 2nd ed. London: Mac Keith Press; 2010.
13. Ciambra G, Arachi S, Protano C, Cellitti R, Caoci S, Di Biasi C, Gualdi G, De Curtis M. Accuracy of transcranial ultrasound in the detection of mild white matter lesions in newborns. *Neuroradiol J* 2013;26:284-9.
14. Graca AM, Cardoso KRV, da Costa JMFP, Cowan FM. Cerebral volume at term age: Comparison between preterm and term-born infants using cranial ultrasound. *Early Human Development* 2013;89:643-8.
15. van Wezel-Meijler G, Steggerda SJ, Leijser LM. Cranial ultrasonography in neonates: role and limitations. *Semin Perinatol* 2010;34:28-38.
16. Steggerda SJ, Leijser LM, Wiggers-de Bruine FT, van der Grond J, Walther FJ, van Wezel-Meijler G. Cerebellar injury in preterm infants: incidence and findings on US and MR images. *Radiology* 2009;252:190-9.
17. Leijser LM, Srinivasan L, Rutherford MA, Counsell SJ, Allsop JM, Cowan FM. Structural linear measurements in the newborn brain: accuracy of cranial ultrasound compared to MRI. *Pediatr Radiol* 2007;37:640-8.
18. Reynolds PR, Dale RC, Cowan FM. Neonatal cranial ultrasound interpretation: a clinical audit. *Arch Dis Child Fetal Neonatal Ed* 2001;84:F92-5.
19. Maalouf EF, Duggan PJ, Counsell SJ, Rutherford MA, Cowan F, Azzopardi D, Edwards AD. Comparison of findings on cranial ultrasound and magnetic resonance imaging in preterm infants. *Pediatrics* 2001;107:719-27.

20. Miller SP, Cozzio CC, Goldstein RB, Ferriero DM, Partridge JC, Vigneron DB, Barkovich AJ. Comparing the diagnosis of white matter injury in premature newborns with serial MR imaging and transfontanel ultrasonography findings. *AJNR Am J Neuroradiol* 2003;24:1661-9.
21. Mirmiran M, Barnes PD, Keller K, Constantinou JC, Fleisher BE, Hintz SR, Ariagno RL. Neonatal brain magnetic resonance imaging before discharge is better than serial cranial ultrasound in predicting cerebral palsy in very low birth weight preterm infants. *Pediatrics* 2004;114:992-8.
22. Horsch S, Skiold B, Hallberg B, Nordell B, Nordell A, Mosskin M, Lagercrantz H, Aden U, Blennow M. Cranial ultrasound and MRI at term age in extremely preterm infants. *Arch Dis Child Fetal Neonatal Ed* 2010;95:F310-4.
23. Leijser LM, Liauw L, Veen S, de Boer IP, Walther FJ, van Wezel-Meijler G. Comparing brain white matter on sequential cranial ultrasound and MRI in very preterm infants. *Neuroradiology* 2008;50:799-811.
24. de Vries LS, Benders MJ, Groenendaal F. Imaging the premature brain: ultrasound or MRI? *Neuroradiology* 2013;55:13-22.
25. Govaert P, Ramenghi L, Taal R, de Vries L, Deveber G. Diagnosis of perinatal stroke I: definitions, differential diagnosis and registration. *Acta Paediatr* 2009;98:1556-67.
26. Papile LA, Burstein J, Burstein R, Koffler H. Incidence and evolution of subependymal and intraventricular hemorrhage: a study of infants with birth weights less than 1,500 gm. *J Pediatr* 1978;92:529-34.
27. Ecury-Goossen GM, Dudink J, Lequin M, Feijen-Roon M, Horsch S, Govaert P. The clinical presentation of preterm cerebellar haemorrhage. *Eur J Pediatr* 2010;169:1249-53.
28. Richardson DK, Corcoran JD, Escobar GJ, Lee SK. SNAP-II and SNAPPE-II: Simplified newborn illness severity and mortality risk scores. *J Pediatr* 2001;138:92-100.
29. Patra K, Wilson-Costello D, Taylor HG, Mercuri-Minich N, Hack M. Grades I-II intraventricular hemorrhage in extremely low birth weight infants: effects on neurodevelopment. *J Pediatr* 2006;149:169-73.
30. Berfelo FJ, Kersbergen KJ, van Ommen CH, Govaert P, van Straaten HL, Poll-The BT, van Wezel-Meijler G, Vermeulen RJ, Groenendaal F, de Vries LS, de Haan TR. Neonatal cerebral sinovenous thrombosis from symptom to outcome. *Stroke* 2010;41:1382-8.
31. Parodi A, Morana G, Severino MS, Malova M, Natalizia AR, Sannia A, Rossi A, Ramenghi LA. Low-grade intraventricular hemorrhage: is ultrasound good enough? *J Matern Fetal Neonatal Med* 2013.
32. Woodward LJ, Anderson PJ, Austin NC, Howard K, Inder TE. Neonatal MRI to predict neurodevelopmental outcomes in preterm infants. *N Engl J Med* 2006;355:685-94.
33. Fumagalli M, Bassi L, Sirgiovanni I, Mosca F, Sannia A, Ramenghi LA. From germinal matrix to cerebellar haemorrhage. *J Matern Fetal Neonatal Med* 2013.
34. Tam EWY, Rosenbluth G, Rogers EE, Ferriero DM, Glidden D, Goldstein RB, Glass HC, Piecuch RE, Barkovich AJ. Cerebellar hemorrhage on magnetic resonance imaging in preterm newborns associated with abnormal neurologic outcome. *J Pediatr* 2011;158:245-50.
35. Messerschmidt A, Brugger PC, Boltshauser E, Zoder G, Sterniste W, Birnbacher R, Prayer D. Disruption of cerebellar development: potential complication of extreme prematurity. *AJNR Am J Neuroradiol* 2005;26:1659-67.
36. Zwicker JG, Grunau RE, Adams E, Chau V, Brant R, Poskitt KJ, Synnes A, Miller SP. Score for neonatal acute physiology-II and neonatal pain predict corticospinal tract development in premature newborns. *Pediatr Neurol* 2013;48:123-9 e1.

37. Card D, Nossin-Manor R, Moore AM, Raybaud C, Sled JG, Taylor MJ. Brain metabolite concentrations are associated with illness severity scores and white matter abnormalities in very preterm infants. *Pediatr Res* 2013;74:75-81.
38. Stokowski LA. Ensuring safety for infants undergoing magnetic resonance imaging. *Adv Neonatal Care* 2005;5:14-27; quiz 52-4.
39. Skiold B, Horsch S, Hallberg B, Engstrom M, Nagy Z, Mosskin M, Blennow M, Aden U. White matter changes in extremely preterm infants, a population-based diffusion tensor imaging study. *Acta Paediatr* 2010;99:842-9.

7

CHAPTER 8

General Discussion and Future Perspectives

General discussion

Prematurity is increasing and due to ongoing improvements in neonatal intensive care, viability of extreme prematurity has substantially improved[1]. However, risk of brain injury and subsequent neuromotor and neurocognitive deficits continue to exist[2-5]. The number of neurologically impaired infants that were born preterm will increase exponentially in the near future.

Because of the large magnitude of this problem, neonatal neuroimaging centers are currently focused on efforts to increase the abilities to predict long term outcome[6-8]. Due to active and rapid developments in advanced neuroimaging and neuromonitoring techniques, the possibilities to allow comprehensive understanding of neuropathology are most promising[9-11]. However, with infants becoming more vulnerable and techniques becoming more complex, the demands for standardized procedures will become stricter to guarantee safety, quality and proper patient care.

Magnetic resonance imaging (MRI) scans are increasingly performed during early preterm life[12]. However, it remains debatable whether this is currently in the patients' best interest. As **chapter 2** outlines, individual prognostic information from MRI scans at term equivalent age (TEA) greatly outweighs that from early MRI scans. In general, the extent of abnormality, demonstrated on conventional MRI scans, diffusion tensor imaging (DTI) or with volumetric MRI, is directly related to measures of functional outcome. Damage to the white matter (WM), either primary or secondary, seems to be by far the most predicting factor[13-17]. Inherently, MRI techniques to assess WM in more detail, such as with the use of DTI, are increasingly performed in preterm infants[11, 18-21]. DTI has unique capabilities and may become the leading technique to assess the preterm brain. Even in infants with normal conventional brain MRI scans, serial DTI studies, have detected abnormal maturation of WM microstructure, which may be considered as an early proxy sign of injury[22, 23]. Furthermore, correlations between early detected brain injury and neurodevelopmental outcome have been demonstrated and yield the use of early MRI scanning[12, 24-26]. Timely identification of early predictors of injury may provide a window of opportunity to undertake preventative measures to minimize destructive effects on further neurodevelopment and may further enable the development of possible targeted intervention therapies. Currently, there is no accepted therapy for preterm brain injury, but neuroprotective agents are currently under development. Candidate agents include: erythropoietin, melatonin, stem cell therapy, magnesium sulfate and progesterone. Surrogate measures of injury, provided by quantitative MRI sequences, may establish efficacy of these intervention trials and subsequently may allow objective selection of infants at risk that need intervention[27, 28]. In view of present perspectives regarding personalized medicine, early MRI scans seem therefore highly appropriate to provide early biomarkers of long term outcome[9, 29] and may be helpful to achieve customized healthcare for individual patients.

Because of these considerations, early MRI scanning is incorporated as part of standard clinical care for all preterm infants born before 29 weeks gestational age in the Sophia's Children Hospital in Rotterdam. Scans are preferably performed around 30 weeks postmenstrual age, provided that infants are clinically stable enough for MRI scanning. However, although we use a tailored guideline that has been developed in collaboration with different disciplines and includes careful evaluation of individual clinical condition[30, 31], avoidable adverse events and logistical problems are still common when performing early MRI scanning procedures. The reported results in **chapter 3** demonstrate the high number of events (50%) that complicate MRI procedures. Body temperature was significantly decreased after the procedure and respiratory instability was frequently encountered within 24 hours after the MRI scan. These results seem to conflict with those from other studies that suggested that MRI scanning can be safely performed in preterm infants[30, 32, 33]. This contrast can be explained by differences in study design, population and outcome measures. Our study was specifically aimed at early MRI scans, performed at 30 weeks postmenstrual age and the occurrence of adverse events was monitored up to 24 hours after the MRI scan. Therefore, findings of this paper raise awareness regarding the important limitations of clinical use of early MRI scanning and stress the necessity to use comprehensive, adapted guidelines to scan vulnerable infants. Accordingly, clinical guidelines for early MRI scans in the Sophia's Children Hospital have been adjusted to prevent avoidable adverse events. Furthermore, a dedicated team of nurses and physicians still continues to strive for improving patient safety and quality of neonatal MRI procedures.

Because of very promising and unique possibilities to assess microstructural changes, such as pre-myelination, advanced DTI sequences allow more sensitive characterization of brain tissue. These are especially suitable to study complex WM features and may further unravel important aspects regarding brain ontogenesis, injurious events, plasticity and functionality[6, 11]. Due to vast improvements regarding sensitivity and clinical use, DTI has also gained much recognition in adult neuropsychiatry, oncology and neurosurgery. However, acquisition, processing and analysis of neonatal DTI are challenging because of specific characteristics with respect to brain size, changes in tissue composition during maturation and higher likelihood of motion as sedation is generally not recommended[31, 34]. Therefore, before considering important implications regarding long term outcomes, pitfalls of DTI need to be recognized, addressed and solved[35, 36].

The crucial importance of addressing these problems is amplified by the contradiction between increasing number of DTI studies in preterm infants and the negligence to address the importance of standardized adapted DTI acquisition and processing in most published papers. Consequently, **chapter 4, 5 and 6** focus in more detail on these important matters. Because of specific challenges of brain imaging in newborns, **chapter 4** provides a clinical perspective regarding general aspects and limitations of neonatal DTI. In addition, frequently encountered artifacts and pitfalls are illustrated by examples from our own population. Furthermore, recommendations to minimize corrupting effects and optimize processing and

analysis of DTI are outlined. For instance, several techniques to estimate the diffusion tensor have been developed. These methods differ considerably with regard to speed, principle and how they deal with data outliers, all of which can have considerable impact on final results[35]. In general, reliability can be improved by dealing with data outliers carefully and is especially important when patients are scanned with high likelihood of subject motion, such as in the neonatal population[37, 38]. However, there seems to be no clarity regarding the exact definition of data outliers and how to properly handle them. This calls for awareness regarding the importance to determine what types of data processing can reliably be performed without affecting data quality. Accordingly, **chapter 5** demonstrates the importance of well-informed data processing and quality of data by investigating their effect on fiber tractography of the fornix in prospectively collected preterm DTI data. This proof of concept shows how processing methodology significantly affects visualization quality of tract reconstruction, quantitative tract parameters and how improper consideration of DTI data quality negatively impacts on the obtained results. Given the insufficient attention to these aspects in the majority of clinical studies to date, our work calls for attention regarding compliance with minimum requirements for processing pipelines: future studies should apply dedicated acquisition setups, standardized quality evaluation and reliable processing of neonatal DTI data. These aspects are indispensable and only if they are properly applied, conclusions can be drawn regarding associations between microstructural brain properties and outcome.

Subsequently, the importance of diligence in using preterm DTI data is further elaborated in the next chapter. For an individual clinical benefit from DTI scans, reference values are needed. They might be derived from DTI templates of the developing brain, which are currently being developed[39-41]. However, because of many aspects that may affect and complicate data analysis, DTI measurements are center, scanner and population specific and can typically not be exchanged across centers. The entire pipeline of DTI data, from acquisition to final analysis, need therefore to be standardized[42]. Another way to allow clinical utility for the individual infant can be achieved by developing a site- and population-specific brain DTI template. This includes that processing software for template construction, rather than quantitative indices, should be exchanged across imaging sites. **Chapter 6** introduces a site-specific workflow for development of DTI templates of preterm brains. This method included robust estimation of the tensor to improve reliability of analysis and a well-informed registration technique to minimize bias due to misalignment. The proof of concept by regional analysis showed significantly deviated DTI measurements in severe brain injury. The presented workflow for template construction seems therefore effective to identify injury. Furthermore, the used software will be integrated in DTI post processing software to enable other centers to create similar site-specific brain templates.

In summary, MRI has great potentials to provide unique objective information regarding neurodevelopment of preterm infants. Because these imaging markers are highly needed to design tailored intervention strategies to prevent effects of brain injury, MRI could become even more essential in neonatal clinical care. However, the clinical use of early MRI scans in

preterm infants is unfortunately still frequently limited because of safety and quality issues, needing our ongoing attention.

Chapter 7 describes findings of a large prospective cohort study, which was aimed to investigate clinical feasibility and detection accuracy of focal preterm brain injury of a single early MRI scan compared with serial extensive cranial ultrasonography (CUS) scans performed by a dedicated, well-trained researcher. Because a large number of MRI scans had to be postponed or completely canceled due to the suboptimal clinical condition of many infants, CUS excelled in clinical feasibility. In agreement with current literature[43, 44], results of this study also show that serial CUS may be an adequate diagnostic tool in most common types of focal preterm brain injuries. However, MRI was needed to detect all posterior fossa abnormalities, such as cerebellar hemorrhages, which are correlated with poor outcome[26, 45]. This chapter stresses the importance of combined use of serial advanced CUS and MRI to detect common patterns of preterm brain injury. Future research should therefore focus on improving their complementary applications.

Although performing early preterm MRI brain scans still has several limitations, some of which are outlined in this thesis, they do have major clinical advantages compared to any other imaging modality. Quantitative MRI scanning during early preterm life allows to objectify microstructural brain properties during an extremely critical period of brain development[6, 46, 47]. Perfusion sequences, such as arterial spin labeling, have gained clinical and research interest and are promising new tools to study hemodynamic consequences of preterm birth. The unique anatomical details that conventional MRI sequences additionally offer, enable localization of injuries in relation to future functional consequences[48]. Finally, functional MRI will provide additional important insights into adapting responses to injury in the concept of brain plasticity[49].

Because of all of these unique opportunities, MRI could bring us to a very promising future. Fully in compliance with current research to discover early origins of long term outcome[29], MRI could provide appropriate biomarkers to allow tailored treatment[9]. Furthermore, MRI will be necessary to evaluate therapeutic effects. Nevertheless, important limitations with regard to patient safety, clinical individual utility and data quality, still have to be dealt with. In order to make full use of MRI, ongoing improvements in terms of safety, clinical accessibility, quality and reliability are highly needed – *'safer better faster stronger'.*

Future perspectives

The unique property of DTI to quantify tissue characteristics is invaluable for early detection of brain abnormalities, prediction of outcome and provision of specific biomarkers for neuroprotective intervention in prematurity[6, 9]. Although DTI has already gained many credits[20, 46, 50], advances are rapidly developing and seem very promising as they allow higher accuracy to explore trajectories of brain development:

Projects to explore whole-brain macrostructural connectivity, or the 'Human Connectome' are under development. Recently, US president Obama announced the 'Brain Research through Advancing Innovative Neurotechnologies' initiative, which, like similar projects, is aimed to map neural circuits that are activated during cognitive processes and may revolutionize our understanding of the human brain. Such projects have already demonstrated reductions in connection strength throughout cerebral WM that seem to be associated with preterm birth. Moreover, as higher cognitive domains, such as intellect, memory and personality, are suggested to be encoded in inter-neuronal connections[51], mapping brain connectomes in preterm born infants will further contribute to a better understanding of underlying injurious mechanisms in neurocognitive impairments and might elucidate fetal origins of adult neuropsychiatric diseases[11, 52, 53].

High angular resolution diffusion imaging (HARDI) and diffusion kurtosis imaging (DKI) are sophisticated extensions based on higher order diffusion models that can be obtained by applying multiple higher b-values and more gradient directions. Both DKI and HARDI offer better reconstruction of multiple fiber directions within a single voxel, resulting in improved and more accurate characterization of complex and heterogeneous WM architecture[54, 55]. Consequently, these techniques have already established better clinical benefits by aiding surgical planning for brain and spinal cord tumors in adults[56, 57]. Providing more sensitive characterization of neural tissues in preterm population seems feasible[58] and very interesting as it may provide more detailed insights into complex circuitry of brain development, destruction and subsequent consequences on further development[59].

Ax Caliber imaging and neurite orientation dispersion and density imaging are other extensions to assess axonal and dendritic complexity[9, 60]. These approaches are suggested to provide direct and more specific representation of brain microstructure than standard DTI parameters, such as fractional anisotropy and will provide new opportunities for better understanding[9, 60, 61]. Although clinical use is not yet established, an important aspect of WM injury is characterized by wide spread axonal degeneration[59]. Quantification of this destruction may fill in the gap of knowledge regarding exact nature and causality in diffuse non-cystic types of WM injury[25, 62-64].

Abilities to study the brain objectively are not limited to DTI, pioneering developments in these fields will also become of great interest in the near future:

Arterial spin labeling (ASL) uses magnetically labeled arterial blood water to trace cerebral blood flow in vivo. It allows monitoring of brain function by quantifying cerebral perfusion, which is suggested to increase during maturation[65, 66]. Furthermore, perinatal injurious events resulting in fluctuated cerebral blood flow are well known to affect normal brain development. Consecutive monitoring of blood flow patterns in preterm brains could provide early identification of infants at risk for injury, resulting in better understanding of causality and may represent an important step forward to find tailored neuroprotective therapies[28, 29].

Functional MRI (fMRI) non-invasively measures changes in blood oxygenation levels, which are thought to reflect functional activity[49]. Neonatal fMRI studies revealed important maturational functional processes, including development of behaviorally relevant resting state networks that reflect neuronal network connectivity in cognitive processes. Furthermore, combining structural MRI with functional imaging may identify timing and location of maturational processes. Etiology of neurosensory, neuromotor and cognitive abilities could be further discovered, including effects of recovery and plasticity after injury. Thus, fMRI can bring valuable new insights into development, organization and integration of functional activity during brain maturation[67].

T2 mapping objectively assesses specific tissue characteristics. The T2 relaxation time is a physical property of tissue that reflects free water content. Prolonged T2 relaxation times in cerebral WM seems to represent impaired myelination and has been correlated to neurodevelopmental impairment[68]. Translational studies, in which T2 mapping and histologic studies are combined, will reveal more information regarding pathophysiology of preterm brain injury[69].

In addition to these technical advances, clinical improvements are equally important to be accomplished. Developments designed to improve patient comfort are ongoing. Recent innovations include "silent" MRI scanning, in which excessive acoustic noise is reduced to near ambient (background) sound levels during MR acquisition. Furthermore, tailored scanning setups are needed, in which safety issues, quality aspects, acquisition parameters and limited availability are no longer of concern. Establishment of a dedicated neonatal MRI suite at continuous disposal in the neonatal intensive care unit will be highly appreciated. Moreover, in order to provide high-quality MRI scanning of the most critically ill infants, such setups should be approached in comprehensive collaboration between medical specialists, technicians and neuroscientists.

In this point of view, using "near-bedside" multimodal imaging as part of standard clinical care seems within reach. Important techniques to assess hemodynamic and functional adaptive processes during maturation include color Doppler imaging[70], near infrared spectroscopy (NIRS)[71] and electroencephalography (EEG)[72]. In addition, by accessing raw ultrasound data, objective measurements of periventricular WM can consecutively be monitored in infants with severe critical illness. Combining and registering these techniques with advanced MRI techniques has great potentials. For instance, EEG and NIRS during fMRI acquisition are currently under development and may contribute to an even deeper understanding of brain organization, neuronal connectivity, intracranial hemodynamics and adapted processes to injurious events in the preterm brain.

Technological advances in medical imaging can be anticipated to enable personalized medicine for preterm infants and consequently a tailored approach with very promising results. Because of the significance of MRI in these developments, its potential pitfalls need to be addressed. This thesis outlines important aspects of early MRI scanning, with the emphasis on a dedicated approach. Furthermore, by offering solutions regarding optimal brain imaging to the fullest extent, this thesis contributes to the overall purpose to improve the long term outcome of premature birth.

References

1. Saigal S, Doyle LW. An overview of mortality and sequelae of preterm birth from infancy to adulthood. *Lancet* 2008;371:261-9.
2. Incidence of and risk factors for neonatal morbidity after active perinatal care: extremely preterm infants study in Sweden (EXPRESS). *Acta Paediatr* 2010;99:978-92.
3. Larroque B, Ancel PY, Marret S, Marchand L, Andre M, Arnaud C, Pierrat V, Roze JC, Messer J, Thiriez G, Burguet A, Picaud JC, Breart G, Kaminski M. Neurodevelopmental disabilities and special care of 5-year-old children born before 33 weeks of gestation (the EPIPAGE study): a longitudinal cohort study. *Lancet* 2008;371:813-20.
4. Marlow N, Wolke D, Bracewell MA, Samara M. Neurologic and developmental disability at six years of age after extremely preterm birth. *N Engl J Med* 2005;352:9-19.
5. Moore T, Hennessy EM, Myles J, Johnson SJ, Draper ES, Costeloe KL, Marlow N. Neurological and developmental outcome in extremely preterm children born in England in 1995 and 2006: the EPICure studies. *BMJ* 2012;345:e7961.
6. Pandit AS, Ball G, Edwards AD, Counsell SJ. Diffusion magnetic resonance imaging in preterm brain injury. *Neuroradiology* 2013;55 Suppl 2:65-95.
7. de Vries LS, Benders MJ, Groenendaal F. Imaging the premature brain: ultrasound or MRI? *Neuroradiology* 2013.
8. Smyser CD, Kidokoro H, Inder TE. Magnetic resonance imaging of the brain at term equivalent age in extremely premature neonates: to scan or not to scan? *J Paediatr Child Health* 2012;48:794-800.
9. Ment LR, Hirtz D, Huppi PS. Imaging biomarkers of outcome in the developing preterm brain. *Lancet Neurol* 2009;8:1042-55.
10. Ramenghi LA, Rutherford M, Fumagalli M, Bassi L, Messner H, Counsell S, Mosca F. Neonatal neuroimaging: going beyond the pictures. *Early Hum Dev* 2009;85:S75-7.
11. Ball G, Boardman JP, Aljabar P, Pandit A, Arichi T, Merchant N, Rueckert D, Edwards AD, Counsell SJ. The influence of preterm birth on the developing thalamocortical connectome. *Cortex* 2013;34:1124-36.
12. Miller SP, Ferriero DM, Leonard C, Piecuch R, Glidden DV, Partridge JC, Perez M, Mukherjee P, Vigneron DB, Barkovich AJ. Early brain injury in premature newborns detected with magnetic resonance imaging is associated with adverse early neurodevelopmental outcome. *J Pediatr* 2005;147:609-16.
13. De Bruine FT, Van Den Berg-Huysmans AA, Leijser LM, Rijken M, Steggerda SJ, Van Grond JD, Van Wezel-Meijler G. Clinical implications of MR imaging findings in the white matter in very preterm infants: A 2-year follow-up study. *Radiology* 2011;261:899-906.
14. Edgin JO, Inder TE, Anderson PJ, Hood KM, Clark CAC, Woodward LJ. Executive functioning in preschool children born very preterm: Relationship with early white matter pathology. *J Int Neuropsychol Soc* 2008;14:90-101.
15. Iwata S, Nakamura T, Hizume E, Kihara H, Takashima S, Matsuishi T, Iwata O. Qualitative brain MRI at term and cognitive outcomes at 9 years after very preterm birth. *Pediatrics* 2012;129:e1138-e47.
16. Spittle AJ, Cheong J, Doyle LW, Roberts G, Lee KJ, Lim J, Hunt RW, Inder TE, Anderson PJ. Neonatal white matter abnormality predicts childhood motor impairment in very preterm children. *Dev Med Child Neurol* 2011;53:1000-6.

17. Woodward LJ, Anderson PJ, Austin NC, Howard K, Inder TE. Neonatal MRI to predict neurodevelopmental outcomes in preterm infants. *New Engl J Med* 2006;355:685-94.
18. Bassi L, Ricci D, Volzone A, Allsop JM, Srinivasan L, Pai A, Ribes C, Ramenghi LA, Mercuri E, Mosca F, Edwards AD, Cowan FM, Rutherford MA, Counsell SJ. Probabilistic diffusion tractography of the optic radiations and visual function in preterm infants at term equivalent age. *Brain* 2008;131:573-82.
19. Counsell SJ, Rutherford MA, Cowan FM, Edwards AD. Magnetic resonance imaging of preterm brain injury. *Arch Dis Child Fetal Neonatal Ed* 2003;88:F269-74.
20. Dudink J, Kerr JL, Paterson K, Counsell SJ. Connecting the developing preterm brain. *Early Hum Dev* 2008;84:777-82.
21. van Kooij BJ, de Vries LS, Ball G, van Haastert IC, Benders MJ, Groenendaal F, Counsell SJ. Neonatal tract-based spatial statistics findings and outcome in preterm infants. *AJNR Am J Neuroradiol* 2012;33:188-94.
22. Glass HC, Berman JI, Norcia AM, Rogers EE, Henry RG, Hou C, Barkovich AJ, Good WV. Quantitative fiber tracking of the optic radiation is correlated with visual-evoked potential amplitude in preterm infants. *Am J Neuroradiol* 2010;31:1424-9.
23. Drobyshevsky A, Bregman J, Storey P, Meyer J, Prasad PV, Derrick M, MacKendrick W, Tan S. Serial diffusion tensor imaging detects white matter changes that correlate with motor outcome in premature infants. *Dev Neurosci* 2007;29:289-301.
24. Cornette LG, Tanner SF, Ramenghi LA, Miall LS, Childs AM, Arthur RJ, Martinez D, Levene MI. Magnetic resonance imaging of the infant brain: Anatomical characteristics and clinical significance of punctate lesions. *Arch Dis Child Fetal Neonatal Ed* 2002;86:F171-F7.
25. Dyet LE, Kennea N, Counsell SJ, Maalouf EF, Ajayi-Obe M, Duggan PJ, Harrison M, Allsop JM, Hajnal J, Herlihy AH, Edwards B, Laroche S, Cowan FM, Rutherford MA, Edwards AD. Natural history of brain lesions in extremely preterm infants studied with serial magnetic resonance imaging from birth and neurodevelopmental assessment. *Pediatrics* 2006;118:536-48.
26. Tam EWY, Rosenbluth G, Rogers EE, Ferriero DM, Glidden D, Goldstein RB, Glass HC, Piecuch RE, Barkovich AJ. Cerebellar hemorrhage on magnetic resonance imaging in preterm newborns associated with abnormal neurologic outcome. *J Pediatr* 2011;158:245-50.
27. Mathur AM, Neil JJ, Inder TE. Understanding brain injury and neurodevelopmental disabilities in the preterm infant: the evolving role of advanced magnetic resonance imaging. *Semin Perinatol* 2010;34:57-66.
28. Rees S, Harding R, Walker D. The biological basis of injury and neuroprotection in the fetal and neonatal brain. *Int J Dev Neurosci* 2011;29:551-63.
29. Mussap M, Noto A, Cibecchini F, Fanos V. The importance of biomarkers in neonatology. *Semin Fetal Neonatal Med* 2013;18:56-64.
30. Benavente-Fernandez I, Lubian-Lopez PS, Zuazo-Ojeda MA, Jimenez-Gomez G, Lechuga-Sancho AM. Safety of magnetic resonance imaging in preterm infants. *Acta Paediatrica* 2010;99:850-3.
31. Mathur AM, Neil JJ, McKinstry RC, Inder TE. Transport, monitoring, and successful brain MR imaging in unsedated neonates. *Pediatr Radiol* 2008;38:260-4.
32. Battin M, Maalouf EF, Counsell S, Herlihy A, Hall A, Azzopardi D, Edwards AD. Physiological stability of preterm infants during magnetic resonance imaging. *Early Hum Dev* 1998;52:101-10.

33. Merchant N, Groves A, Larkman DJ, Counsell SJ, Thomson MA, Doria V, Groppo M, Arichi T, Foreman S, Herlihy DJ, Hajnal JV, Srinivasan L, Foran A, Rutherford M, Edwards AD, Boardman JP. A patient care system for early 3.0 Tesla magnetic resonance imaging of very low birth weight infants. *Early Hum Dev* 2009;85:779-83.
34. Pannek K, Guzzetta A, Colditz PB, Rose SE. Diffusion MRI of the neonate brain: acquisition, processing and analysis techniques. *Pediatric Radiology* 2012;42:1169-82.
35. Jones DK, Cercignani M. Twenty-five pitfalls in the analysis of diffusion MRI data. *NMR Biomed* 2010;23:803-20.
36. Mukherjee P, Chung SW, Berman JI, Hess CP, Henry RG. Diffusion tensor MR imaging and fiber tractography: technical considerations. *AJNR Am J Neuroradiol* 2008;29:843-52.
37. Heemskerk AM, Plaisier A, Reiss IKM, Lequin MH, Leemans A, Dudink J. DTI in neonates: data corruption due to motion. ISMRM; 2012; Melbourne, Australia; 2012.
38. Malamateniou C, Malik SJ, Counsell SJ, Allsop JM, McGuinness AK, Hayat T, Broadhouse K, Nunes RG, Ederies AM, Hajnal JV, Rutherford MA. Motion-Compensation Techniques in Neonatal and Fetal MR Imaging. *AJNR Am J Neuroradiol* 2013;34:1124-36.
39. Huang H. Delineating neural structures of developmental human brains with diffusion tensor imaging. *ScientificWorldJournal* 2010;10:135-44.
40. Oishi K, Mori S, Donohue PK, Ernst T, Anderson L, Buchthal S, Faria A, Jiang H, Li X, Miller MI, van Zijl PC, Chang L. Multi-contrast human neonatal brain atlas: application to normal neonate development analysis. *Neuroimage* 2011;56:8-20.
41. Rose J, Vassar R, Cahill-Rowley K, Guzman XS, Stevenson DK, Barnea-Goraly N. Brain microstructural development at near-term age in very-low-birth-weight preterm infants: An atlas-based diffusion imaging study. *Neuroimage* 2013.
42. Pannek K, Scheck SM, Colditz PB, Boyd RN, Rose SE. Magnetic resonance diffusion tractography of the preterm infant brain: a systematic review. *Dev Med Child Neurol* 2013.
43. Horsch S, Skiold B, Hallberg B, Nordell B, Nordell A, Mosskin M, Lagercrantz H, Aden U, Blennow M. Cranial ultrasound and MRI at term age in extremely preterm infants. *Arch Dis Child Fetal Neonatal Ed* 2010;95:F310-4.
44. Leijser LM, de Vries LS, Cowan FM. Using cerebral ultrasound effectively in the newborn infant. *Early Hum Dev* 2006;82:827-35.
45. Messerschmidt A, Brugger PC, Boltshauser E, Zoder G, Sterniste W, Birnbacher R, Prayer D. Disruption of cerebellar development: potential complication of extreme prematurity. *AJNR Am J Neuroradiol* 2005;26:1659-67.
46. Huppi PS, Dubois J. Diffusion tensor imaging of brain development. *Semin Fetal Neonatal Med* 2006;11:489-97.
47. Volpe JJ. Neuronal Proliferation, Migration Organization and Myelination. In: *Neurology of the Newborn*. (ed). Philadelphia: Saunders; 2008.
48. Rutherford MA. What's new in neuroimaging? Magnetic resonance imaging of the immature brain. *Eur J Paediatr Neurol* 2002;6:5-13.
49. Seghier ML, Lazeyras F, Huppi PS. Functional MRI of the newborn. *Semin Fetal Neonatal Med* 2006;11:479-88.

50. Jones DK. Studying connections in the living human brain with diffusion MRI. *Cortex* 2008;44:936-52.
51. Allen M, Williams G. Consciousness, plasticity, and connectomics: the role of intersubjectivity in human cognition. *Front Psychol* 2011;2:20.
52. Pandit AS, Robinson E, Aljabar P, Ball G, Gousias IS, Wang Z, Hajnal JV, Rueckert D, Counsell SJ, Montana G, Edwards AD. Whole-Brain Mapping of Structural Connectivity in Infants Reveals Altered Connection Strength Associated with Growth and Preterm Birth. *Cereb Cortex* 2013.
53. Collin G, van den Heuvel MP. The Ontogeny of the Human Connectome: Development and Dynamic Changes of Brain Connectivity Across the Life Span. *Neuroscientist* 2013;19:616-28.
54. Wahl M, Barkovich AJ, Mukherjee P. Diffusion imaging and tractography of congenital brain malformations. *Pediatr Radiol* 2010;40:59-67.
55. De Santis S, Gabrielli A, Palombo M, Maraviglia B, Capuani S. Non-Gaussian diffusion imaging: a brief practical review. *Magn Reson Imaging* 2011;29:1410-6.
56. Kuhnt D, Bauer MH, Sommer J, Merhof D, Nimsky C. Optic radiation fiber tractography in glioma patients based on high angular resolution diffusion imaging with compressed sensing compared with diffusion tensor imaging - initial experience. *PLoS One* 2013;8:e70973.
57. Hori M, Fukunaga I, Masutani Y, Taoka T, Kamagata K, Suzuki Y, Aoki S. Visualizing non-Gaussian diffusion: clinical application of q-space imaging and diffusional kurtosis imaging of the brain and spine. *Magn Reson Med Sci* 2012;11:221-33.
58. Kudzinava M, Poot D, Plaisier A, Sijbers J. Optimized workflow for diffusion kurtosis imaging of newborns IEEE International Symposium on Biomedical Imaging: From Nano to Macro Chicago, USA; 2011.
59. Volpe JJ. Brain injury in premature infants: a complex amalgam of destructive and developmental disturbances. *Lancet Neurol* 2009;8:110-24.
60. Zhang H, Schneider T, Wheeler-Kingshott CA, Alexander DC. NODDI: practical in vivo neurite orientation dispersion and density imaging of the human brain. *Neuroimage* 2012;61:1000-16.
61. Winston GP. The physical and biological basis of quantitative parameters derived from diffusion MRI. *Quant Imaging Med Surg* 2012;2:254-65.
62. Kidokoro H, Anderson PJ, Doyle LW, Neil JJ, Inder TE. High signal intensity on T2-weighted MR imaging at term-equivalent age in preterm infants does not predict 2-year neurodevelopmental outcomes. *Am J Neuroradiol* 2011;32:2005-10.
63. Rutherford MA, Supramaniam V, Ederies A, Chew A, Bassi L, Groppo M, Anjari M, Counsell S, Ramenghi LA. Magnetic resonance imaging of white matter diseases of prematurity. *Neuroradiology* 2010;52:505-21.
64. Counsell SJ, Shen Y, Boardman JP, Larkman DJ, Kapellou O, Ward P, Allsop JM, Cowan FM, Hajnal JV, Edwards AD, Rutherford MA. Axial and radial diffusivity in preterm infants who have diffuse white matter changes on magnetic resonance imaging at term-equivalent age. *Pediatrics* 2006;117:376-86.
65. Wang Z, Fernandez-Seara M, Alsop DC, Liu WC, Flax JF, Benasich AA, Detre JA. Assessment of functional development in normal infant brain using arterial spin labeled perfusion MRI. *Neuroimage* 2008;39:973-8.
66. De Vis JB, Petersen ET, de Vries LS, Groenendaal F, Kersbergen KJ, Alderliesten T, Hendrikse J, Benders MJ. Regional changes in brain perfusion during brain maturation measured non-invasively with Arterial Spin Labeling MRI in neonates. *Eur J Radiol* 2013;82:538-43.
67. Lee W, Morgan BR, Shroff MM, Sled JG, Taylor MJ. The development of regional functional connectivity in preterm infants into early childhood. *Neuroradiology* 2013;55 Suppl 2:105-11.

68. Abernethy LJ, Klafkowski G, Foulder-Hughes L, Cooke RWI. Magnetic resonance imaging and T2 relaxometry of cerebral white matter and hippocampus in children born preterm. *Pediatric Research* 2003;54:868-74.
69. Deng W. Neurobiology of injury to the developing brain. *Nat Rev Neurol* 2010;6:328-36.
70. Govaert PP, de Vries L.S. *An atlas of neonatal brain sonography.* 2nd ed. London, Cambridge: Mac Keith Press; 2010.
71. Marin T, Moore J. Understanding near-infrared spectroscopy. *Adv Neonatal Care* 2011;11:382-8.
72. Vanhatalo S, Kaila K. Development of neonatal EEG activity: from phenomenology to physiology. *Semin Fetal Neonatal Med* 2006;11:471-8.

CHAPTER 9

Samenvatting
Summary
About the author
List of publications
PhD Portfolio
Dankwoord
Color section

Samenvatting

Hoofdstuk 1

Prematuriteit is wereldwijd een groot probleem voor de gezondheidszorg. Hoewel er in de afgelopen jaren grote vorderingen zijn geboekt die de overlevingskansen hebben vergroot, hebben prematuur geboren kinderen nog steeds een verhoogde kans op cognitieve en motorische ontwikkelingsproblemen. De verhoogde kans op hersenschade door perinatale problemen ligt hier voor een groot deel aan ten grondslag. Nauwkeurige herkenning van deze schade is daarom van groot belang. Magnetic resonance imaging (MRI) biedt zeer gedetailleerde beeldvorming van het brein. Met behulp van verschillende sequenties (scaninstellingen) kan het hersenweefsel op verschillende unieke manieren worden beoordeeld. Zo kan bijvoorbeeld door middel van diffusion tensor imaging (DTI) microstructurele weefselkenmerken objectief worden beoordeeld. Echter, het uitvoeren van een MRI scan bij een prematuur geboren neonaat in de klinische situatie heeft enkele beperkingen ten aanzien van patiëntveiligheid, beeldkwaliteit en het toepassen van de juiste sequenties om de latere neurologische uitkomst nauwkeurig te kunnen voorspellen. In dit proefschrift worden deze beperkingen beschreven. Daarnaast wordt uiteengezet dat het van groot belang is om de klinische toepasbaarheid van MRI te vergemakkelijken, zodat op deze wijze optimale hersenbeeldvorming door middel van MRI bij prematuren gerealiseerd kan worden.

Hoofdstuk 2

Door belangrijke ontwikkelingen en vorderingen in de neonatale hersenbeeldvorming is vroege opsporing van hersenschade bij prematuren aanzienlijk verbeterd. Echter, er lijkt geen consensus te zijn over de optimale timing van MRI scans om de neurologische ontwikkeling het beste te kunnen voorspellen. In dit hoofdstuk worden de resultaten van een systematische review van de huidige literatuur beschreven. Deze literatuurstudie had als doel te onderzoeken wat het beste moment voor een MRI scan bij premature zuigelingen is om de lange termijn uitkomst te kunnen voorspellen. In deze review zijn 26 artikelen opgenomen: acht seriële MRI studies, twee uitgevoerd op ≤35 weken en 52 MRI studies uitgevoerd op >35 weken postmenstruele leeftijd. Eén van de belangrijkste bevindingen was dat cerebrale witte stof schade, hetzij beoordeeld met behulp van conventionele structurele MRI, DTI, volume MRI of proton MR spectroscopie, veruit de belangrijkste factor lijkt te zijn voor het voorspellen van de neurologische uitkomst. Duidelijke aanknopingspunten ten aanzien van de optimale timing van MRI scans zijn niet aangetroffen. Echter, gezien het overgrote aandeel van de studies die uitgevoerd zijn rond de aterme leeftijd, lijkt de individueel prognostische waarde van een MRI scan op die leeftijd hoger dan die van een MRI scan uitgevoerd op jongere leeftijd. Desondanks zijn vroege MRI scans veelbelovend om tijdig schade te kunnen detecteren en om interventiestudies, gericht op het beperken van hersenschade, te kunnen begeleiden.

Hoofdstuk 3

Vanwege het verhoogd risico op respiratoire en hemodynamische instabiliteit, is het uitvoeren van een MRI scan in de premature periode niet voor de hand liggend en zijn specifieke maatregelen vereist. Hoofdstuk 3 presenteert gegevens over patiëntveiligheid van 52 prematuren die MRI scans ondergingen rond de postmenstruele leeftijd van 30 weken. In deze studie werden op vaste tijdstippen in de 24 uur voor en in de 24 uur na de MRI scan gegevens ten aanzien van klinische conditie en patiëntveiligheid verzameld. Hoewel ernstige complicaties zich niet hebben voorgedaan en de vitale parameters doorgaans stabiel zijn gebleven, trad er in de helft van de MRI procedures een (milde) complicatie op. Met name ging dit om toegenomen respiratoire insufficiëntie (23,1%), welke significant geassocieerd was met een kortere zwangerschapsduur bij de geboorte, een lager geboortegewicht en een intensievere vorm van ademhalingsondersteuning. Hypothermie (lichaamstemperatuur onder 36˚C) werd gezien in 17,3% van de procedures. Deze resultaten tonen de hoge incidentie van complicaties bij vroege MRI scans in prematuren en benadrukken de noodzaak van specifieke en alomvattende richtlijnen voor het uitvoeren van MRI scans bij kwetsbare patiënten.

Hoofdstuk 4

Hoewel de mogelijkheden van DTI veelbelovend zijn, is het goed toepassen en interpreteren van DTI sequenties complex: verschillende technische, klinische en fysiologische aspecten kunnen nauwkeurige analyse bemoeilijken. Specifieke acquisitie, weloverwogen beeldverwerking en zorgvuldige interpretatie van neonatale DTI data zijn dan ook essentieel om betrouwbare analyse mogelijk te maken. In dit hoofdstuk worden de algemene aspecten, specifieke technische kenmerken, belangrijke beperkingen en de voornaamste valkuilen ten aanzien van de acquisitie van neonatale DTI vanuit een klinisch oogpunt uiteengezet. Eveneens wordt het belang van zowel acquisitie van hoogwaardige DTI data, als het gebruik van specifieke beeldverwerkingsprocessen benadrukt door middel van klinische voorbeelden. Tenslotte worden praktische aanbevelingen en strategieën om beeldartefacten te verminderen en datakwaliteit te evalueren beschreven.

Hoofdstuk 5

In de huidige literatuur wordt er onvoldoende aandacht besteed aan het belang van specifieke maatregelen om de juiste acquisitie en beeldverwerking van premature DTI data te bewerkstelligen. In hoofdstuk 5 wordt een studie beschreven betreffende dit belang. Het effect van verschillende diffusie tensor berekeningsmethoden en datakwaliteit op reconstructies van de fornix door middel van tractografie in het premature brein werd onderzocht. DTI scans van 28 prematuren, verkregen op een postmenstruele leeftijd van 30 weken, zonder hersenletsel, werden prospectief verzameld. Acquisitie, kwaliteitsbeoordeling en correctiemethoden waren identiek voor alle datasets. Er werden vier verschillende methoden toegepast om de diffusie

tensor vast te stellen: linear least squares (LLS), weighted linear least squares (WLLS), non-linear least squares (NLLS) en robust estimation of tensors by outlier rejection (RESTORE). Tractografie resultaten werden voor elke methode afzonderlijk geëvalueerd. Kwantitatieve witte stof parameters werden significant beïnvloed door de methode van tensor berekening: NLLS en RESTORE resulteerden in lagere gemiddelde fractionele anisotropie waarden dan LLS en WLLS. Daarnaast werd de kwaliteit van witte stof reconstructie ook significant beïnvloed: er werd met RESTORE een hogere kwaliteit verkregen. Kwaliteit van de DTI data was ook significant geassocieerd met de nauwkeurigheid van tractografie. Resultaten van deze studie tonen hoe de gekozen beeldverwerkingsmethode tractografie resultaten beïnvloedt. Voordat men daarom over kan gaan op het associëren van microstructurele eigenschappen van hersenweefsel met lange termijn uitkomsten, dienen alle stappen van acquisitie tot en met interpretatie van premature DTI data weloverwogen gekozen te worden en dienen deze stappen te voldoen aan strikte kwaliteitseisen om betrouwbare interpretatie te garanderen.

Hoofdstuk 6

Voor klinisch individueel profijt van DTI scans zijn kwantitatieve metingen van de normale hersenontwikkeling nodig. Dergelijke referentiewaarden kunnen worden afgeleid van DTI atlassen, die momenteel in verschillende centra worden ontwikkeld. Het belang van een gestandaardiseerde benadering van beeldverwerkingsprocessen, zoals beschreven in hoofdstuk 5, is eveneens van toepassing op hersenatlassen. DTI parameters zijn centrum-, scanner- en populatie-specifiek en kunnen in beginsel niet worden uitgewisseld tussen centra. Om dit probleem op te lossen, wordt in hoofdstuk 6 een manier geschetst om een centrum-specifieke DTI atlas van het premature brein te ontwikkelen en toe te passen. In deze studie, zoals beschreven in dit hoofdstuk, werden DTI scans van 24 prematuren, gescand op 30 weken postmenstruele leeftijd, zonder hersenschade, prospectief verzameld. Segmentatie van verschillende hersengebieden werd handmatig verricht door een expert. Alle scans werden op elkaar geregistreerd in een standaardruimte met behulp van een robuuste registratietechniek. Het gemiddelde en de standaarddeviatie van DTI parameters werden voor elk hersengebied berekend. Effectiviteit van de atlas werd getest op nieuwe data van prematuren, met of zonder hersenletsel. Bij een pasgeborene met ernstig hersenletsel was de gemiddelde diffusiviteit in de witte stof (Z-score: 4,15) en basale kernen (Z-score 11,18) significant afwijkend ten opzichte van de atlaswaarden. Om andere centra de mogelijkheid te bieden om een soortgelijke atlas te ontwerpen, zal deze methode beschikbaar worden gesteld in "*ExploreDTI*".

Hoofdstuk 7

Zoals beschreven in dit proefschrift, is het uitvoeren van een MRI scan bij premature pasgeborenen een bijzondere aangelegenheid vanwege veiligheidsaspecten, logistieke problemen en de invloed van beeldkwaliteit waardoor de klinische toepasbaarheid beperkt kan zijn.

Schedelechografie krijgt daarentegen, door voortdurende technische ontwikkelingen en het gebruik van andere fontanellen, een steeds belangrijkere rol in het opsporen van premature schadepatronen. Bovendien is door schedelechografie seriële beeldvorming van ernstig zieke pasgeborenen aan het bed mogelijk. In hoofdstuk 7 worden de bevindingen van een grote prospectieve cohortstudie beschreven. Deze studie had als doel om de klinische waarde van één vroege MRI scan te vergelijken met seriële schedelechografie door een ervaren onderzoeker. Er werden 307 neonaten, geboren <29 weken zwangerschapsduur, geïncludeerd. Volgens klinisch protocol werd schedelechografie serieel uitgevoerd vanaf de geboorte tot ontslag en werd een MRI scan uitgevoerd rond 30 weken postmenstruele leeftijd. De MRI scan werd uitgesteld of geannuleerd in geval van klinische instabiliteit. Beoordeling van de hersenbeeldvorming werd uitgevoerd door ervaren onderzoekers. In tegenstelling tot echografie, werd de MRI scan vaak uitgesteld of geannuleerd in respectievelijk 58 en 127 prematuren. De incidentie van hersenletsel was hoog: bijna 48%. Bij 61 pasgeborenen werden tegenstrijdige bevindingen tussen echografie en MRI gevonden. Seriële schedelechografie bleek adequaat om veelvoorkomende schadepatronen in prematuren op te sporen, zoals acute intra-ventriculaire bloedingen en sino-veneuze trombose. Bovendien blonk schedelechografie uit in de klinische toepasbaarheid. Echter, MRI identificeerde kleine cerebellaire bloedingen die niet konden worden gedetecteerd met behulp van echografie. Aangezien verondersteld wordt dat deze bloedingen geassocieerd zijn met slechtere lange termijn uitkomsten, is MRI nodig voor een betere voorspelling van de neurologische uitkomst. Om deze reden dient de klinische toepasbaarheid van MRI scans voor individuele prematuren te worden vergemakkelijkt en dienen MRI procedures te worden verbeterd ten aanzien van patiëntveiligheid.

Hoofdstuk 8

In het laatste hoofdstuk worden de voornaamste bevindingen van dit proefschrift ten opzichte van de huidige literatuur beschreven. Bovendien worden aanbevelingen en voorstellen voor toekomstig onderzoek gedaan.

Summary

Chapter 1

This chapter introduces the main topics of this thesis. The importance of accurate detection of brain injury in preterm infants to predict neurodevelopmental outcome is described and the main challenges of magnetic resonance imaging (MRI) performed in preterm infants for clinical purposes are discussed. Finally, the aims and outline of this thesis are presented.

Chapter 2

Although advances in neonatal neuroimaging have improved early detection of preterm brain injury responsible for abnormal neuromotor and cognitive development, there seems to be no consensus on the optimal timing of MRI scans. This chapter describes the results from a systematic review of current literature, which was set up to investigate how brain MRI in preterm infants should be timed to best predict long term outcome. 62 articles were incorporated in this review: eight serial MRI studies, two performed at ≤35 weeks and 52 MRI studies performed at >35 weeks. Based on these papers, involvement of the white matter in preterm brain injury, assessed with conventional structural MRI, diffusion tensor imaging (DTI), volumetric MRI and proton MR spectroscopy, seems the most important factor for predicting neurodevelopmental outcome. Clear evidence on optimal timing of MRI was not available. However, given the much larger number of studies performed around term age, the individual prognostic value of term-equivalent scanning seems favorable compared to that of early MRI scanning. Nevertheless, early MRI scans are promising as they can guide early neuroprotective intervention studies and are indispensable in ongoing research to understand brain injury in preterm infants.

Chapter 3

Because of the high risk of respiratory and hemodynamic instability of preterm infants, MRI scanning in the preterm period is challenging and requires a dedicated approach. Chapter 3 presents data on patient safety of 52 preterm infants who underwent MRI scans at a mean postmenstrual age of 30 weeks. In this cohort study, data sampling was done at fixed times during the 24 hours before and 24 hours after the MRI scan. No serious adverse events occurred and vital parameters remained generally stable. However, one in two MRI procedures were complicated by minor adverse events, predominantly because of increased respiratory instability (23.1%). This was significantly associated with lower gestational age, lower birth weight and a higher mode of respiratory support. Hypothermia (core temperature below 36˚C) was encountered in 17.3% of the procedures. These results raise awareness of important complications of early MRI scans in preterm infants and the necessity of tailored state-of-the-art guidelines for MRI procedures in vulnerable populations.

Chapter 4

Although its possibilities are very promising, DTI is a complex matter; there are many technical, clinical and physiological aspects that may complicate accurate analysis. Dedicated acquisition, well-informed processing and careful interpretation of neonatal DTI data are therefore crucial to enable reliable analysis. In this chapter, general aspects, specific technical characteristics, important limitations and main pitfalls of acquisition of neonatal DTI data are reviewed. In addition, the importance of both acquisition of high-quality DTI data as the use of dedicated processing pipelines is emphasized by giving clinical examples from our own cohort. Practical recommendations regarding strategies to minimize corrupting effects and quality assessment tools of neonatal DTI data are described.

Chapter 5

Current literature seems insufficiently focused on the importance of a dedicated approach towards acquisition and processing pipeline of preterm DTI data. Therefore, the study described in chapter 5 was aimed to raise awareness about this importance by investigating the impact of the chosen method of diffusion tensor estimation and data quality on tractography reconstructions of the fornix in the preterm brain. DTI scans of 28 preterm infants, acquired at 30 weeks' postmenstrual age, without brain injury, were prospectively collected. Image acquisition, quality assessment and correction methods were identical for all datasets. Four different diffusion tensor estimation methods were applied: linear least squares (LLS), weighted linear least squares (WLLS), non-linear least squares (NLLS) and robust estimation of tensors by outlier rejection (RESTORE). Tractography results were evaluated for each method independently. Quantitative tract parameters were significantly affected by the method of tensor estimation: NLLS and RESTORE resulted in lower mean fractional anisotropy values than LLS and WLLS. Furthermore, visualized quality of tract reconstruction was also significantly affected: in general, with RESTORE a higher quality of tract delineation was obtained. Quality of the DTI data correlated significantly with the visualized quality of tract reconstruction. Results of this study demonstrate how processing methodology influences tractography results. Therefore, before microstructural brain properties can be associated with long term outcome measurements, all steps from acquisition to interpretation of preterm DTI data need to be chosen carefully and must comply with strict requirements to ensure reliable interpretation.

Chapter 6

For clinical individual profit from DTI scans in preterm infants, quantitative measurements of normal brain development are needed. Such reference values can be derived from DTI templates, which are currently under development in different neuroimaging centers. The importance of standardization of processing pipelines, as discussed in chapter 5, covers however for brain templates as well. DTI parameters are center, scanner and population specific and can

typically not be exchanged across centers. To overcome this problem, chapter 6 presents the conceptual workflow for the construction and application of a site-specific DTI template of the preterm brain. In this study, DTI data of 24 preterm infants, scanned at 30 weeks' postmenstrual age, without brain injury on conventional MRI, were prospectively collected. Segmentation of different brain regions was manually performed by an experienced observer. All scans were registered to a common space using a nonrigid group-wise registration technique. Mean and standard deviation of DTI parameters were calculated for each brain region. Efficacy of the template was tested using new imaging data of infants, either with or without brain injury. In an infant with severe brain injury, mean diffusivity in the white matter (z-score: 4.15) and basal ganglia (z-score 11.18) deviated significantly from template values. In order to enable other imaging centers to perform similar work, the workflow will be made available in Explore DTI.

Chapter 7

As outlined in this thesis, MRI scanning in preterm infants is particularly challenging due to safety, logistical and quality issues that limit feasibility of MRI in clinical context. Meanwhile, due to ongoing technical developments and by using additional acoustic windows, cranial ultrasonography (CUS) is gaining more credits in detecting preterm brain injury. Furthermore, CUS allows serially bedside scanning of critically ill infants. Chapter 7 describes findings of a large prospective cohort study that was aimed to investigate clinical value of a single early MRI scan compared with serial experienced CUS scans in diagnosing common injury patterns. 307 infants born <29 weeks gestational age, were included in this study. According to clinical protocol, CUS was serially performed from birth until discharge. Early MRI scanning was performed at 30 weeks postmenstrual age, but was postponed or cancelled in case of clinical instability. Experienced observers performed evaluation of brain imaging. In contrast to CUS, MRI scanning was often postponed or canceled in 58 and 127 infants respectively. Brain injury was common as it was detected in almost 48%. In 61 infants, discrepant imaging findings were found. Results of this study show how serial advanced CUS is adequate in diagnosing preterm brain injury, such as acute intraventricular hemorrhage and cerebral sinovenous thrombosis. Furthermore, CUS excelled in clinical feasibility. However, MRI identified small cerebellar hemorrhages that could not be detected with CUS. As these hemorrhages are thought to correlate with poorer long term neurodevelopmental outcome, MRI is needed for better prediction of outcome. Therefore, the clinical limitations of MRI for individual preterm infants need to be addressed and MRI procedures must to be improved in terms of safety and clinical applicability.

Chapter 8

In this last chapter, main findings of this thesis in comparison with current literature are described. In addition, recommendations and directions for future research are discussed.

About the author

Annemarie Plaisier was born in Rotterdam on May 31st 1982. After graduating secondary school at "Develsteincollege" in Zwijndrecht in the year 2000, she started her medical training at the Medical Faculty of the Erasmus University Rotterdam. In 2007, she received her medical degree and started working as a resident at the Department of Pediatrics in the Medical Centre Rotterdam Zuid. After one year, she transferred to the Division of Neonatology at the Leids University Medical Centre in Leiden. She returned to Rotterdam in 2009, when she started working at the division of Neonatology in the Erasmus MC Sophia Children's Hospital, first as a resident and after one year she also worked as a PhD student on this thesis. During her PhD project, she has worked at the Technical University Ghent, Belgium and at the Department of Perinatal Imaging at King's College London, United Kingdom to gain more experience in the field of advanced neonatal neuroimaging. In 2014 she started working as a resident at the Department of Pediatrics in the Sint Franciscus Gasthuis in Rotterdam. Annemarie lives happily ever after with Ronald van Nugteren.

List of publications

Pieterman K, **Plaisier A**, Govaert P, Leemans A, Lequin MH, Dudink J. Systematic review of dedicated acquisition, quality assessment and post processing pipelines in preterm diffusion tensor imaging. *Submitted*

Plaisier A, Raets MMA, Ecury-Goossen GM, Govaert P, Feijen-Roon M, Reiss IKM, Smit LS, Lequin MH, Dudink J. Serial cranial ultrasonography and early MRI are complementary in detecting preterm brain injury. *Submitted*

Plaisier A, Pieterman K, Lequin MH, Govaert P, Heemskerk AM, Reiss IKM, Krestin GP, Dudink J. Choice of diffusion tensor estimation approach affects fiber tractography of the fornix in the preterm brain. *AJNR Am J Neuroradiol. January 2014*

Plaisier A, Govaert P, Lequin MH, Dudink J. Optimal timing of cerebral MRI in preterm infants to predict long term neurodevelopmental outcome: a systematic review. *AJNR Am J Neuroradiol. May 2013*

Heemskerk AM, Leemans A, **Plaisier A**, Pieterman K, Lequin MH, Dudink J. Acquisition guidelines and quality assessment tools for analyzing neonatal diffusion tensor MRI data. *AJNR Am J Neuroradiol. 2013; 34:1496-505*

Plaisier A, Raets MMA, van der Starre C, Feijen-Roon M, Govaert P, Lequin MH, Heemskerk AM, Dudink J. Safety of routine early MRI in preterm infants. *Pediatric Radiology, 2012; 42:1205-11*

Raets MMA, Lequin MH, **Plaisier A**, Dudink J, Govaert P. Incidental sonographic diagnosis of neonatal carotid occlusion. *Acta Paediatr. 2013; 102:187-90*

Kudzinava M, Poot D, **Plaisier A**, Sijbers J. Optimized workflow for diffusion kurtosis imaging of newborns. *IEEE International Symposium on Biomedical Imaging: From Nano to Macro Chicago, USA; 2011*

Plaisier A, Maingay-de Groof F, Mast-Harwig R, Kalkman PM, Wulkan RW, Verwers R, Neele M, Hop WC, Groeneweg M. Plasma water as a diagnostic tool in the assessment of dehydration in children with acute gastroenteritis. *Eur J Pediatr. 2010; 169:883-6*

PhD Portfolio

Summary of PhD training and teaching activities

Erasmus MC Department:	Pediatrics, Division of Neonatology
PhD period:	January 2010 – December 2014
Promotors:	Prof.dr. I.K.M. Reiss
	Prof.dr. G.P. Krestin
Copromotor:	Dr. J. Dudink

1. PhD training

	Year	*ECTS*
General courses		
CPO-mini-course, Erasmus MC	2010	0.3
Good Clinical Practice, Erasmus MC	2011	1
Biostatistical Methods I: Basic Principles, NIHES, Erasmus MC	2011	5.7
Specific courses		
MRI of the Neonatal Brain, Hammersmith Hospital, London, UK	2010	0.6
MRI safety course, Erasmus MC	2010	0.6
Seminars and workshops		
European neonatal neuro experts meeting, Rotterdam	2010	0.3
Neuroimaging, genetics and endophenotypes: development and psychopathology, Rotterdam	2010	0.3
Annual Flemish-Dutch neonatology meeting, Ghent, Belgium	2011	0.3
Annual ESMRN meeting, Amsterdam	2011	1
Advances in MR imaging in the preterm infant, Utrecht	2011	0.3
Annual ISMRM Benelux chapter meeting, Leuven, Belgium	2012	0.3
Annual OBNEO meeting, Veldhoven	2012	0.3
Annual neonatal neurology meetings	2011-2013	0.9
Conferences		
International		
Annual ESPR meeting, Newcastle, UK (poster presentation)	2011	1
Annual ESPR meeting, Istanbul, Turkey (oral presentation)	2012	1
Annual Flemish-Dutch neonatology meeting, Antwerp, Belgium (oral presentation)	2013	1
Annual ESPR meeting, Porto, Portugal (oral presentation)	2013	1

National

Annual Dutch neonatal fellow meetings	2012-2013	2
Pediatric research day, Rotterdam	2013	1
VRA course traumatic brain injury, Rotterdam	2013	1

Other

Working visit: department of telecommunications and information processing, Ghent, Belgium	2010	4
Working visit: department of perinatal imaging, King's College, London, UK	2012	7

2. Teaching activities

	Year	*ECTS*
Lecturing		
Clinical lessons about neonatal MRI procedures to nursing staff	2013-2013	1
Tutoring		
Training courses about DTI post processing to graduation students	2011-2013	3

Dankwoord

'Silent gratitude isn't much use to anyone' – G.B. Stern

Hoewel ik hier al voor gewaarschuwd werd, valt het vinden van de juiste woorden om iedereen persoonlijk te bedanken toch niet mee. Het dankwoord betreft misschien wel het meest gelezen hoofdstuk en heeft daarmee de hoogste impact factor van dit proefschrift...

Allereerst wil ik alle kinderen en hun ouders hartelijk bedanken voor deelname aan de studie waarop dit proefschrift is gebaseerd. Dit boekje is voor en door jullie tot stand gekomen.

Mijn promotoren; Prof. Dr. I.K.M. Reiss en Prof. Dr. G.P. Krestin. Beste Irwin, "Hopla!", het boekje van één van je eerste echte promovendi is af! Veel dank voor je superviserende en motiverende rol als promotor, je inspirerende visie op de toekomst en je aansturing bij het afronden van mijn promotietraject. Professor Krestin, de combinatie van Neonatologie en Radiologie als uitgangspunt van dit proefschrift heeft een zeer belangrijke rol gekregen in mijn ambities voor de toekomst. Hartelijk dank voor deze waardevolle aanvulling.

Mijn co-promotor; Dr. J. Dudink, Jeroen, "In Principe" het grote brein achter dit proefschrift. Heel veel dank voor de onuitputtelijke hoeveelheid energie, enthousiasme, steun en begeleiding in de wetenschap, maar ook daarbuiten: StuBru en de Afrekening, Mega Mindy, de papegaai op je schouder en de vele andere leuke grapjes in kamer SK-3202.

De leden van de kleine promotiecommissie; Prof. Dr. D. Tibboel en Prof. Dr. W.J. Niessen, hartelijk dank voor het lezen en beoordelen van mijn proefschrift. Prof. Dr. S.J. Counsell, dear Serena, I am truly honored that you would like to participate in the small committee of my thesis. Many thanks as well for the wonderful and inspiring time I had at King's College!

De overige commissieleden; Prof. Dr. J.B. van Goudoever, beste Hans, ik herinner ons gesprek in de ambulance naar Goes, waarin je dit onderzoeksproject voorstelde, nog als de dag van gisteren. Veel dank voor de mogelijkheid om promotieonderzoek te kunnen doen. Prof. Dr. A. van der Lugt en Dr. T.J.H. White, bedankt voor het plaatsnemen in de grote commissie. Dr. M.H. Lequin, beste Maarten, veel dank voor jouw belangrijke bijdrage aan dit proefschrift; van het aanpassen van het scanprotocol en beoordeling van vrijwel elke MRI scan tot en met de kritische beoordeling van de manuscripten.

The Department of Perinatal Imaging at King's College London; Fran, Katherine, Rui, Georgia, Anand, Tom, Joanna, Andrew, Emer, Michelle, Nora and all others, thank you very much for the warm welcome, the freshly ground coffee, strong tea with lots of milk, the fantastic view at the Houses of Parliament and, of course, Secret Santa.

The Department of Telecommunications and Information Processing van de Technische

Universiteit Gent; Ivana Despotovic, thank you very much for introducing me in the complex world of image processing and "lego-brains". Prof. Dr. Philips en Ewout Vansteenkiste, dank voor de inspirerende researchmeetings.

Graag wil ik ook Alexander Leemans, Kay Pieterman, Stefan Klein, Hakim Achterberg en andere mede-auteurs bedanken voor de zeer prettige samenwerking en mooie publicaties. Ko Hagoort, veel dank voor de altijd snelle en zeer nuttige correcties van de manuscripten.

De kinderradiologen, laboranten en het secretariaat van de afdeling Radiologie, in het bijzonder Nanko, Sylvia, Sita, Hanneke en natuurlijk Carla, hartelijk bedankt voor de fijne samenwerking en de mogelijkheid om zelfstandig neonaten te kunnen scannen. Ton, bedankt voor je hulp met de mooie voorkant en opmaak van dit proefschrift.

Alle (oud-) collega's van de afdeling Neonatologie van het Sophia Kinderziekenhuis; neonatologen, fellows, verpleegkundig specialisten, arts-assistenten, verpleegkundigen en zorgassistenten, dank voor jullie hulp met scannen van patiënten en fijne diensten in de kliniek. Dankzij jullie heb ik een onvergetelijke tijd gehad in het Sophia en kijk ik hier met veel plezier naar terug. In het bijzonder ook veel dank aan de Doppio-momentjes met Daniëlla, Cynthia en André, veel dank voor de ontspanning in drukke tijden. George, dank voor de puntjes op de "i" en de wijze levenslessen. Karin; de rots in de administratieve branding, ik kon altijd bij jou terecht, bedankt voor het vele regelwerk in de laatste periode van dit promotietraject.

Mijn nieuwe collega's van de afdeling Kindergeneeskunde van het Sint Franciscus Gasthuis in Rotterdam, hartelijk dank voor de ondersteuning tijdens de laatste loodjes van dit proefschrift. Ik verheug me op een zeer leerzaam en gezellig jaar!

De BRAINS groep; Liesbeth, Renate, Ginette, Anneriet en Leen, bedankt voor jullie bijdrage aan dit proefschrift en de zeer leerzame periode. Paul Govaert, zonder uw optimisme, kritische noot en doortastende zoektochten zouden de "donderende donderdagen" lang niet zo inspirerend zijn geweest, veel dank ook voor de Bourgondische sfeer in mijn onderzoekstraject.

Monique, heel veel dank voor al je hulp, met scannen, spuien en de rest. Dank voor je heerlijk droge humor en relativering die mij altijd weer met beide benen op de grond hielden, ik weet zeker dat ik jou ga missen!

Marlou; buddy, synaps, paranimf, samen hebben wij alle "fun, excellence and education" doorgemaakt. Dank voor de scroppino's tijdens congressen, pindasoep bij TL-licht, fluctuerende flow op donderdag en het fine-tunen van onze papers.

Ilse en Ilse; de dakduifjes!! De liefste vriendinnen die je maar kan bedenken. Het is altijd goed als ik jullie spreek. Ik hoop dat we samen met onze mannen en kleine dame nog heel lang alles met elkaar kunnen blijven delen!

Mijn schoonfamilie; Hans, Bets, Richard en Yuchen, ik heb het getroffen met zo'n schone familie! Dank voor al jullie hulp, steun en gezelligheid in de afgelopen jaren.

Lucy en Gerard; mijn lieve mamma en pappa, door jullie onvoorwaardelijke steun, liefde en adviezen, in vrijwel alles wat ik doe, kan ik heel de wereld aan. Dit boekje is compleet met de tulpen, die "er leuk bij staan".

Nadine; Zussie, wat ben ik trots op je. Ik ben heel blij dat jij vandaag naast mij wilt staan, ongetwijfeld zal jij je tussen alle toga's veel meer op je gemak voelen dan ik. Dank alvast voor het oplezen van die ene stelling...;)

Ten slotte, Ronald; mijn lief, met en bij jou ben ik thuis; hier, nu, strakjes en hopelijk voor altijd...

Color section

Chapter 1

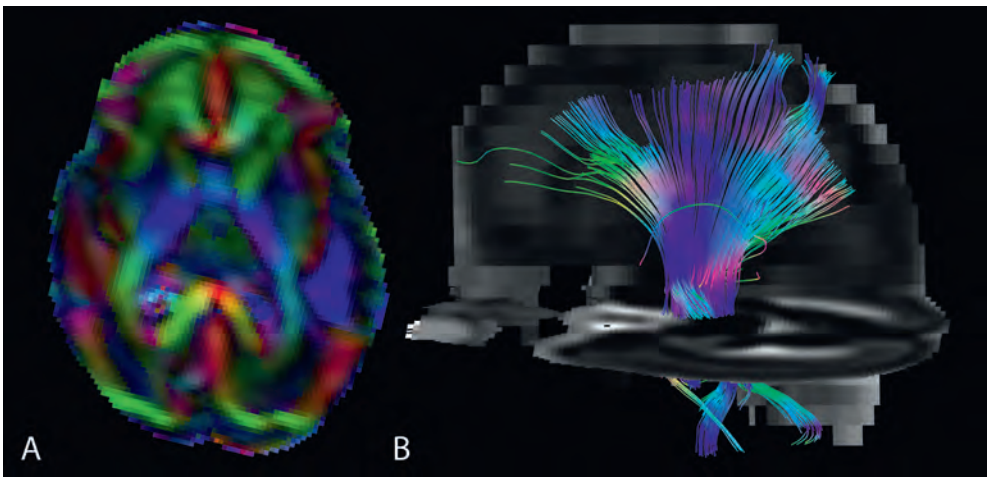

Figure 5 – Applications of diffusion tensor imaging: **A**, color-coded maps; red stands for left–right direction, blue for superior–inferior, and green for anterior–posterior. Brightness of colors is weighted by the FA value. **B**, fiber tractography of the corticospinal tract.

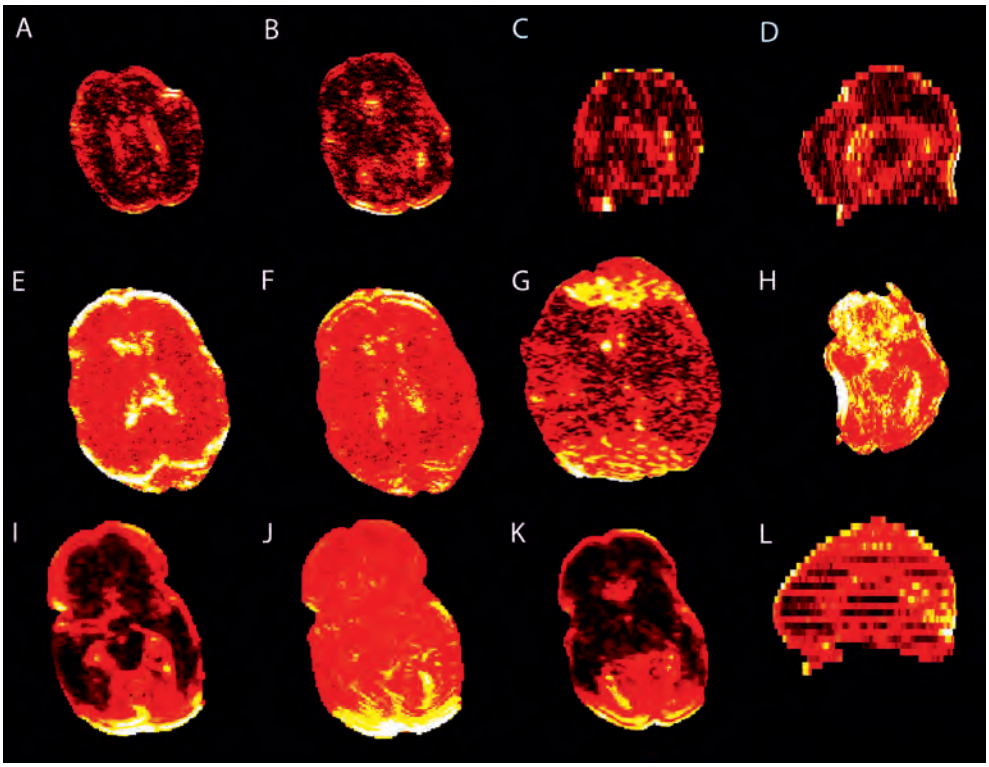

Figure 4 – Examples of residuals. **A** trough **D**, residuals from a subject with good data quality. Higher residuals are present at the border and in the ventricles. **A** and **B**, axial images; **C**, coronal view; and **D**, sagittal view. **E** and **F**, effects of motion and eddy current correction with higher residuals before correction and lower values after correction; **G**, higher residuals caused by ghosting; **H**, higher residuals caused to susceptibility artifacts; **I** through **L**, residuals from a subject with gross motion artifacts showing both sections with low (no motion) and high (motion) residuals. The sagittal view (**L**) shows a pattern with alternating sections of high and lower residuals. Each image is individually scaled.

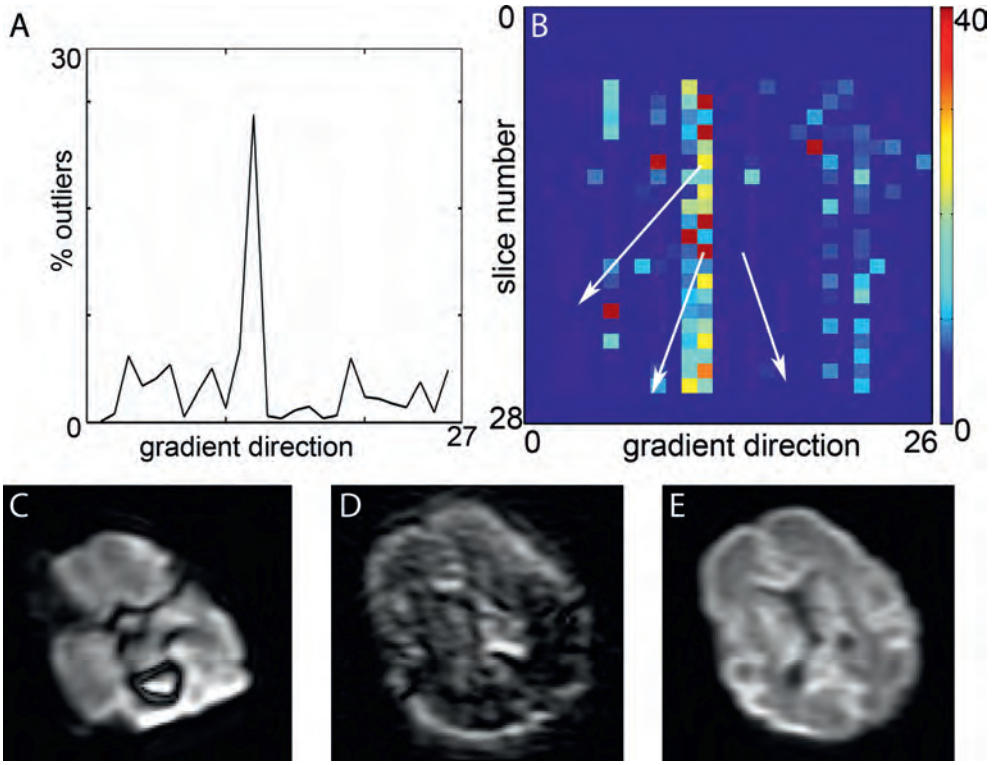

Figure 5 – Detection of outliers. **A**, percentage of outliers per DW image is a tool to indicate potential problems with the DTI dataset. In this case, DW images eleven and twelve have a high percentage of outliers. **B**, percentage outliers per section facilitate easy detection of the problematic sections. During the acquisition of gradient direction twelve, several sections are affected by movement of the infant. **C** and **D**, examples of the resulting images, and **E**, non-affected image. Because of the interleaved section acquisition, there is an alternating pattern for the odd and even sections. Scaling is similar for diffusion weighted images.

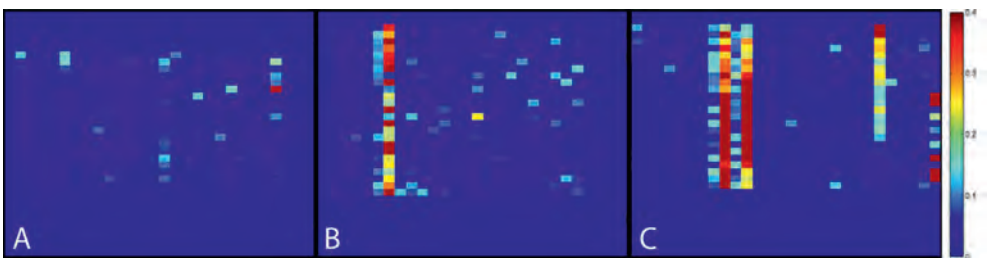

Figure 6 – Outlier profile for different datasets. Outliers are only depicted for those sections that contain >1000 voxels with signal intensity. **A**, dataset without gross motion artifacts; **B**, dataset with one corrupted gradient direction, and **C**, dataset with multiple corrupted gradient directions. Scaling is for 0–40% outliers.

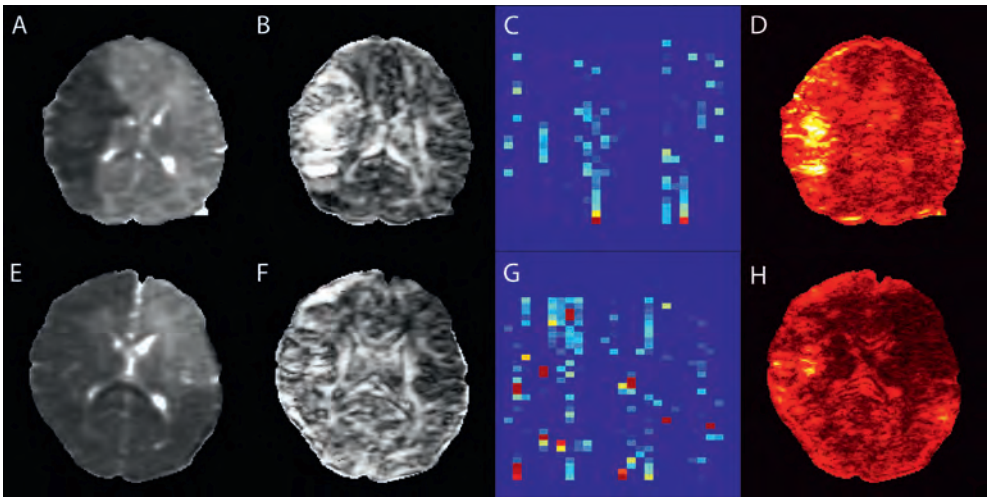

Figure 7 – Quality assessment in two term-born neonates with brain pathology. The damaged brain areas have much lower mean diffusivity (MD) (**A** and **E**) and apparent high fractional anisotropy (FA) (**B** and **F**) values. The percentage outliers (**C** and **G**) are low and are distributed uniformly. Because the residuals are also dependent on the underlying MD and FA values, they (**D** and **H**) are large in the damaged areas. Scaling: MD, 0–2 x 10^{-3} mm^2/s; FA, 0–1; outliers, 0–40%.

Chapter 5

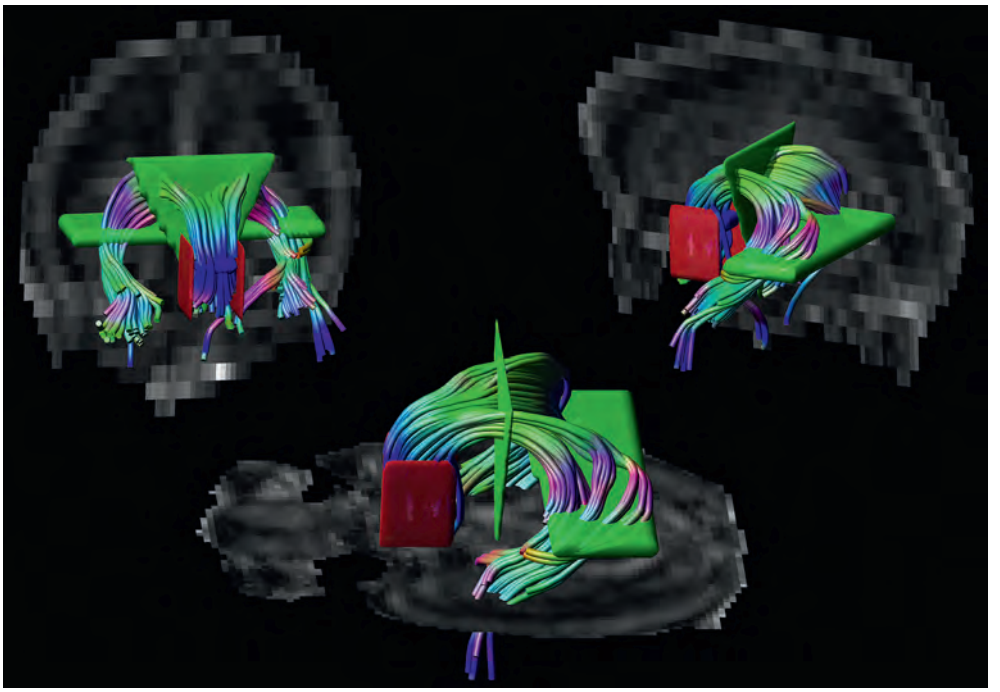

Figure 1 – Placement of regions of interests (ROIs). Tractography of the fornix was performed by placing one "OR" ROI (in blue), two "AND" ROIs (in green) and two "NOT" ROIs (in red) on color-coded fractional anisotropy maps.

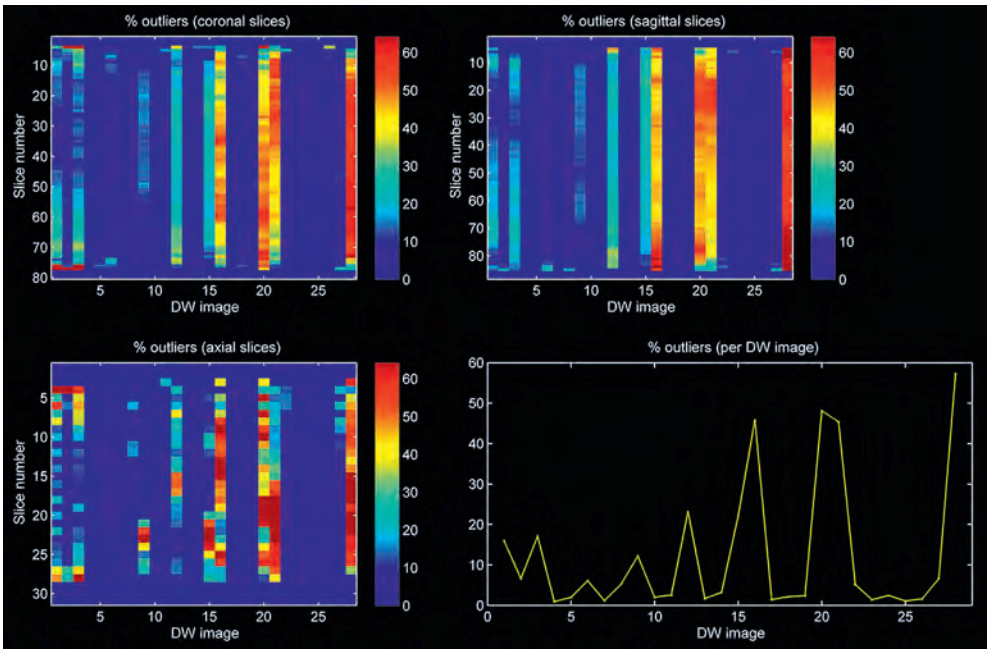

Figure 2 – Outlier profile of DTI data with high percentage of outliers.

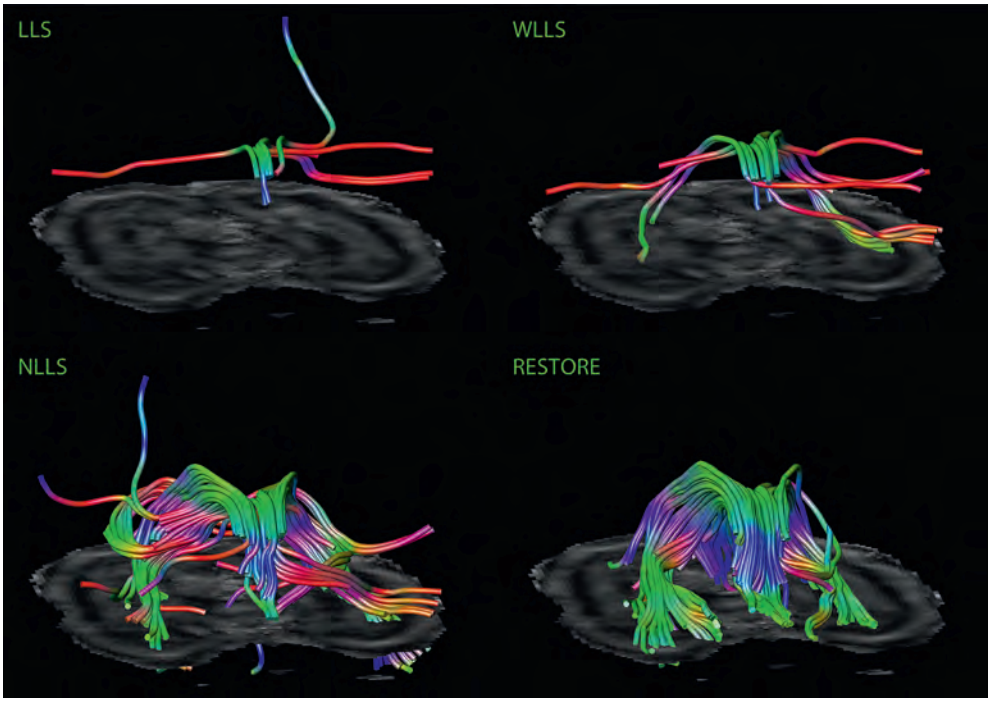

Figure 3 – Impact of diffusion tensor estimation method on tract reconstruction of poor-quality DTI data. Characteristic representations to illustrate the effect of tensor estimation methodology on reconstruction of the fornix with high percentage of data outliers (>10%). Note that reconstruction is not possible using the linear least squares (LLS) and weighted linear least squares (WLLS) methods, seems slightly possible with non-linear least squares (NLLS), but is very well performed if the robust estimation of tensors by outlier rejection (RESTORE) approach is used.

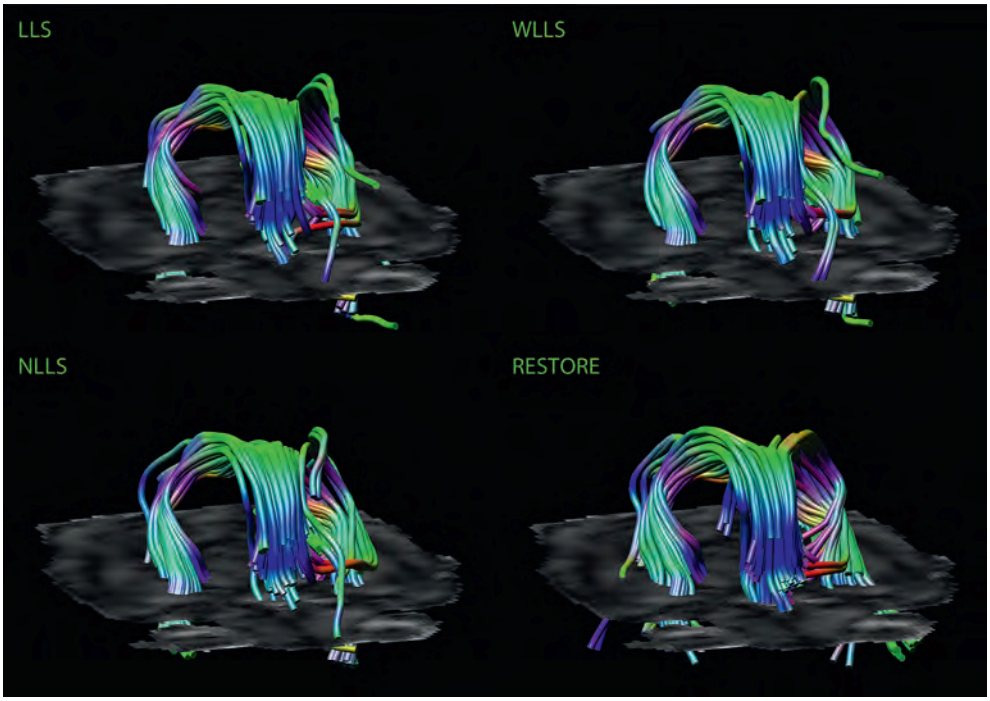

Figure 4 – Impact of diffusion tensor estimation method on tract reconstruction of good quality DTI data. Characteristic representations to illustrate the effect of the tensor estimation on fiber tracking of the fornix with low percentage of data outliers (<10%). Note the more accurate tract reconstruction using the RESTORE approach.

Chapter 6

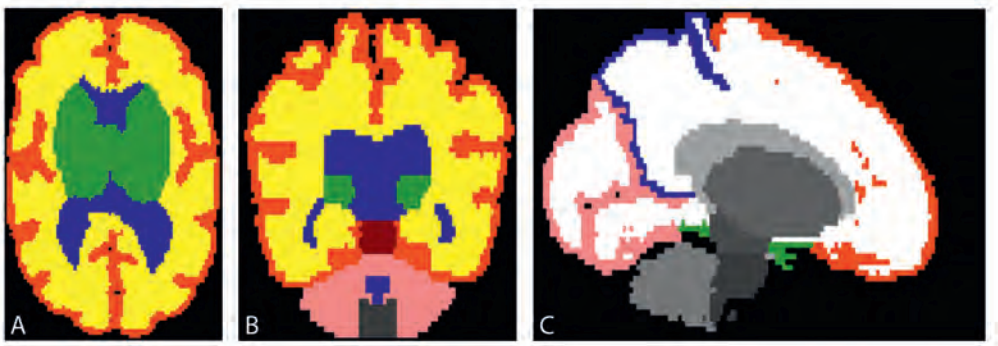

Figure 1 – Manually segmented brain regions in axial (**A**) and coronal (**B**) plane: cortical (orange) and deep (green) gray matter, white matter (yellow), intracranial cerebrospinal fluid (blue), mesencephalon (red), cerebellum (pink) and brain stem (gray). **C**, subdivision of cortical gray matter was further in frontal (orange), parietal (blue), temporal (green) and occipital (pink) cortex. Note that the insular cortex is not shown.

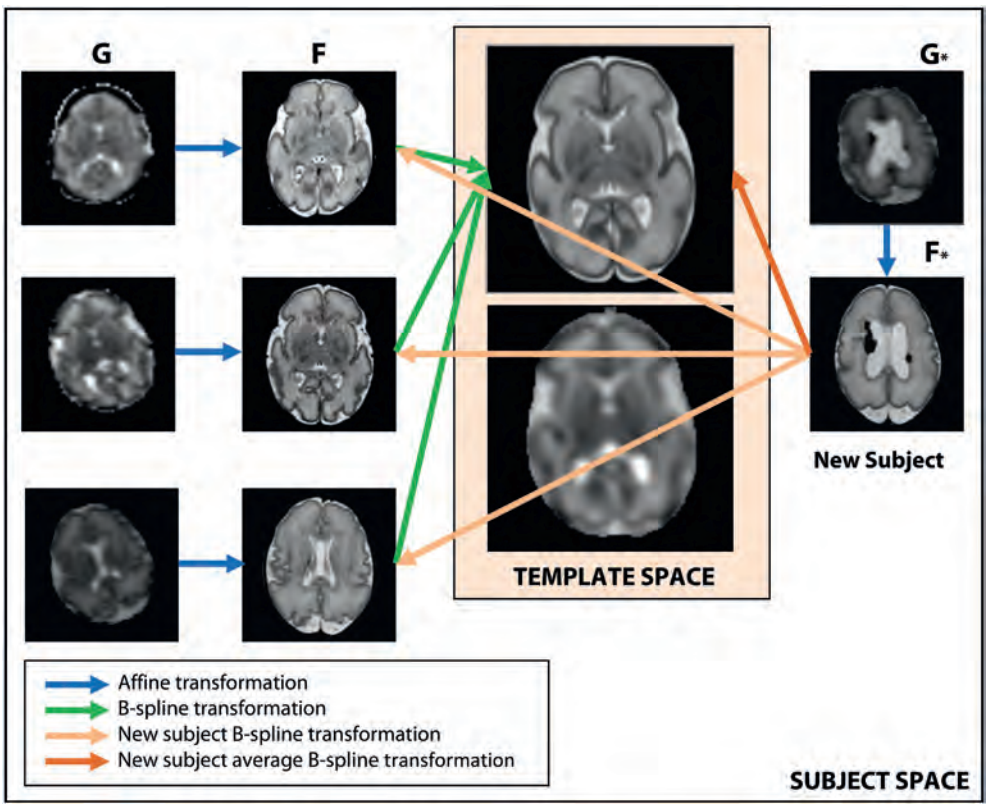

Figure 2 – Schematic representation of image transformation template construction.
F indicates T2-weighted images; **G**, MD/FA maps; **F*,** T2-weighted image from new patients, and **G*,** MD/FA maps from new patients.

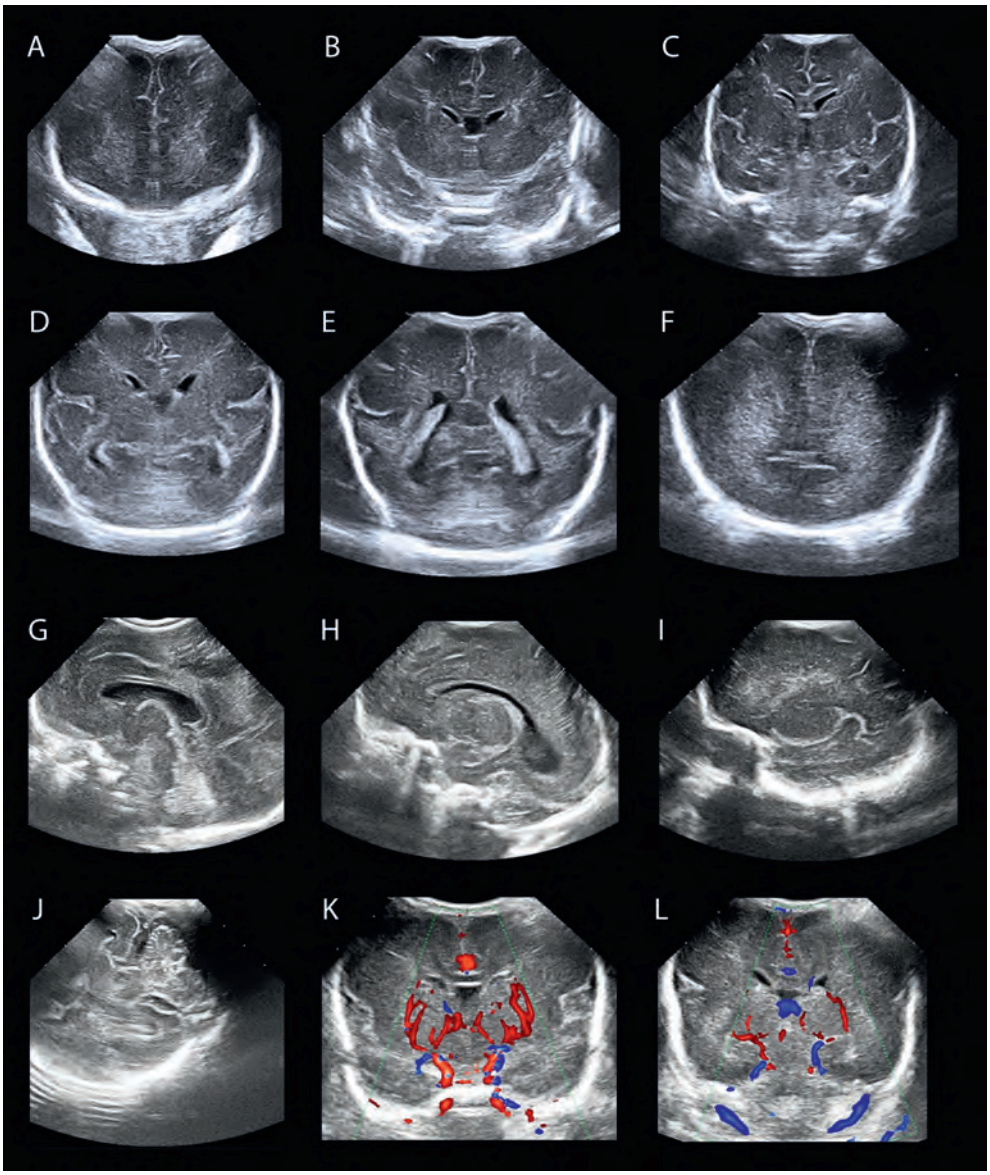

Figure 1 – Ultrasound images were obtained in six coronal (**A**-**F**) and five sagittal/parasagittal planes (**G**-**I**) through the anterior fontanel. Additional images were acquired through the mastoid fontanel (**J**) to visualize the cerebellum and color Doppler images (**K**-**L**) were acquired to assess arterial and (sino-) venous systems.

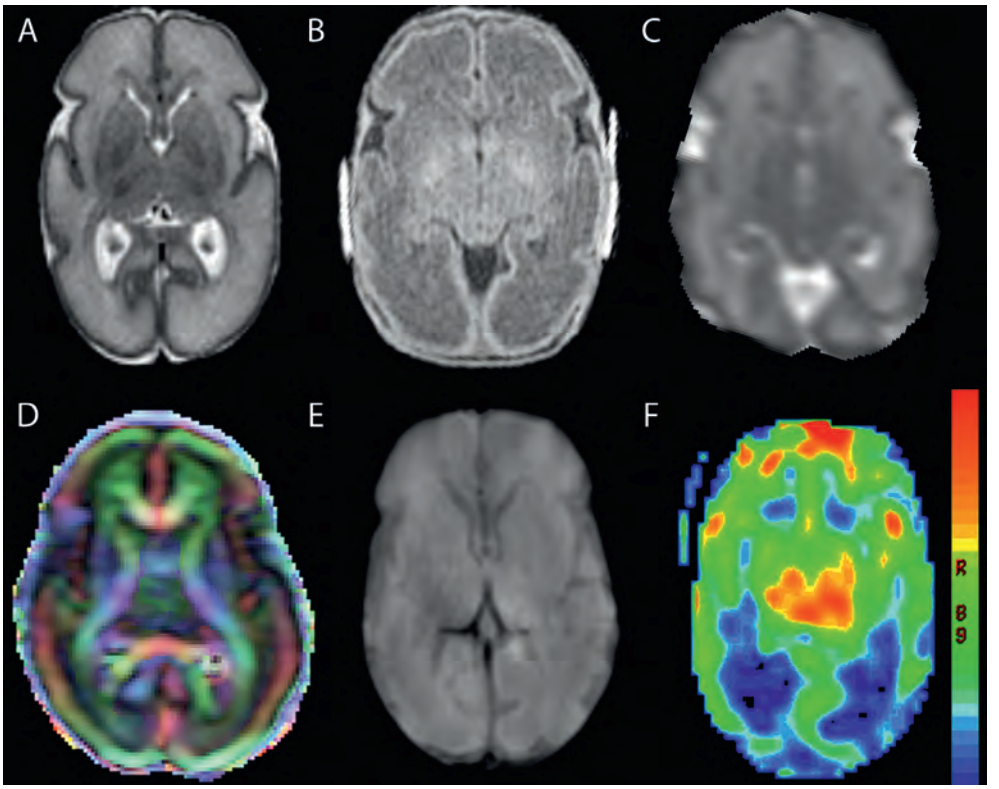

Figure 2 – Applied MRI sequences: **A**, axial T2-weighted fast spin-echo; **B**, axial 3D T1-SPGR; diffusion tensor imaging; **C**, mean diffusivity map; **D**, color-coded directionality map (red represents fibers in the left–right direction, blue represents fibers in the superior–inferior direction, and green represents fibers in the anterior–posterior direction); **E**, susceptibility weighted imaging, and **F**, arterial spin labeling.